UNCLASSIFIED

SECURITY CLASSIFICATION OF THIS PAGE *(When Data Entered)*

AD-A197 150

REPORT DOCUMENTATION PAGE

READ INSTRUCTIONS BEFORE COMPLETING FORM

1. REPORT NUMBER: AFIT/CI/NR 88-170
2. GOVT ACCESSION NO.
3. RECIPIENT'S CATALOG NUMBER: DTIC FILE COPY

4. TITLE *(and Subtitle)*: EFFECTS OF EXPANSION DEVICES ON THE TRANSIENT RESPONSE CHARACTERISTICS OF THE AIR-SOURCE HEAT PUMP DURING THE REVERSE CYCLE DEFROST

5. TYPE OF REPORT & PERIOD COVERED: MS THESIS

6. PERFORMING ORG. REPORT NUMBER

7. AUTHOR(s): KURT T. PETERSON

8. CONTRACT OR GRANT NUMBER(s)

9. PERFORMING ORGANIZATION NAME AND ADDRESS: AFIT STUDENT AT: TEXAS A&M UNIVERSITY

10. PROGRAM ELEMENT, PROJECT, TASK AREA & WORK UNIT NUMBERS

11. CONTROLLING OFFICE NAME AND ADDRESS

12. REPORT DATE: 1988

13. NUMBER OF PAGES: 118

14. MONITORING AGENCY NAME & ADDRESS *(If different from Controlling Office)*: AFIT/NR, Wright-Patterson AFB OH 45433-6583

15. SECURITY CLASS. *(of this report)*: UNCLASSIFIED

15a. DECLASSIFICATION/DOWNGRADING SCHEDULE

16. DISTRIBUTION STATEMENT *(of this Report)*

DISTRIBUTED UNLIMITED: APPROVED FOR PUBLIC RELEASE

17. DISTRIBUTION STATEMENT *(of the abstract entered in Block 20, if different from Report)*

SAME AS REPORT

18. SUPPLEMENTARY NOTES

Approved for Public Release: IAW AFR 190-1
LYNN E. WOLAVER 8 Aug 88
Dean for Research and Professional Development
Air Force Institute of Technology
Wright-Patterson AFB OH 45433-6583

19. KEY WORDS *(Continue on reverse side if necessary and identify by block number)*

20. ABSTRACT *(Continue on reverse side if necessary and identify by block number)*

ATTACHED

DD FORM 1 JAN 73 1473 EDITION OF 1 NOV 65 IS OBSOLETE

UNCLASSIFIED

SECURITY CLASSIFICATION OF THIS PAGE *(When Data Entered)*

THE EFFECTS OF EXPANSION DEVICES ON THE TRANSIENT RESPONSE CHARACTERISTICS OF THE AIR-SOURCE HEAT PUMP DURING THE REVERSE CYCLE DEFROST

A Thesis

by

KURT T. PETERSON

Submitted to the Graduate College of
Texas A&M University
in partial fulfillment of the requirement for the degree of

MASTER OF SCIENCE

August 1988

Major Subject: Mechanical Engineering

THE EFFECTS OF EXPANSION DEVICES ON THE TRANSIENT RESPONSE CHARACTERISTICS OF THE AIR-SOURCE HEAT PUMP DURING THE REVERSE CYCLE DEFROST

A Thesis

by

KURT T. PETERSON

Approved as to style and content by:

Dennis L. O'Neal
(Chairman of Committee)

N.K. Anand
(Member)

Lester L. Boyer
(Member)

for Michael J. Rabins
(Department Head)

August 1988

ABSTRACT

The Effects of Expansion Devices
on the Transient Response Characteristics
of the Air-Source Heat Pump
During the Reverse Cycle Defrost. (August 1988)
Kurt Thomas Peterson, B.S., LeTourneau College
Chairman of Advisary Committee: Dr. Dennis L. O'Neal

The effects of the defrost expansion device on the transient performance of the air-source heat pump during the reverse cycle defrost was investigated. A base case test was established using an average response thermal expansion valve in the experimental setup. The base case test was compared to tests using fast and slow response TXVs and different diameter orifices. The overall performance of each test was analyzed as well as a detailed investigation of the refrigerant dynamics. The results of the investigation for TXVs indicated bulb/suction line contact was more critical to the response of the TXV than the internal bulb charge. The orifice investigation showed a general trend of faster defrost times with larger orifices, although the largest orifices allowed liquid refrigerant to enter the compressor intake. The investigation also described the different refrigerant flow control of the TXV and the orifice.

ACKNOWLEDGEMENTS

I would like to thank Dr. Dennis O'Neal for acting as my advisor and committee chairman. He generously gave advice, support and time to this project when other demands were pressing. Also many thanks to Dr. N.K. Anand and Dr. Lester Boyer for their advice and comments during the writing of this thesis. Special thanks to my research partner, Steve Schleising, for making the long hours at the lab bearable and for the development of the plotting software. Finally, I want to give special thanks to my wife, Wendy, for her love and for maintaining our home and family during my many hours away at the lab and office. Without her support, this would not have been possible.

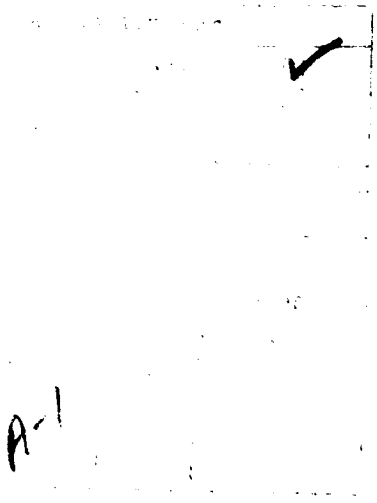

TABLE OF CONTENTS

LIST OF TABLES

LIST OF FIGURES

CHAPTER I

INTRODUCTION

The residential air-source heat pump is an air conditioning unit that has been modified to transfer heat in two modes. During the summer, the heat pump performs the same job as an air conditioner. In the winter, the heat pump extracts heat from the cold outside air and releases the heat inside the living space. The popularity of the heat pump has come from the fact that it can transfer over three times the energy that it consumes and save the consumer utility dollars over electric resistance heating.

The increasing costs of electricity during the seventies and the threat of Federal efficiency standards encouraged manufacturers to improve the efficiency of heat pumps as well as other residential appliances. Research in the 1970's led to the development of steady state heat pump computer design models that have been used to greatly improve the heat pump's steady state efficiency. While the understanding of steady state performance has greatly improved, the heat pump transient effects, which include

---

The style of this thesis conforms to that of the ASHRAE Transactions.

cycling, frosting of the outdoor coil, and defrosting of the outdoor coil, are much more difficult to characterize and are still not well understood.

The objectives of the research are to: (1) characterize the reverse cycle defrost of the air-to-air heat pump and (2) examine the effect of different expansion devices on the performance of the heat pump during the defrost cycle.

The investigation consists of a literature review and an experimental phase. In the literature review, relevant literature on the defrost cycle and transient performance is summarized. During the experimental phase, a test setup was constructed which contained a nominal 3-ton capacity residential air-to-air heat pump. Refrigerant temperature and pressure measurements were made throughout the system as well as refrigerant flow rates, air-side capacity, compressor/outdoor fan power and refrigerant level in the accumulator. Modifications were also made on the heat pump to allow for easy switching of defrost cycle expansion devices without shutting the system off. System parameters and testing procedures are documented to ensure the experimental results are reproducible.

Selection of the expansion device for the focus of this research was done after receiving input from an advisory

committee from The American Society of Heating, Refrigerating, and Air-conditioning Engineers (ASHRAE). Two types of expansion devices were tested: thermal expansion valves(TXVs) and orifices. Capillary tubes were not considered, since the majority of new units are equipped with TXVs or orifices.

A literature review was performed to identify the present state of research in the area of transient heat pump performance and establish the need for further research. A summary of the literature is contained in Chapter II. Chapter III presents a complete description of the experimental setup and procedures used to collect the required data. The results of the research are presented in three parts starting with the analysis of the base case test in Chapter IV. Chapter V contains the comparison of TXVs (Thermal Expansion Valves) with different response times. Chapter VI provides a description of the performance using orifices of different diameters. The analyses in Chapters IV through VI include the "macro" features of the heat pump such as power usage, capacity and cycle times and a detailed analysis of system characteristics such as temperature and pressure fluctuations, suction and discharge pressures, and refrigerant flow. Finally, conclusions and recommendations from this research are presented in chapter VII.

CHAPTER II

LITERATURE REVIEW

One of the key features of the reverse cycle defrost is that it is a transient process that occurs in the heat pump. Because of the general lack of relevant literature directed at the reverse cycle defrost, it was decided to also examine other literature that may deal with the transient startup of both heat pumps and air conditioners. The available literature was divided into five general categories: (1) Performance Measurement, (2) Transient Performance, (3) Cycling Losses, (4) Frosting Performance, and (5) Defrost Performance. Each topic is discussed below.

PERFORMANCE MEASUREMENT

Heat pump efficiency is measured by taking the usable heating effect and dividing it by the work input. This is called the Coefficient of Performance(COP)[1]. Until 1979, published heat pump heating performance was based solely on the capacity and COP measured at the operating conditions of 47^{o}F and 17^{o}F outside temperature with an indoor temperature of 70^{o}F[2]. This rating method enabled all heat pumps to be compared on a common basis. However, there was no provision

for comparing heat pumps on a seasonal energy basis, which would include cycling, frosting, and defrosting losses.

During the mid and late 70's the National Bureau of Standards(NBS)[3] conducted extensive tests on residential heat pumps. Their tests revealed two transient effects that significantly degrade heat pump performance: (1) cycling effects and (2) frosting effects on the outdoor coil. The NBS work led to the development of a new rating procedure that includes transient losses due to both cycling and frosting/defrosting losses. Several researchers have run experimental tests on heat pumps to determine the amount of degradation caused by transient characteristics. Baxter, et al[4], arrived at the degradation factor from cycling and frosting/defrosting of 20% and suggested it could be as high as 40% in warm weather. Wildin, et al[5], arrived at losses from defrosting of 2 to 5%, while Goldschmidt and Hart[6] found losses of 5% for cycling and less than 3% for frosting. Finally Bittle and Goldschmidt[7] found a 1 to 2% loss factor from frosting and a 2 to 17% loss rate for cycling. There is a wide variation in results. Bittle[7] concluded that the contradictions in the available data can not be resolved without more information on data from each of the individual investigations.

TRANSIENT PERFORMANCE

A typical heat pump heating cycle during startup, frosting, defrosting, and defrost recovery spends very little time in steady state. The performance approaches steady state for short periods, but its overall operation is far from steady state. Baxter and Moyers[8] monitored a residential unit for eight winter months and were able to break down the seasonal energy consumption into the separate steady state and transient components of the heat pump cycle as shown in Table 2.1.

Table 2.1. Breakdown of Seasonal Energy Use in the Air-to-Air Heat Pump [8].

Condition	% Energy Use
Steady state	74.3
Transient state	25.7
* Defrost cycle w/o temp.	10.2
* Cycling (Start-up)	8.5
* Frosting of coil	3.7
* Off-cycle parasites	3.3

They showed that over 25% of the energy used for heating the house was used during transient conditions when the heat pump performance was low.

CYCLING LOSSES

Efficiency losses occur in a heat pump during startup and shutdown. Examining the sources of losses during startup may provide some understanding of the losses that occur during the defrost cycle after the reversing valve has been engaged.

One of the major variables affecting these losses is the location of the refrigerant in the system either right before startup or shutdown. When a heat pump in running at steady state, the refrigerant is not equally distributed throughout the system. The location of the refrigerant depends on the outdoor and indoor ambient conditions, the amount of refrigerant charge in the unit, and the components used in the system. For instance, in the heating mode for those units containing a suction line accumulator, some investigators have found that over 60% of the refrigerant is located in the condenser and accumulator[9],[10].

As the unit shuts down, the pressure is allowed to equalize through the compressor and the TXV. During the winter months the outdoor coil is much colder than the indoor coil so most of the refrigerant migrates to the outdoor coil. A recent study by Mulroy indicated that when the unit is restarted the refrigerant fills the accumulator

and is trapped there as the accumulator slowly dispenses it back into the system[11]. He concluded that[11]:

> "...for units allowing migration of refrigerant during the off-cycle and which have accumulators, the primary source of cyclic performance loss after the first minute of operation is the result of refrigerant being trapped in the accumulator. The [heat pump] unit will not reach steady state until the accumulator level has been reduced to its steady state value..[Page 815-6]"

Mulroy's results indicated that during the summer, the warmer outdoor temperatures help boil off the refrigerant from the accumulator[11]. However, during the heating season, the colder outdoor temperatures cause the unit to take over 20 minutes before it reaches steady state after startup. Because the accumulator can store a relatively large mass of refrigerant, it effectively creates a thermal lag in the system during startup.

Mulroy[11] eliminated all cycle migration by installing solenoid valves in the refrigerant lines. By eliminating refrigerant migration during the off cycle, the unit was able to reach 90% of capacity in about 3 minutes instead of close to 15 minutes when migration was allowed. Young[12] recommended a heat exchanger be attached to the accumulator that would draw heat from the liquid line before the expansion valve and speed up the transient process. A reduction in system volume will also speed up the transient

response of the unit as there will be less refrigerant trapped in the accumulator[11].

FROSTING LOSSES

The only reason a heat pump undergoes a reverse cycle defrost is to eliminate frost that has built up on the outdoor evaporator during heating operation. To extract heat from the outdoor air, the outdoor coil must be at a lower temperature than the outdoor air. If the temperature of the coil is below the dew point of the outdoor air and also below 32^{o}F, then moisture will condense on the coil and freeze. As the frost builds on the coil, the pressure drop across the coil increases and the frost acts as an insulating layer between the cold heat exchanger surface and the relatively warm, moist air. As the pressure drop increases, the airflow produced by the outdoor coil propeller fan decreases. This decrease in airflow reduces the capacity of the evaporator and the capacity of the heat pump. Eventually, the performance of the heat pump is reduced enough that the unit must be defrosted to return the heat pump to peak performance.

Miller[13] found the conditions that will promote frosting of the outdoor coil are when the outdoor temp is between 17°F and 40°F and the relative humidity is greater then 70%. He showed typical results of heat pump performance during frosting conditions. At outdoor conditions of 35°F DB, Miller found that frosting was not evident until the humidity rose to 70% RH and then the frosting rate steadily increased with humidity.

DEFROSTING LOSSES

Frost accumulation on the outdoor coil of the heat pump degrades it's performance by insulating the coil and reducing the airflow through the coil. Restoring the heat pumps performance is accomplished with the use of a reverse cycle defrost. The reverse cycle defrost is a procedure that switches the condenser and the evaporator from the heating mode where the outdoor coil is the evaporator to the cooling mode where the outdoor coil is now the condenser. The hot gas which was being pumped into the indoor coil to heat the house is now, during the defrost cycle, pumped into the outdoor coil to melt the frost off of the coil. When the ice is melted from the outdoor coil the heat pump is switched back to heating and resumes normal operation.

During the defrost cycle, the heat pump removes heat from the house to melt the ice on the outdoor coil. This cooling effect must be offset by resistance electric heaters which are mounted in the indoor air handler. The electric heaters have a COP of 1, which is less than half as efficient as the heat pump so the overall COP of the heat pump decreases. Thus, the fewer times and more efficiently the unit can be defrosted, the less energy will be consumed during the defrost cycle.

A recent study on defrost cycle losses was conducted by Young[12]. One of the purposes of his study was developing an "efficient and dependable means of defrosting the outdoor coil..p.671"[12]. He conducted tests on two specially constructed heat pumps. Some of the features of the first heat pump included:

* Nominal heating capacity of 2.5 tons,
* Outdoor coil had fin density of 8 fins/inch,
* Outdoor fan was 3 blade propeller unit, belt driven,
* Electric expansion valve in heating mode,
* Outdoor coil was horizontal,
* Defrost cycle refrigerant control: capillary tubes,
* Condenser outlet had receiver,
* Reversing valve: sliding port,

* Accumulator had heat exchanger (exchanged heat from the outlet of the condenser before expansion device),
* Compressor was indoors,
* Defrost initiation: Demand, based on outdoor fan current.

The second heat pump was a modified version of the first heat pump. The key modifications included:

* Larger compressor (2.75 tons vs. 2.25 tons),
* Outdoor fan was 4 blade propeller unit, direct drive,
* Outdoor coil was at 45°F angle,
* Defrost cycle refrigerant control: large orifice valve,
* Reversing valve replaced with four solenoid valves.

Young claims that an accumulator heat exchanger enhances the transient response of the heat pump following defrost reversal or system startup[12]. However, nowhere in his paper is data provided on how much it improves the transient response of the unit during the defrost cycle. Data on how much faster the accumulator empties, effect on defrost time, energy use, etc. would have been useful. This may be one area for further investigation.

An important piece of equipment affecting the length of the defrost cycle in Young's study was the defrost cycle

expansion device. By installing a larger defrost orifice than the normal cooling mode capillary tubes, he was able to produce a 30% reduction (almost 1 minute) in defrost cycle time[10]. Young did not give any data on the size of the capillary tubes or orifice he used. The larger orifice almost eliminated the suction pressure drop at the beginning of the defrost cycle and allowed a higher mass flow rate and heat delivery to the outdoor coil. He recommends the installation of a separate expansion device for reverse cycle defrost rather than using the cooling mode device.

Young also found that the common sliding port reversing valve degraded the performance of his first heat pump by as much as 10%. These losses occur from both heat and mass leakage from the high side to the low side of the system. It was not apparent from the study whether this valve was exceptional or typical of reversing valves. He was able to eliminate the losses by installing multiple solenoid valves in the second heat pump.

For the heating mode, Young[12] used an electric expansion device that was opened wider during the recovery period following defrost. This shortened the recovery time to steady state by 50%.

Both of the units that Young tested were significantly different than most heat pumps currently found on the market. For instance, one unit had a horizontal outdoor coil and the other had a 45 degree angle tilt. Most manufacturers use a vertically mounted outdoor heat exchanger. This difference means that his units probably drain water from the melted frost faster than current models. His outdoor coil had only 8 fins/inch which is significantly less than the 14 to 19 typically found on units sold today. Because of the wider fin spacing, one would expect Young's units to go longer before defrosting. Thus, it appears that caution should be used when trying to extend his results to units currently made by many U.S. manufacturers.

Young's paper provided some excellent ideas on ways to improve performance during the defrost cycle. However, in general he did not quantify how each piece of hardware affected system dynamics during the defrost cycle.

Another recent study of the heat pump reverse cycle defrost was published by Miller[10]. His purposes included: (1) gaining a better understanding of the physical processes that occur during the frost/defrost cycle and (2) quantifying the losses during the cycle. All of Miller's

work was conducted on a single heat pump whose characteristics included:

* 2.75 Ton nominal capacity,
* Split system,
* Plate fin heat exchanger,
* Liquid line- suction line heat exchanger (only active during heating cycle)
* Suction line accumulator,
* Outdoor coil fin density of 14 fins/inch,
* Demand defrost initiation (based on 0.51 inches WG pressure drop across the outdoor coil),
* Capillary tube expansion during defrost cycle and heating mode,
* Indoor coil is A-frame style with 3 tube rows,
* Sliding port reversing valve.

Miller collected system data such as instantaneous capacity and power as well as component data such as instantaneous temperatures and pressures at different locations throughout the system. While he collected data at a variety of outdoor temperatures and humidities, most of his published frosting/defrost data is at an outdoor air temperature of 35^{o}F and relative humidity of 70%. While the data at those conditions may be useful from a qualitative perspective, it would have been more useful if data had been

published for the DOE/ARI heavy frosting tests which are at 35°F and 80% relative humidity. Another possible limitation of his data is that the unit used capillary tubes for the expansion device. Capillary tubes are more common on older heat pumps. However, many of the units currently manufactured use either thermal expansion valves or orifices.

For the 35°F, 70% relative humidity conditions, Miller's heat pump ran approximately 2 hours before defrost was initiated[10]. His defrost cycle lasted approximately 7 minutes. At defrost initiation, Miller estimated that 50% of the refrigerant was in the indoor coil. However, he based this estimate on previous steady state weight measurements and not measured immediately before defrost initiation. Also, conditions were not specified for his previous weight measurements. Pressure measurements across the capillary tubes indicated that there was no refrigerant flow in the system for approximately 1.5 minutes after defrost initiation. The units capacity dropped close to zero in the first 30 seconds, then increased about 4000 Btu/hr for approximately a minute, then decreased until reaching a maximum cooling capacity at 6.5 minutes. He stated that after 30 seconds of defrosting, the indoor coil held only low-pressure vapor. Miller's unit took

approximately 5 to 6 minutes to completely melt the frost from the outdoor coil.

While he published the temperature exiting the outdoor coil, it is not clear from his paper whether this temperature is the average of all the circuits leaving the coil, or the temperature of the circuit used to determine when defrost should be terminated. Some manufacturers will monitor the temperature on a specific circuit (usually the bottom) on a coil to determine when the defrost cycle should be terminated. For Miller's unit, defrost was terminated when the exiting refrigerant temperature from the outdoor coil reached 75^{o}F

Trask[14] recommends taking the accumulator out of the line between the reversing valve and compressor and mounting it between the reversing valve and the outdoor coil. A check valve mounted at the accumulator would channel the refrigerant through the accumulator in the heating mode, but upon defrost initiation, the hot gas would bypass the accumulator and go directly into the compressor. He claims this would keep the refrigerant from being cooled down by the accumulator and allow more heat directly into the outdoor coil. As the pressures in the indoor coil drop below 40 psi, Trask recommends using a constant pressure valve to bypass the cooling TXV allowing refrigerant to flow

freely to the indoor coil. Trask claims the valve would help prevent the large accumulation of refrigerant in the outdoor coil and the subsequent flushing of refrigerant into the accumulator.

Currently, there are two basic methods of controlling when and how long the heat pump is in the defrost mode[15]. These methods are the time-temperature defrost control and the demand defrost control. The time-temperature defrost control is energized when the entering refrigerant to the outdoor coil drops to approximately 30^{o}F. When energized, a timer which can be set for 30,45, or 90 minutes is started and the unit will defrost after each timer interval. After energizing the defrost cycle, the control senses the leaving refrigerant temperature and terminates the cycle when it rises to approximately 65^{o}F or after ten minutes whichever comes first.

The second control is the demand defrost control which senses the unit's operating conditions and initiates defrost when the conditions indicate heavy frosting. A common demand defrost control monitors the ambient outside air temperature and the outdoor coil temperature. The manufacturer runs tests on a certain unit and monitors the combinations of air-coil temperatures that occur when defrosting is required. This information is programed into

the control and defrost is initiated when those conditions are met. Termination of the cycle is accomplished in the same manner as the time-temperature defrost.

Baxter and Moyers[8] monitored a residential heat pump with time-temperature defrost controls for two years. They used the temperature and humidity frosting criteria developed by Miller[13] to track the total number of unit defrost cycles and how many of the cycles occurred when there was potential for frosting. The results of their survey showed that 27% of a total of 665 defrost cycles occurred when no frost was on the coil. Baxter and Moyers recommended using demand defrost to cut down on the useless defrost cycles.

SUMMARY OF LITERATURE REVIEW

There are many system components and operating conditions that affect the transient characteristics of a heat pump. The suction line accumulator, because of its ability to store large quantities of refrigerant, apparently slows down the startup process. The result is larger transient losses in the system. From the visual observation made by Miller[10], much liquid refrigerant is contained in the accumulator immediately after the reverse cycle defrost. With the accumulator full of refrigerant, the heat pump

remains undercharged until the refrigerant is fed back into the system[11]. By the addition of a heat exchanger in the accumulator, Young claimed a reduction in time to get the refrigerant out of the accumulator[12]. The accumulator (or lack of one) appears to be one area for possible further investigation.

Another system component that appears to have a significant effect on performance during defrost was the defrost cycle expansion device[12,14]. In particular, Young found that increasing the expansion device size decreased the defrost time. Miller's unit, which had capillary tubes, experienced no refrigerant flow for approximately 1.5 minutes after defrost initiation. This condition could possibly be due to the size of the capillary tubes. A systematic study of expansion device size and its effect on system performance should be performed.

Two significant limitations to the work published to date are: (1) the uniqueness of each experiment and (2) the general lack of adequate documentation to be able to reproduce the researchers experiment. Young's[12] experiments were conducted on "prototype" laboratory constructed heat pumps. The components (8 fin/inch heat exchanger, liquid receiver, etc.) were constructed in such a manner that they were not typical of current practice in the

industry. Unfortunately, even an experiment conducted on a unit more typical of what is currently sold on the market would have unique features that were installed by the manufacturer of the unit. For instance, an experiment on a unit with a suction line accumulator would provide results that may differ from the performance of units that do not use an accumulator. This factor would point toward the need for a series of experiments that would include multiple units having features used by a majority of industry. This type of study would provide results to separate trends that are equipment specific and those that are generic to the defrost cycle.

The second limitation was mentioned several times in discussing results from various researchers. If a researcher does not adequately document his experiment, it makes it difficult for the next investigator to compare results. Bittle[7] was cognizant of the lack of documentation as she attempted to explain the large variation in results from different investigators.

CHAPTER III

EXPERIMENTAL APPARATUS

The objective of the experimentation is to collect accurate data on the transient characteristics of an air-source heat pump during the frost/defrost cycle. The data includes pressures and temperatures throughout the system, power consumption, and refrigerant and air flow rates. A testing apparatus was constructed that would allow measurement of important performance parameters and provide flexibility so the heat pump system could be modified without losing unit charge. Modifications of the apparatus included changing the expansion devices and the compressor.

The heat pump testing apparatus and testing procedure are described below.

GENERAL DESCRIPTION

The test apparatus is located in the psychrometric rooms of the Energy Systems Laboratory at Texas A&M University Research Annex. The general layout of the test apparatus is given in Figure 3.1. The psychrometric rooms

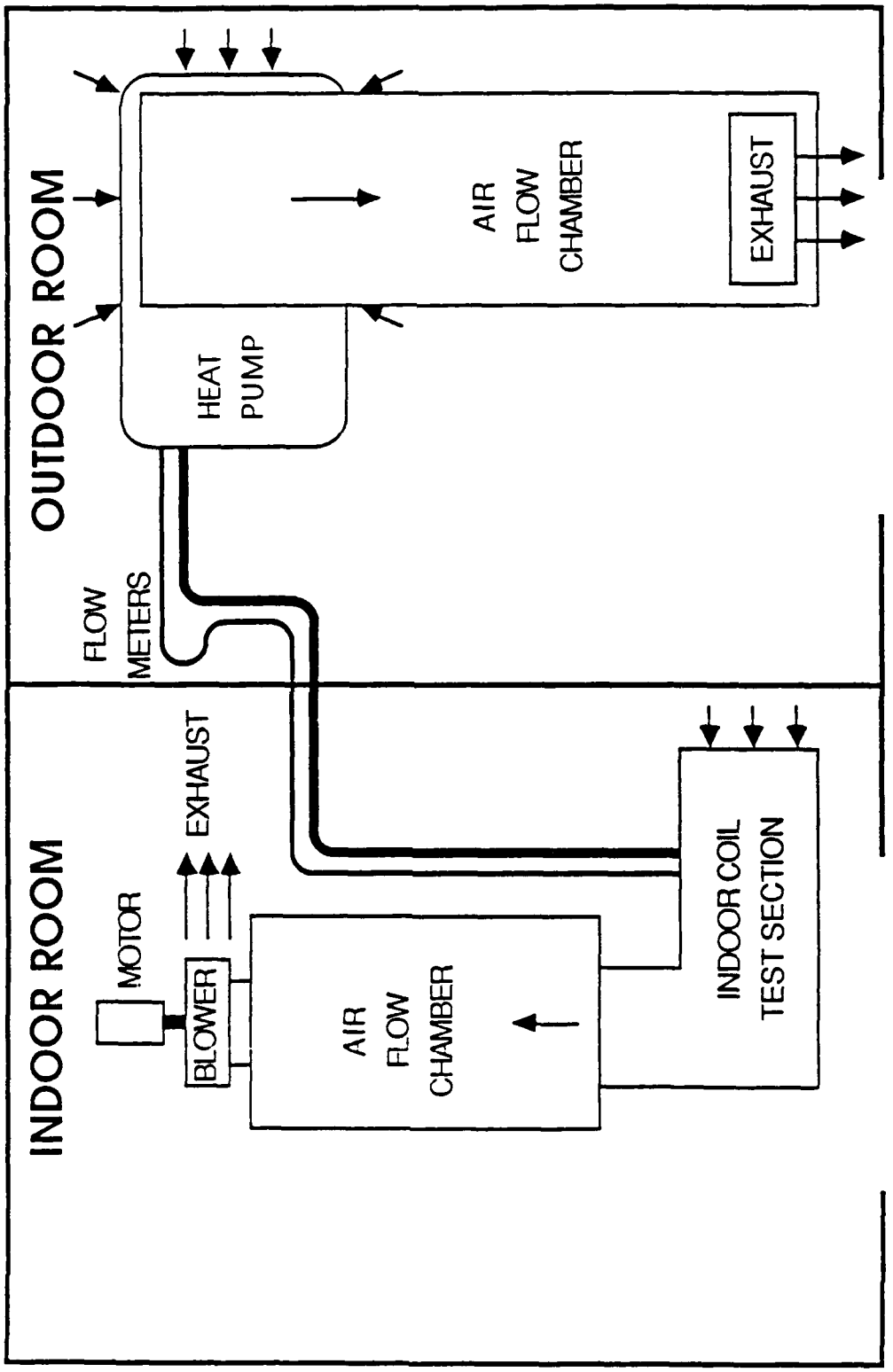

Figure 3.1. General Layout of Test Setup.

simulate the indoor and outdoor conditions (temperature and humidity) necessary for heat pump performance testing.

The indoor test section consists of the indoor coil and the indoor air flow chamber. Conditioned air from the indoor room at 70°F DB and 20% relative humidity(RH), is drawn through the indoor test section by the air flow chamber fan. The air flow chamber, which is used to measure the air flow through the test section, has a damper mounted on the outlet that is adjustable and is set to maintain a constant air flow of 1200 cfm through the indoor test coil. The air is routed back into the indoor room after leaving the chamber.

The outdoor test section consists of the compressor, accumulator, outdoor coil, and outdoor air flow chamber. The conditioned outdoor air at 35°F DB and 30°F DP, enters the outdoor coil and is exhausted by the unit fan into the air flow chamber. Air flow is regulated to maintain zero static pressure at the chamber entrance by a set of dampers located in the airflow chamber. The air is then exhausted back into the room.

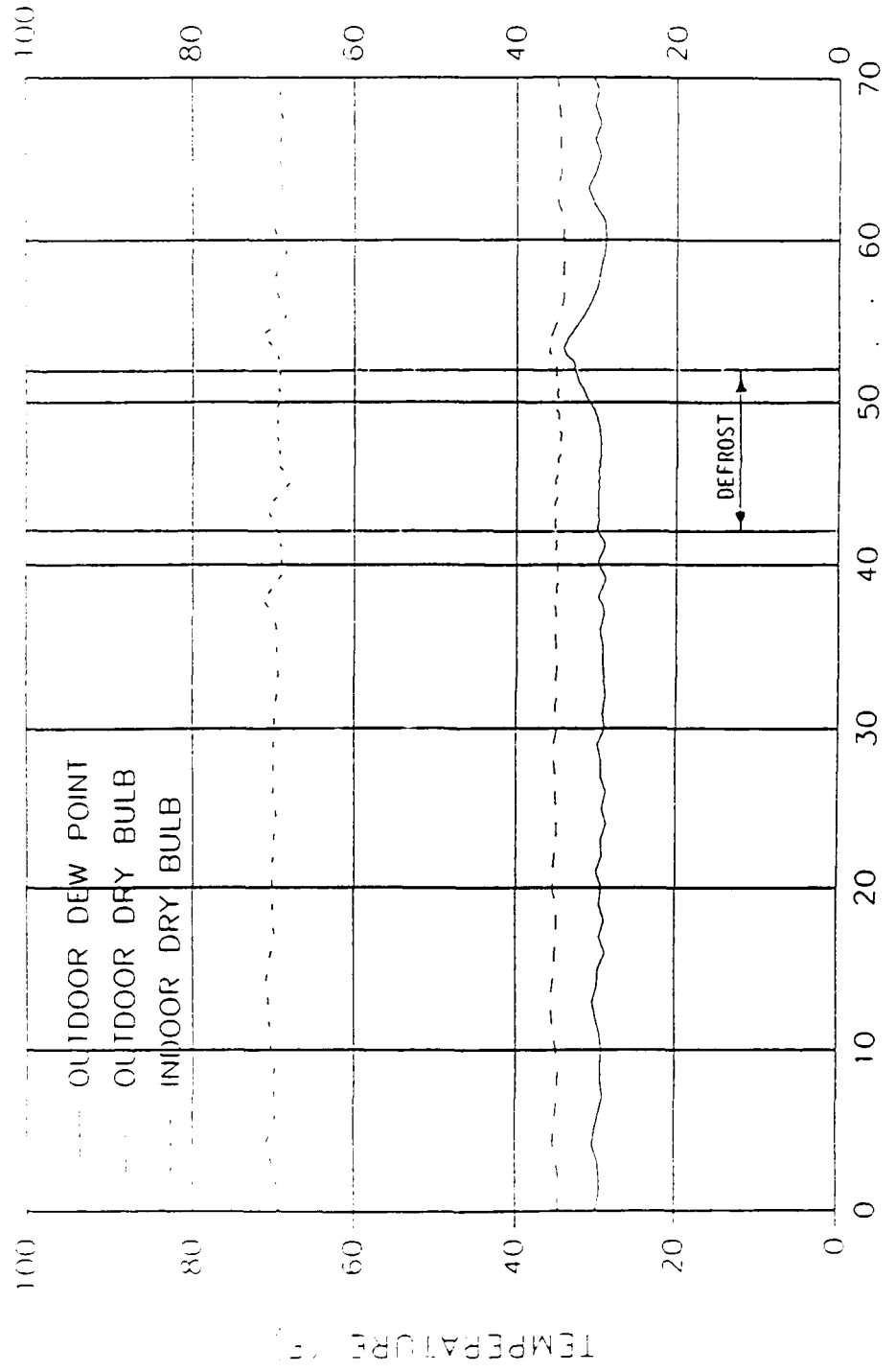

Figure 3.2. Temperature and Humidity Variations in Psychrometric Rooms.

PSYCHROMETRIC ROOMS

The psychrometric rooms can simulate all testing conditions required for air-conditioning and heat pump performance testing. Dew point and room temperatures can be maintained within $1^{\circ}F$ of the set point. Variations of the temperature and dew point in the outdoor room and temperature in the indoor room during a typical frost/defrost cycle are shown in Figure 3.2. The rise in the dew point during the defrost cycle at 50 minutes is caused by the vapor from the warm coil. The dew point sampler is located next to the coil and it picks up the vapor from the coil generated toward the end of defrost. This is a local effect, and room conditions are still well within tolerance.

Room temperatures are maintained with chilled water coils and electric resistance heaters. The chilled water coils are fed with an ethylene glycol solution that is chilled by a 105 ton capacity chiller. A 300 gallon chilled water thermal storage tank is mounted in the chilled water system to stabilize chilled water temperature. There are four banks of electric heaters in each room with 9900 watts per bank.

Humidity levels in the rooms are controlled by electric humidifiers and dehumidification coils. The dehumidification coils are fed from the same circuit as the cooling coils. The humidifiers are mounted in each room and supply steam directly into the supply air duct.

TESTING CONDITIONS

The testing conditions used for the frost/defrost tests are those prescribed for the frost build up test in the Department of Energy(DOE) - Test Procedures for Central Air Conditioners, Including Heat Pumps(1979)[16]. The entering dry bulb temperature for the outdoor coil is 35°F(+/- 1° during the heating cycle and +/- 2° during defrost) with a dew point temperature of 30°F(+/- 1°). This corresponds to a relative humidity of approximately 80%. The indoor conditions are 70°F DB(+/- 1°) with a maximum wet bulb temperature of 60°F. For this testing the wet bulb temperature in the indoor room is maintained at approximately 52°F.

The outdoor conditions for the frosting/defrosting cycling test were selected because of the rapid frosting of the outdoor coil at these conditions. Miller's[13] research agrees favorably with these test conditions. The indoor

conditions of 70°F DB and less than 60°F WB were chosen to eliminate any condensation on the indoor coil during the reverse cycle defrost. This means the dew point of the air will remain constant as it passes through the indoor coil.

INDOOR TEST SECTION

The indoor test section is shown in Figure 3.3. Conditioned air flows through a set of straighteners(A) as it enters the section. A 16 element thermocouple grid(B) is then used to measure the temperature of the entering air before it proceeds into the coil(C). After leaving the coil the air flows through two sets of mixers(D) and another set of straighteners(E). Its temperature is then measured by a second 16 element thermocouple grid(F).

The indoor coil has vertical plate fins at 12 fins per inch with 17 passes and four rows of 3/8" copper tubing divided into four refrigerant circuits. The coil is 30"x18" and has a rated capacity of 3 tons.

After leaving the test section the air is drawn into an AMCA 210, Figure 15 flow chamber[17] where the air flow is measured. The chamber contains four ASME air flow nozzles(one-8",two-5",one-3") that can be used in any

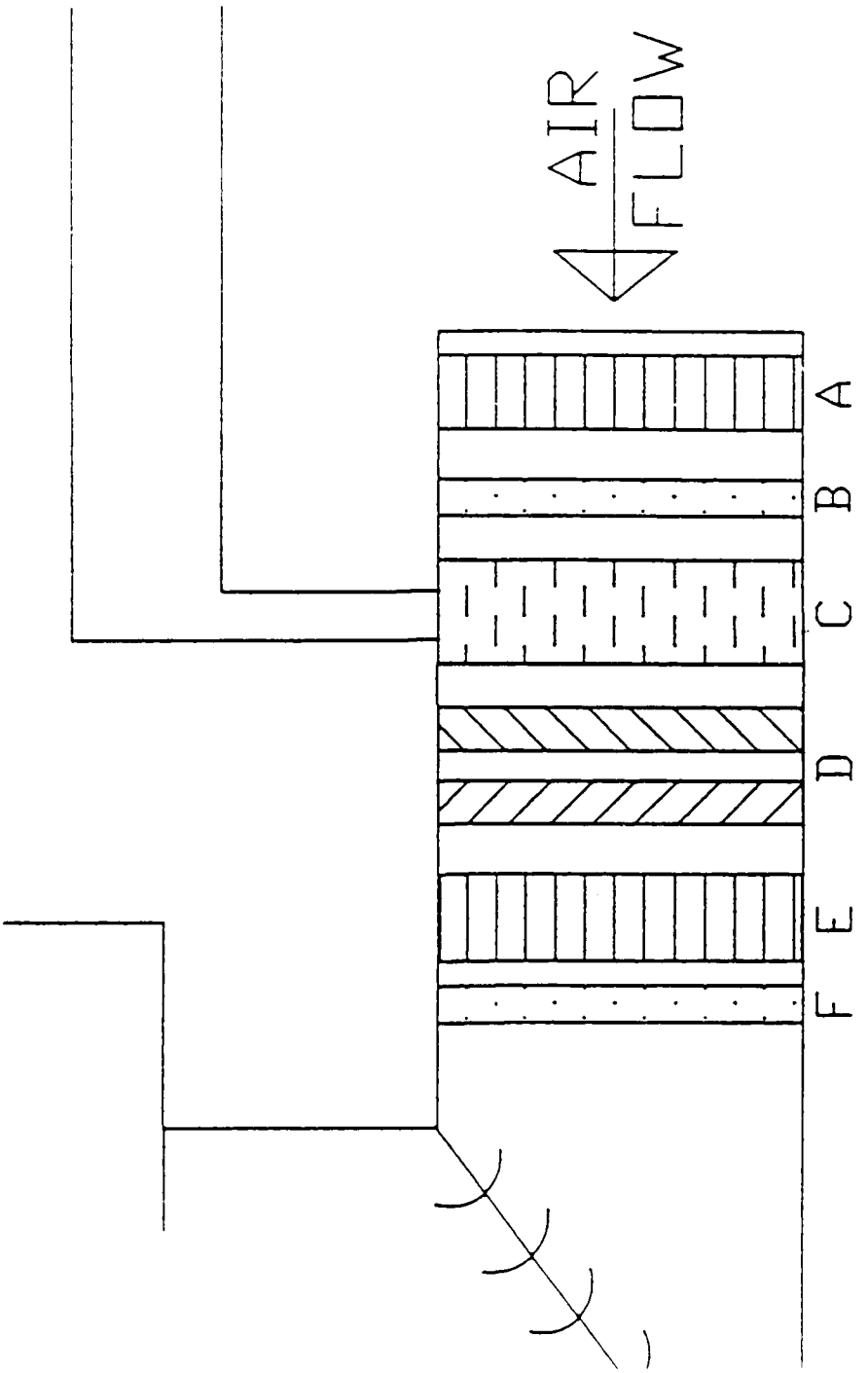

Figure 3.3. Detail of Indoor Test Section.

combination to accurately measure a flow range of 100 to 5000 cfm[17]. A booster fan mounted on the end of the chamber provides the air flow through the setup. The air flow is adjusted by operating a set of dampers mounted on the fan outlet. For the frost/defrost test, two 5" nozzles are used in the chamber to achieve a pressure drop of 1.3" WG which is equivalent to 1250 cfm through the indoor test coil.

OUTDOOR TEST SECTION

The outdoor test section(Figure 3.4) includes the outdoor air flow chamber and the outdoor portion of the heat pump(compressor, accumulator, reversing valve, and outdoor coil).

The three ton compressor supplied with the heat pump was installed in the base case setup. An accumulator with sight glasses mounted in the shell was used instead of the accumulator supplied with the heat pump since it provided a method of visualizing refrigerant flow in the system.

A two row, U-shaped coil is used for the outdoor heat exchanger. The coil has thirty passes per row with four separate refrigerant circuits. The coil fins are wavy with

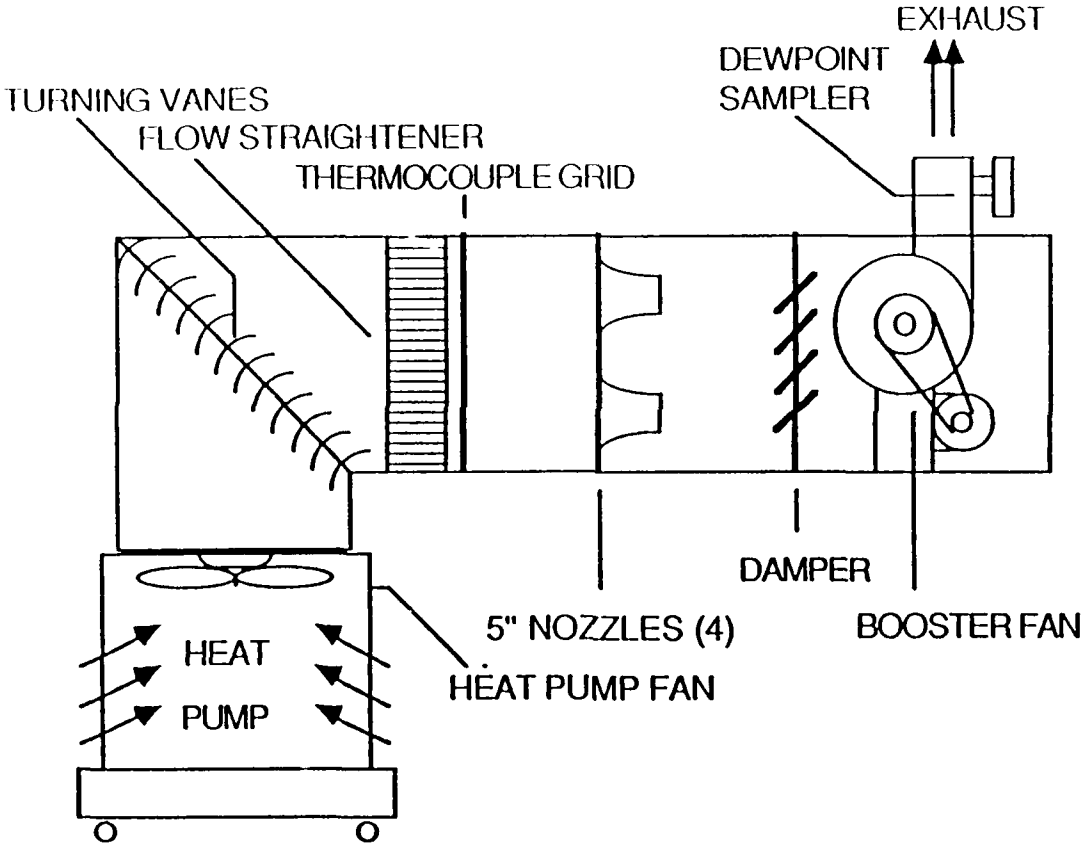

Figure 3.4. Elevation of Outdoor Test Section

a fin density of 20 fins per inch. The face area of the coil is approximately 18.3 ft^2. A sheet metal pan is mounted under the coil and is sloped so the melted frost will drain into a collection pan during and after the defrost cycle.

The outdoor air flow chamber is used to monitor the air flow through the outdoor coil by measuring the pressure drop as the air passes through four 5" ASME flow nozzles that are mounted in the duct. A pressure drop of 1.15" WG is equivalent to 2300 cfm through the outdoor coil[17]. The temperature and dew point of the air leaving the outdoor coil is measured in the chamber by a 9 element thermocouple grid and a dew point sensor.

Correct air flow through the outdoor coil is regulated by manipulating the damper mounted on the inlet side of the chamber booster fan. The static pressure at the entrance to the air chamber (outlet of the outdoor unit) is maintained at zero during the testing. This simulates free flow conditions on the outdoor fan and lets the heat pump fan maintain the airflow through the coil.

To accurately measure the dew point temperature, the dew point sensors must be mounted in an air stream of 500 to 3000 fpm. An air sampler was constructed to sample the air

entering the outdoor coil. The sampler, which is pictured in Figure 3.5, is made of PVC pipe that wraps around the outdoor coil approximately 6 inches from the coil surface. Holes in the pipe are evenly spaced around the coil on the side of the pipe facing away from the coil. The hole sizes range from 3/8" at the ends of the sampler to 1/8" at the entrance to the sampler fan. This allows for the lower suction at the ends of the sampler and will provide more accurate air sampling. The fan draws air through the holes in the pipe and into a channel where the dew point sensor is mounted. The air flow in the channel is approximately 2000 fpm which is within the operating range of the sensor. The leaving dew point temperature is measured by mounting the dew point sensor in the air chamber outlet. The air flow across the second dew point sensor varies with the airflow through the coil. However, it stays within the allowable range of the sensor when the fan is in operation.

REFRIGERANT CIRCUIT

A schematic of the refrigerant circuit is shown in Figure 3.6. Refrigerant pressures are monitored at the 10 points shown with the use of 0-300 psig pressure transducers. To accurately measure the refrigerant

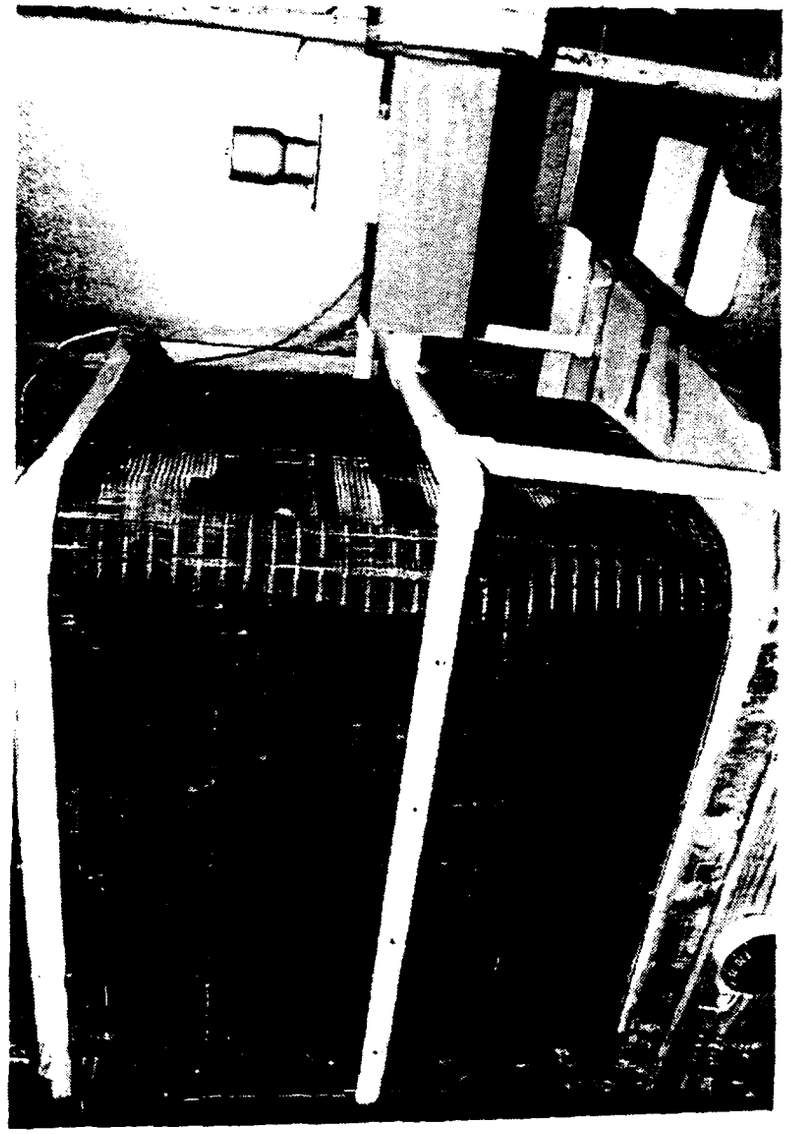

Figure 3.5. Outdoor Coil with Dew Point Sampler.

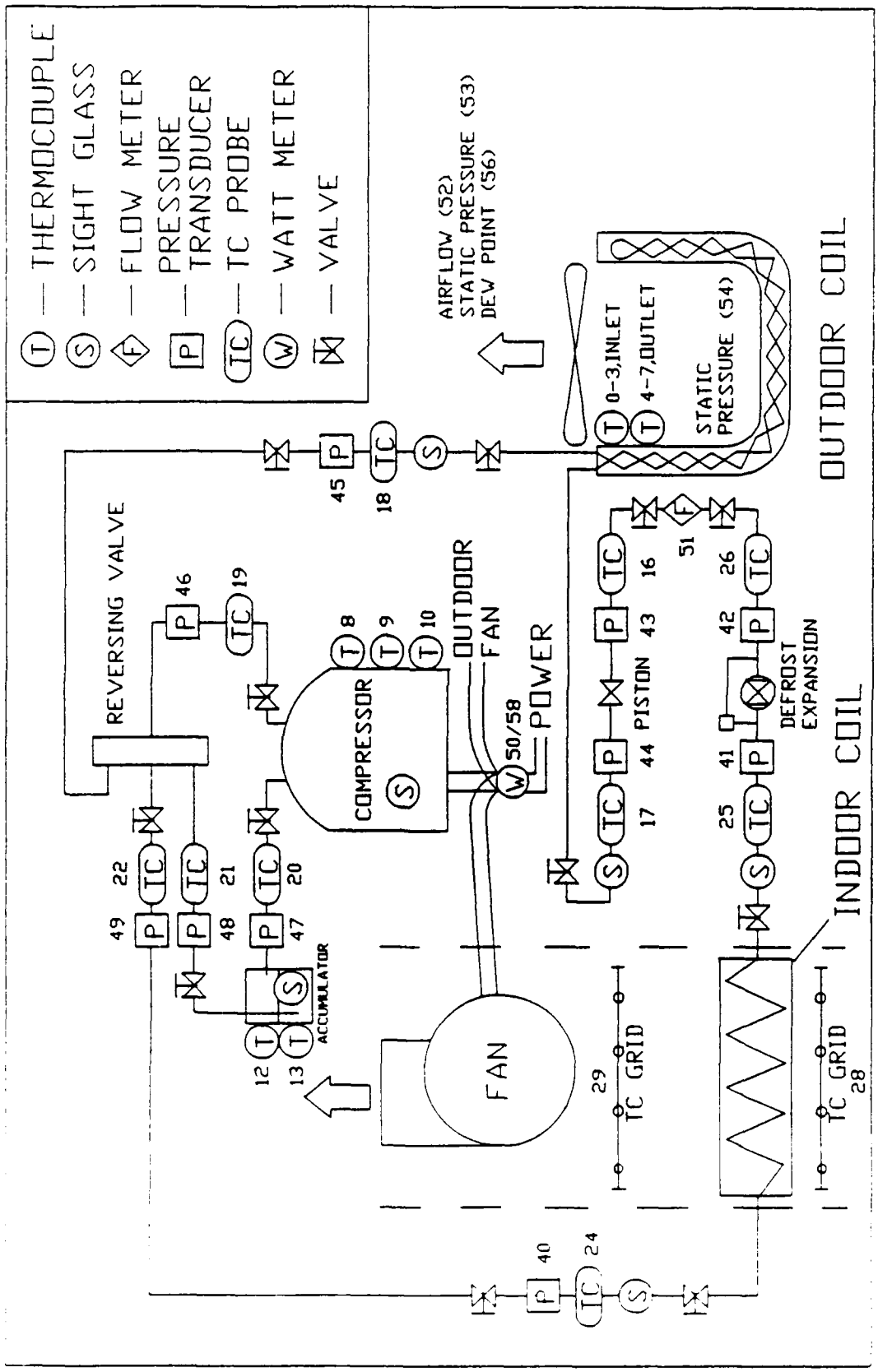

Figure 3.6. Schematic of Refrigerant Circuit.

temperatures and reduce the conduction effects of the copper tubing, thermocouple probes were installed in the refrigerant lines(Figure 3.7). The probes are thin (1/16" dia.) and mounted far enough into the flow of the refrigerant(approx. 8 diameters) that any conduction effects from the tube surface will be minimal.

Refrigerant flow is measured with two mass flow meters mounted in parallel. The flow meters measure mass flow according to the Coriolis principle as the refrigerant flows through a U-shaped tube. The flow rate through the meters varies from 0 to 10 pounds per minute with a pressure drop at the maximum flow rate of approximately 10 psi. This is within the standards of ASHRAE 116-1983 which establishes a maximum pressure drop equivalent to a $3^{o}F$ temperature change[18]. At the testing conditions a $3^{o}F$ temperature change is equivalent to a 12 psi pressure drop.

As mentioned in the objectives, a major consideration to the refrigerant system design was the ability to change expansion devices, the compressor, or make other adjustments to the system without losing the refrigerant charge. This is accomplished with the use of ball valves mounted around all sections of the refrigerant circuit that might need to be isolated. This has proven extremely effective in

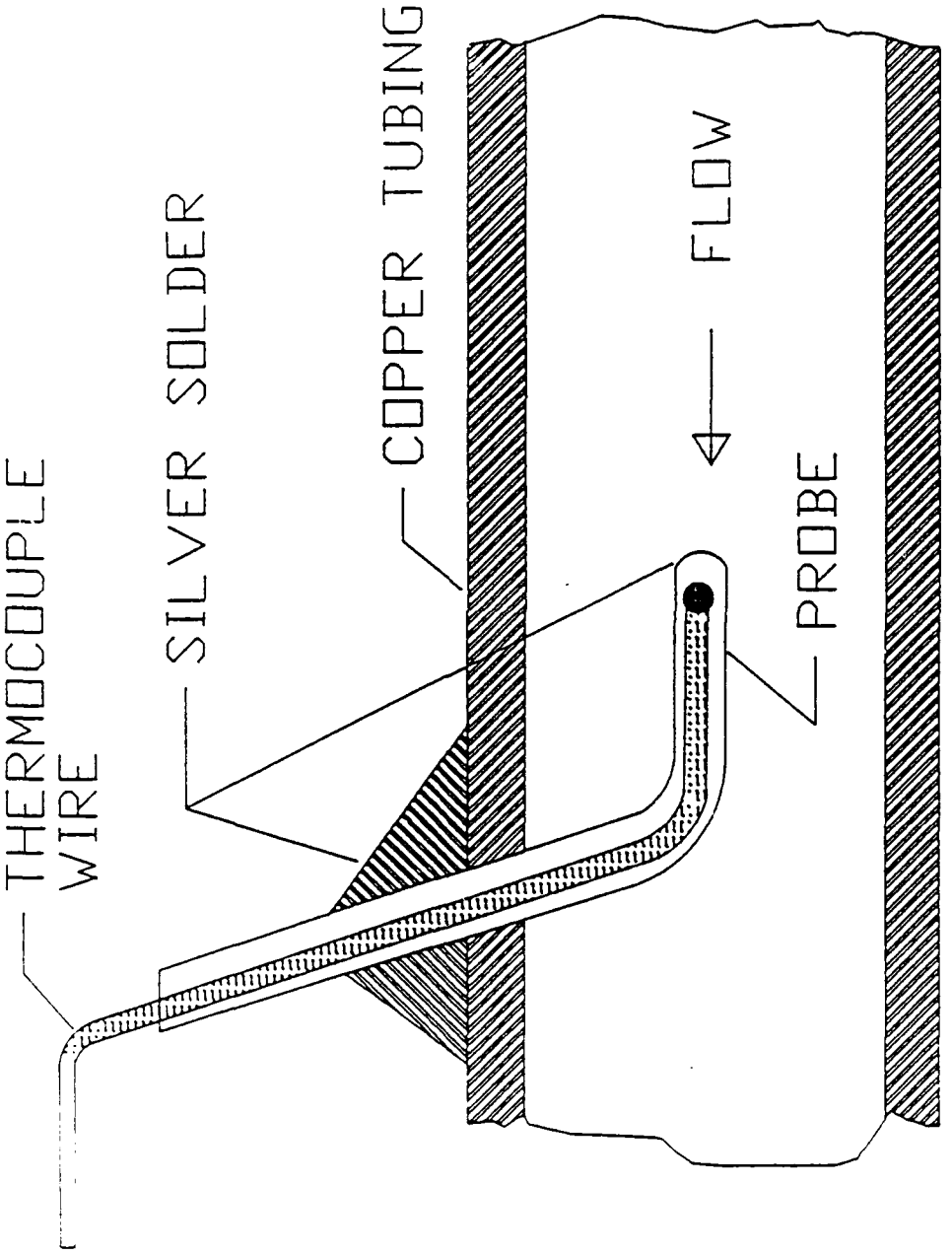

Figure 3.7. Refrigerant Temperature Probe.

changing out components and also in identifying refrigerant leaks. The valve locations are shown in Figure 3.6.

The ability to change expansion devices during the testing sequence without losing the testing charge was made possible by mounting expansion devices and a bypass line in parallel(Figure 3.8). Ball valves are mounted in each of the four lines and any of three expansion devices can be selected without shutting down the heat pump. The base case TXV is not changed out because it must be in line to set the charge. During testing, the system charge is set with the base TXV and then either of the other two expansion devices, one TXV and one orifice, can be valved into the line during the run, between defrost cycles. This saves many hours of testing time as it takes over six hours for the system to attain a steady state mode of frost/defrost cycling.

SYSTEM CONTROLS

The controls for the heat pump are located in the psychrometric room control room. The heat pump can be energized in either the cooling or heating mode. During the heating mode, the reversing valve and the outdoor fan are controlled separately for manual variations in the defrost cycle, or the automatic defrost control supplied with the

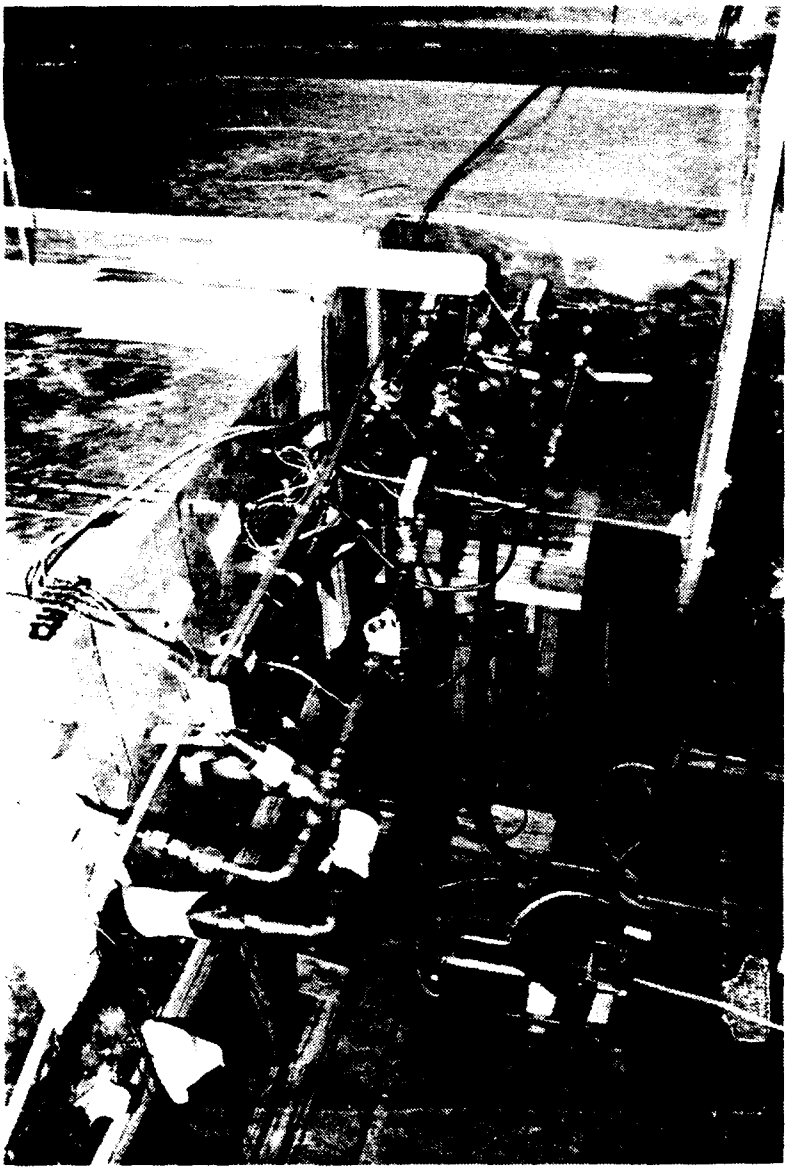

Figure 3.8. Defrost Expansion Devices, Mounted in Parallel.

test heat pump can be energized if desired. The outdoor air chamber damper is also controlled from the control room by varying the voltage input to the hydraulic actuator mounted on the side of the duct.

DATA ACQUISITION

A data logger was used to collect data from the testing apparatus. The data logger reads up to 65 data points at a maximum scan rate of approximately 8 seconds. An IBM PC compatible computer was used to store the data on a 10 megabyte hard drive. All data were transmitted to a mini-computer for analysis and backed up on floppy disks. A description of the data points is given on Table 3.1. The channel numbers in Table 3.1 correspond to the numbers in the schematic of the test setup in Figure 3.6.

One series of tests with the heat pump running continuously lasted approximately 36 hours. This could not be monitored with one continuous scan so the scans were terminated at 15 minutes after the defrost termination. This was at a period when the heat pump was running at near steady state conditions. One minute scans were used for the period outside the defrost cycle and 10 second scans were used during the defrost cycle. The 10 second scans were

Table 3.1 Description of Test Points

CHANNEL	TYPE	LOCATION
0-3	THERMOCOUPLE	OUTDOOR COIL - INLET (T to B)
4-7	THERMOCOUPLE	OUTDOOR COIL - OUTLET (T to B)
8-10	THERMOCOUPLE	COMPRESSOR - SURFACE (T to B)
11	TC-GRID	OUTDOOR ROOM
12-13	THERMOCOUPLE	ACCUMULATOR - SURFACE (T to B)
14	TC-GRID	OUTDOOR AIR CHAMBER
15	THERMOCOUPLE	CHILLED WATER TEMPERATURE
16-19	TC-PROBE	PROBE IN REFRIG. LINE
20-22	TC-PROBE	PROBE IN REFRIG. LINE
23		----NOT USED----
24-26	TC-PROBE	PROBE IN REFRIG. LINE
27		----NOT USED----
28	TC-GRID	UPSTREAM OF INDOOR COIL (16pt)
29	TC-GRID	DNSTREAM OF INDOOR COIL (16pt)
30-39		----NOT USED----
40-49	PRESSURE TRAN.	REFRIGERANT LINES
50	WATT TRAN.	208 VAC - 1 PHASE
51	FLOWMETER	REFRIGERANT LIQUID LINE
52	DIFF. PRESS.	OUTDOOR AIR CHAMBER (NOZZLES)
53	DIFF. PRESS.	OUTDOOR AIR CHAMBER (INLET)
54	DIFF. PRESS.	OUTDOOR COIL (PRESS. DROP)
55	DEW POINT SENS	UPSTREAM OUTDOOR COIL
56	DEW POINT SENS	DOWN STREAM OUTDOOR COIL
57	FLOW METER	IN PARALLEL WITH #51
58	WATTHOUR TRAN.	COMPRESSOR/OUTDOOR FAN

initiated 3 minutes before defrost initiation and continued to approximately 3 minutes after defrost termination.

REFRIGERANT CHARGING PROCEDURE

The proper refrigerant charge for the test setup was accomplished during the cooling mode. Charging in the heating mode was not considered because a large amount of refrigerant is stored in the accumulator during normal heating operation. Adding or removing charge during the heating mode would only raise or lower the level of refrigerant in the accumulator and wouldn't affect system characteristics. Though refrigerant charge is not critical during the heating mode, the charge will affect the defrost cycle as the unit switches to the cooling mode and the refrigerant is pumped into the outdoor coil to melt the frost.

Factory recommendations called for 14^{o}F of subcooling leaving the condensor(outdoor coil) in the cooling mode. The setup was charged to this level with the outdoor room at 95^{o}F DB and the indoor room at 80^{o}F DB and 57^{o}F WB. This prevented condensation on the indoor coil during the charging procedure.

EQUIPMENT

A complete listing of equipment used in the testing apparatus is given in Appendix A. All testing instrumentation was calibrated prior to data collection and the accuracies are also listed in Appendix A.

TESTING PROCEDURE

The first step in the testing session was to set or verify the unit charge at the room conditions mentioned previously. With the refrigerant charge set, the defrost expansion device to be tested was valved into position and the rooms were brought down to testing conditions. This took approximately two hours. Finally, with the rooms at testing conditions, the testing instrumentation was readjusted as necessary and the heat pump started.

After the heat pump was started, the outdoor airflow chamber was adjusted to zero static pressure above the unit. The outdoor chamber damper had to be manually adjusted throughout the frosting cycle as the air flow changed with varying levels of frost accumulation.

The defrost cycle was initiated manually when the capacity of the heat pump dropped by 20%. The capacity was calculated by measuring the temperature difference and airflow across the indoor coil. Defrost termination was also done manually when the bottom circuit temperature in the outdoor coil rose above 65°F. The outdoor unit fan and chamber fan were both turned off during the defrost cycle. These initiation and termination criteria were selected because they depict a common type of demand defrost control that is currently being used by the manufacturer of this heat pump.

The heat pump was run through 3 to 5 defrost cycles before it reached a point where consecutive defrost times and the amount of defrost water collected were repeatable. One or two cycles were run between test cases for the same reason. At least three consecutive tests were then run for each expansion device or defrost strategy.

As stated previously, the data scans were terminated 15 minutes after the defrost termination. At this time a new scan was begun for the next defrost cycle and the defrost water was collected and recorded. Collecting the water at this time had the advantages of allowing the water to completely drain into the collection pan and making a consistent time of collection for testing.

CHAPTER IV

THE BASE CASE DEFROST CYCLE

This chapter provides a detailed description of the frosting/defrost cycle for the base case test. A description of the base case defrost expansion device is presented first, followed by the overall performance of the heat pump using the base case expansion device and then a more detailed description of the refrigerant dynamics during the frosting/defrost cycle.

BASE CASE DEFROST EXPANSION DEVICE

To evaluate the effect of various expansion devices on the frosting/defrost cycle, a base expansion device was selected which would serve as a reference to compare the performance of other expansion devices. The expansion device used during the base case defrost cycle was a thermal expansion valve(labeled as TXV #57). In selecting TXV #57, nine TXVs of the same model and capacity were tested* for stroke response time. TXV #57 was selected as the base case

---

* Tests were conducted by the TXV manufacturer.

because it represented the average response time of the group. Table 4.1 provides a brief description of TXV #57.

Table 4.1. Charactersitics of Base Case Defrost Expansion Device - TXV #57.

ITEM	TYPE OR VALUE
NOMINAL CAPACITY	2 1/2 TON
STATIC SUPERHEAT	$6^{O}F$
SYSTEM SUPERHEAT	$10^{O}F$
INLET	3/8" SAE
OUTLET	1/2" SAE
BULB/TXV LINE	5 FEET
BULB FILL	STANDARD RESIDENTIAL A/C and HEATPUMP
PRESSURE EQUALIZATION	BLEED TYPE
CONFIGURATION	STRAIGHT THROUGH
MAXIMUM OPENING	0.0059 $IN.^2$
STROKE	0.024 IN.

OVERALL SYSTEM PERFORMANCE OF THE BASE CASE

Four operating characteristics are used to measure the overall base case performance using TXV #57 as the defrost expansion device. These parameters are the Coefficient of

Performance(COP), defrost cycle time, melt time, and drain time. The operating characteristics are averages taken from three consecutive test runs. The average deviations during the tests were +/- 1% for the COP and defrost time, while the deviation was +/- 2% for the melt and drain time.

Table 4.2 contains the four operating characteristics for the base case test.

Table 4.2. Heat Pump System Characteristics* for Base Case Test Using TXV #57.

DEFROST EXPANSION DEVICE	INTEGR. CYCLIC COP	DEFROST TIME (minutes)	MELT TIME (minutes)	DRAIN TIME (minutes)
TXV #57	2.26	8.06	4.22	3.83

* System characteristics are averages taken from three consecutive test runs.

The defrost time is the time from defrost initiation to defrost termination of the same cycle. For a more accurate comparison of the performance of different expansion devices, the defrost time was divided into two phases, the melt phase and the drain phase. The melt phase started at defrost initiation and ended when the frost on the outdoor coil was melted. As the melt time ended, the drain phase

started and lasts until the cycle is terminated and the melted frost was drained from the coil.

CALCULATION OF COP

The integrated cyclic COP is the ratio of the integrated heating output (measured at the indoor coil) over the integrated energy consumption. The integration is done over a complete frosting/defrost cycle which starts at the termination of the previous defrost and ends at the termination of the present defrost.

Heating output from the indoor coil was calculated using the air-enthalpy method found in ASHRAE Standard 116-1983[18]. In the air-enthalpy method, the instantaneous capacity of the indoor coil is calculated as follows:

$$\text{Capacity} = \frac{\text{cfm}}{v} \times (h_2 - h_1),$$

where

h_1 = Enthalpy of air entering indoor coil (Btu/lb),

h_2 = Enthalpy of the air leaving the indoor coil (Btu/lb),

cfm = cubic feet per minute of dry air passing through the indoor coil, and

v = specific volume of the air passing through the coil (ft^3/lb).

Values for h_1, h_2, and v were obtained from methods contained in the ASHRAE 1985 Fundamentals Handbook[19]. The airflow calculations were done using a method provided in ANSI/ASHRAE Standard 51-1985[17]. The instantaneous capacity is integrated over time during a complete frosting/defrost cycle to produce the cyclic heating output.

The energy consumption is the integrated value over time of the instantaneous power usage. A watt transducer is mounted in the heat pump which provided the instantaneous power usage.

Correction factors had to be added to the integrated heating usage and energy consumption because the test unit operated without an indoor unit fan. The indoor air chamber provided the airflow through the coil so correction factors were used to simulate the power consumption and heat output from an indoor unit fan[16]. The correction factor for power usage is 0.365 kW per 1000 cfm airflow through the indoor coil. For heating capacity, the indoor unit would give up heat to the room so the correction factor for heating capacity is 1250 Btu/hr/1000 cfm. These correction factors were added to the instantaneous values before integration.

BASE CASE ENERGY BALANCE

To verify the calculations for air-side heating capacity, an energy balance was performed on the indoor coil. Figure 4.1 shows a plot of the refrigerant side and air side capacity for the indoor coil during the base case test. The energy balance was done without the correction factors for the indoor fan, since the refrigerant side does not contain the same correction.

The refrigerant side capacity was calculated by multiplying the refrigerant mass flow rate by the change in enthalpy of the refrigerant entering and leaving the indoor coil. The enthalpy of the refrigerant was calculated using subroutines developed by Kartsounes and Erth[20].

The difference in refrigerant and air side capacities averaged under 5% during the frosting portion of the cycle when the system was close to steady state.

DESCRIPTION OF BASE CASE TEST

This section provides a detailed description of the frosting /defrost cycle for the base case test. Relevant data(pressure, temperature, capacity, etc.) are plotted and discussed as to their effect on the cycle. Figure 4.2 shows a plot of the power usage(compressor plus outdoor and indoor

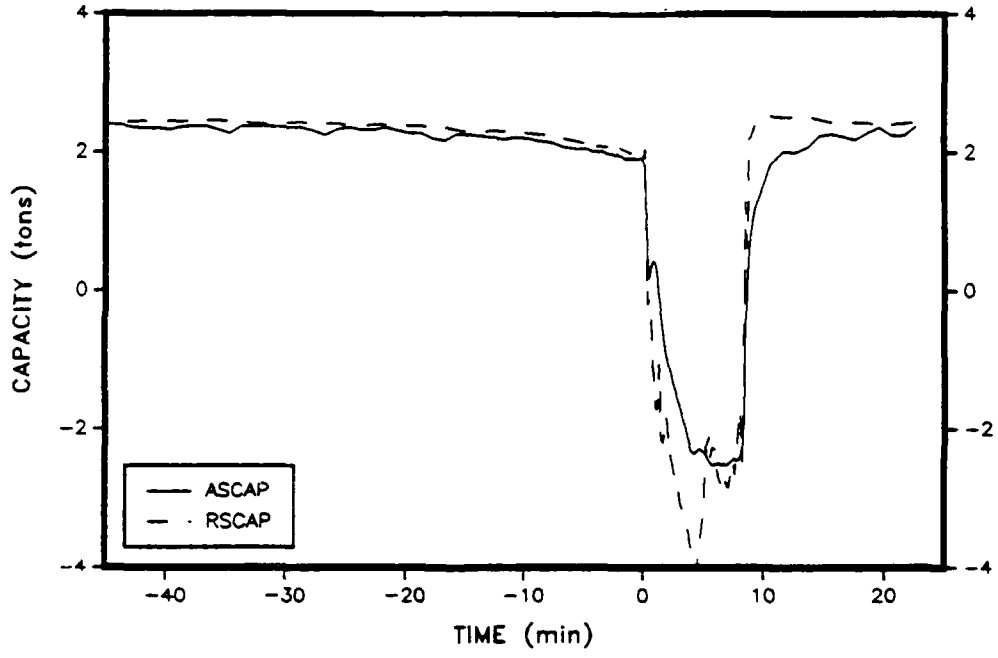

Figure 4.1. Refrigerant-Side/Air-Side Capacity Comparison.

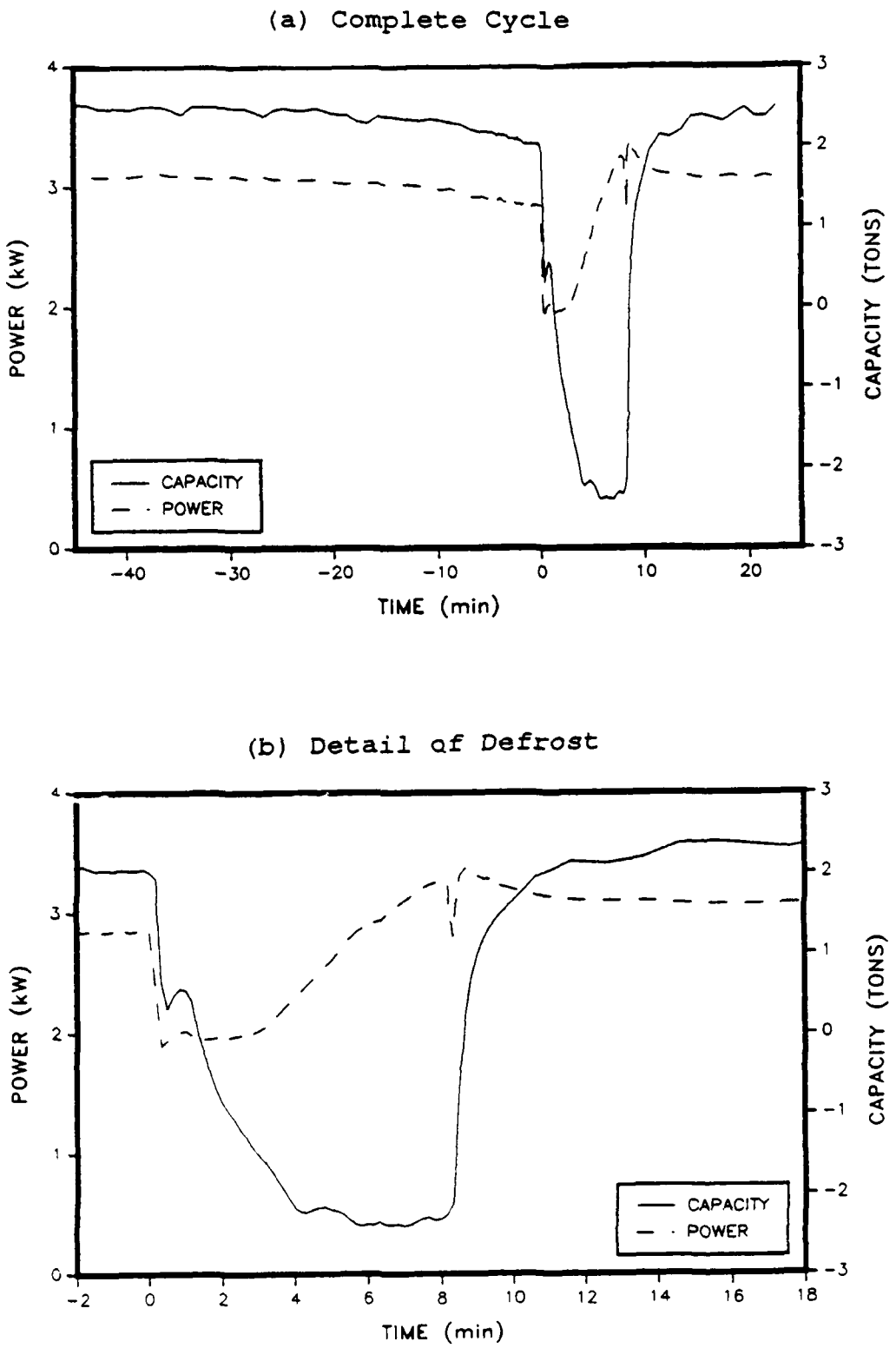

Figure 4.2. Power Usage and Heating Capacity for Base Case.

fans) and capacity for the heat pump with the base expansion device during a complete frosting/defrosting cycle. Figure 4.2a shows a plot of the complete cycle, while Figure 4.2b provides an expanded plot of the defrost portion of the cycle. Figure 4.2a starts 45 minutes before defrost initiation(-45 minutes), which was approximately 15 minutes after the termination of the previous defrost. Time is equal to 0 minutes at defrost initiation and the plot continues until 25 minutes after defrost initiation(25 minutes). Figure 4.2b starts at 2 minutes before defrost initiation and continues until 18 minutes after initiation of defrost.

FROSTING OF THE OUTDOOR COIL

-45 to 0 minutes

At the start of Figure 4.2a(-45 minutes), the heat pump had been running 15 minutes since the completion of the previous defrost cycle. At this point, the unit was also running at its maximum capacity of approximately 2.5 tons @ 35^{o}F ambient and the accumulator was approximately half full of liquid refrigerant.. Frost was visible on the bottom circuit of the outdoor coil(Figure 4.3) and the air pressure drop through the outdoor coil was just beginning to

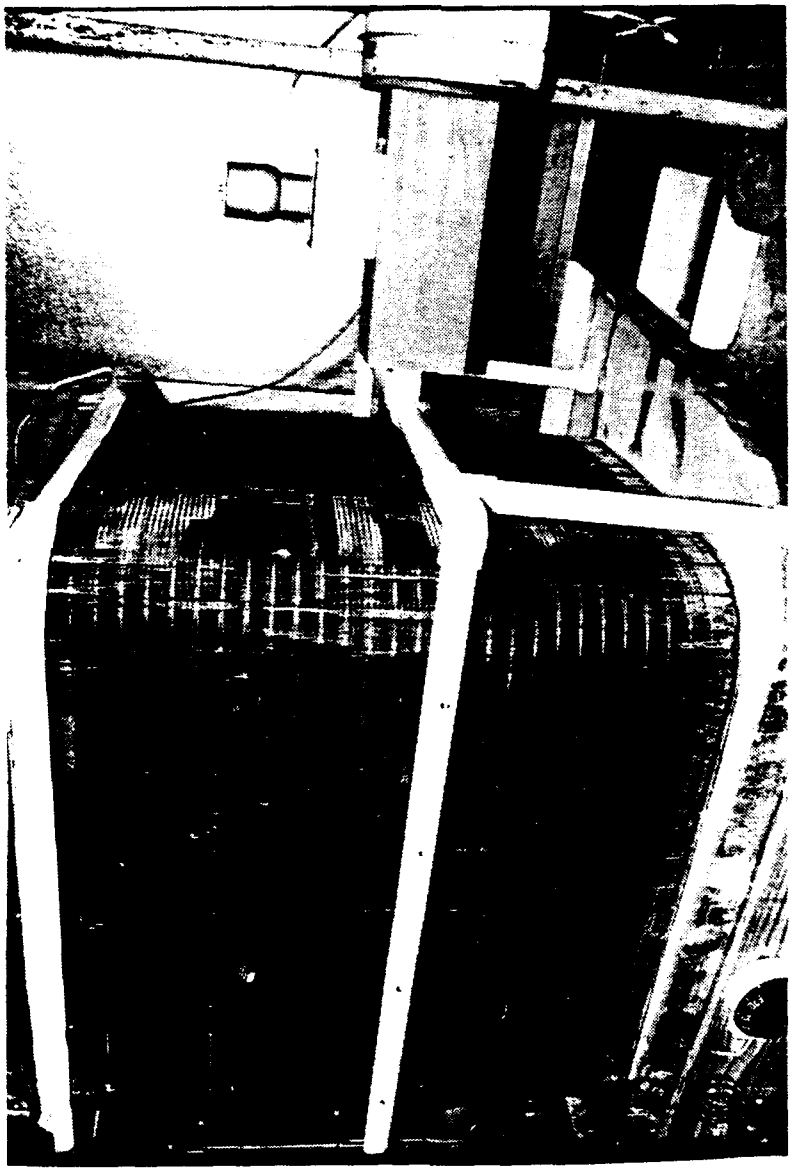

Figure 4.3. Outdoor Coil at 45 Minutes Before Defrost.

rise(Figure 4.4a). As the frost continued to grow, the pressure drop across the outdoor coil increased and at -32 minutes, the airflow started to decrease from the maximum of 1900 cfm. The unit's heating capacity was not significantly affected by the frost growth until about -15 minutes, when it began to decrease(Figure 4.2a). At this point, the airflow had fallen to 1500 cfm(Figure 4.4a) and frost was now located mainly on the edges and corners of the coil(Figure 4.5).

After -15 minutes, frost began to spread throughout the coil, until at -8 minutes, frost was visible over most of the surface(Figure 4.6). During those 7 minutes, the air pressure drop through the coil rose to a maximum of 0.15 inches WG at -9 minutes and then abruptly dropped to 0.09 inches WG when the outdoor unit fan motor "stalled" under the high static pressure.(Figure 4.4a). The outdoor unit fan was a 3-blade propeller fan designed to efficiently move large volumes of air but unable to handle large static pressures[21].

With the fan motor unable to maintain torque under the high static pressure, there is a rapid drop in airflow from 1400 cfm to 1000 cfm through the outdoor coil(Figure 4.4a). With the rapid drop in airflow, the heat pump's capacity

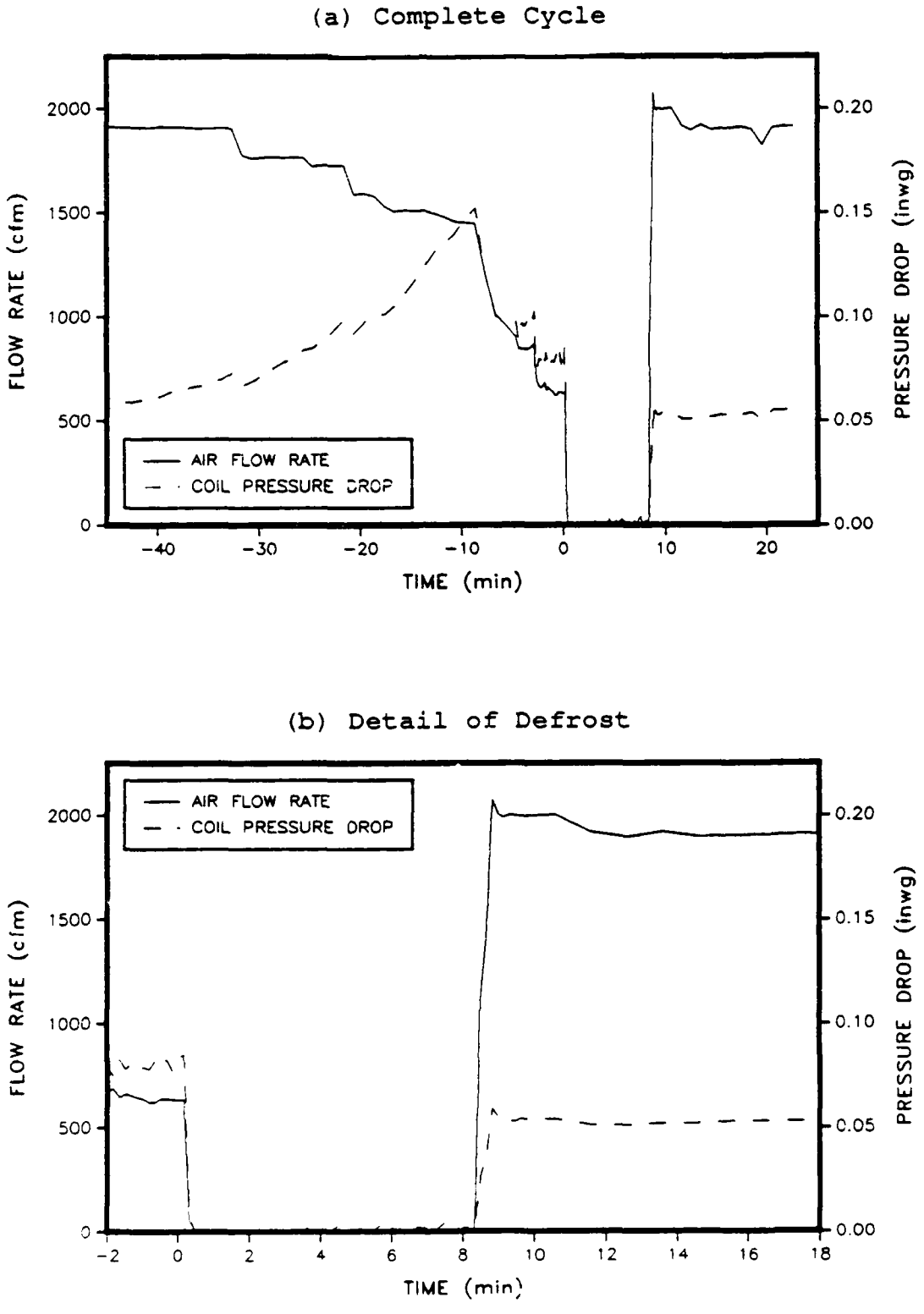

Figure 4.4. Airflow and Pressure Drop Through Outdoor Coil (Base Case).

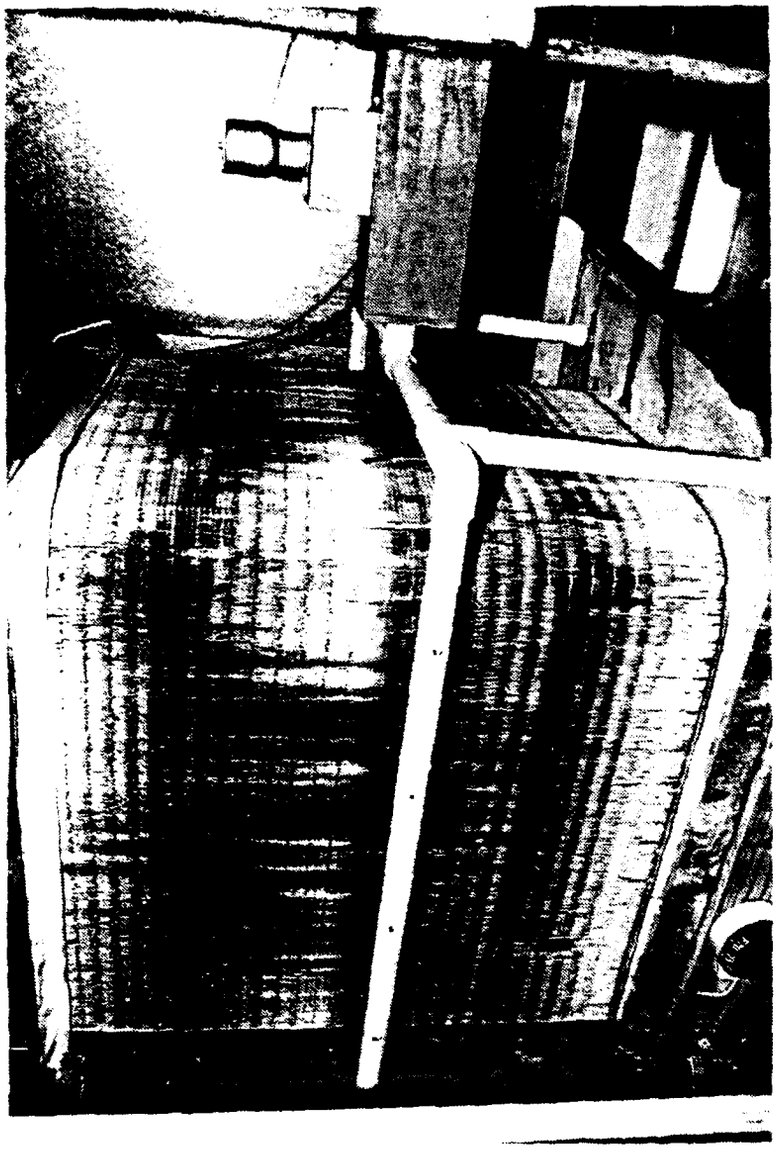

Figure 4.5. Outdoor Coil at 15 Minutes Before Defrost.

Figure 4.6. Outdoor Coil at 8 Minutes Before Defrost.

dropped from 2.4 tons to 2.2 tons over the same two minutes(Figure 4.2a).

As the frost accumulation increased, the outdoor coil temperature decreased(Figure 4.7a), causing an acceleration in frost growth, an increase in pressure drop through the coil and a decrease in heating capacity. The vapor line temperature, which is the suction line temperature during the heating mode, dropped from 23°F at -45 minutes to 15°F at -5 minutes as frost grew on the coil. The frost blocked the airflow through the coil which reduced the heat transfer into the coil and the amount of vapor supplied to the compressor. This reduced the density of the suction line vapor which also reduced the pressure and temperature in the outdoor coil and the indoor coil. The colder refrigerant temperatures reduced capacity in the indoor coil and encouraged frost growth in the outdoor coil, further dropping the liquid and vapor line temperatures and reducing system capacity.

(a) Complete Cycle

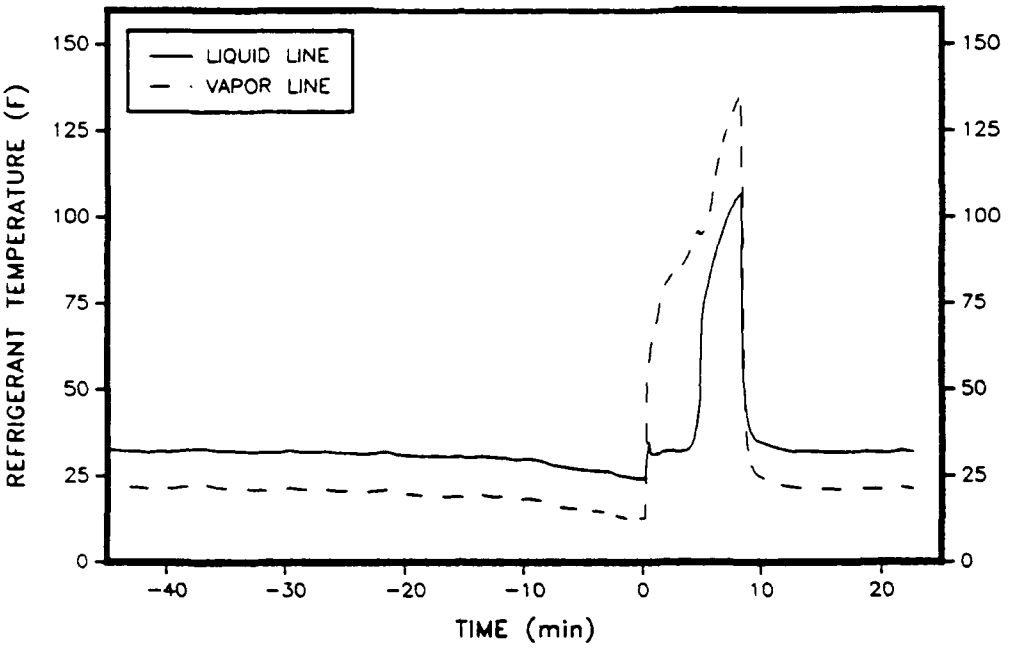

(b) Detail of Defrost

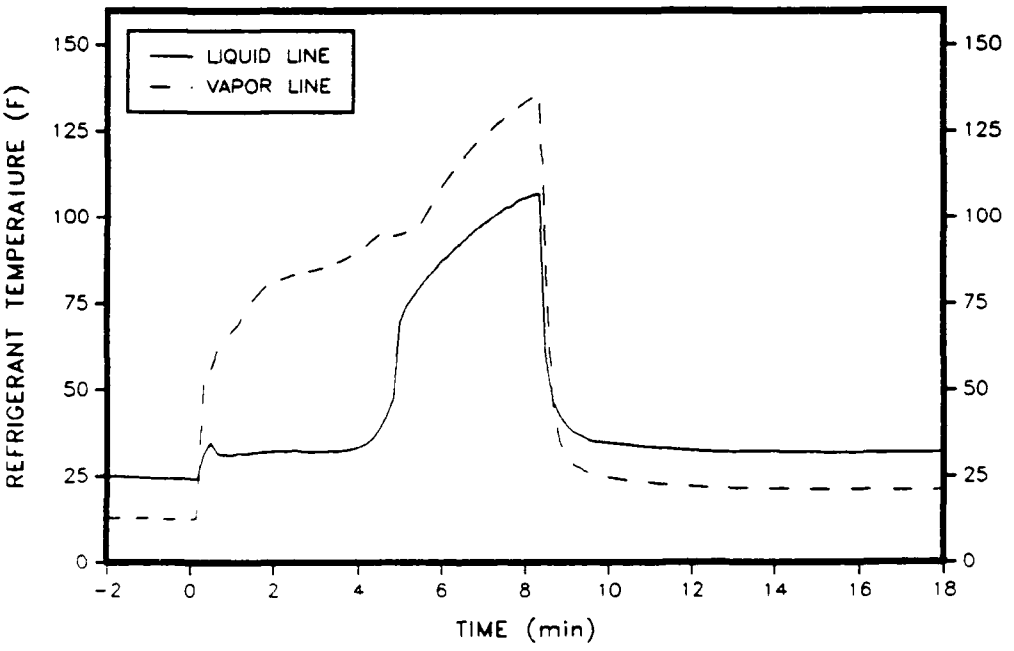

Figure 4.7. Refrigerant Temperatures Near Outdoor Coil. (Base Case).

DEFROST INITIATION

0.0 to 1.0 minutes

As discussed in Chapter III, the test criteria for defrost initiation was a 20% drop in system capacity from the maximum capacity(2.5 tons) reached after a defrost. Defrost was initiated when the capacity fell to 2.0 tons, at 0 minutes (Figure 4.2). The coil was fully covered with frost(Figure 4.8) and the accumulator was approximately 80% filled with refrigerant before defrost initiation. This is equal to 55% of the system charge since the capacity of the accumulator and the system charge are approximately 125 ounces and 184 ounces, respectively. At defrost initiation, the reversing valve was energized and the outdoor fan was shut off, which dropped the outdoor airflow and pressure drop through the coil to zero. The reversing valve switched the direction of refrigerant flow from the heating mode, where the outdoor coil was the evaporator, to the cooling mode, making the outdoor coil the condenser.

As the reversing valve changed the direction of the refrigerant flow, an apparent equalization between the suction and discharge pressure lines occured(Figure 4.9). The discharge pressure dropped from 190 psia to 75 psia in 5 to 10 seconds, while the suction pressure surged upward from

Figure 4.8. Outdoor Coil at Defrost Initiation.

(a) Complete Cycle

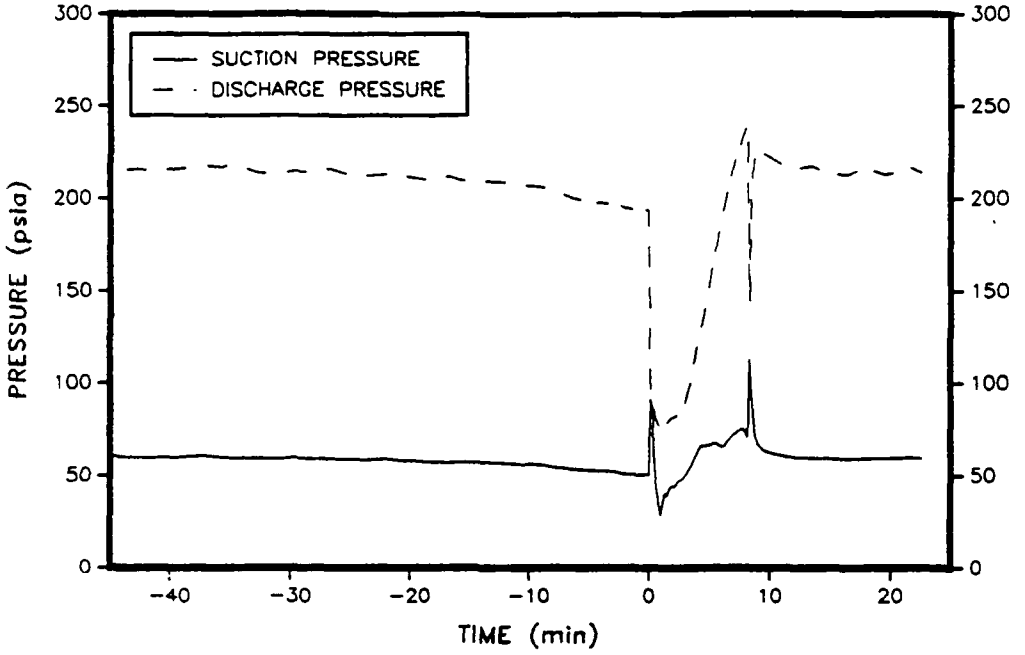

(b) Detail of Defrost

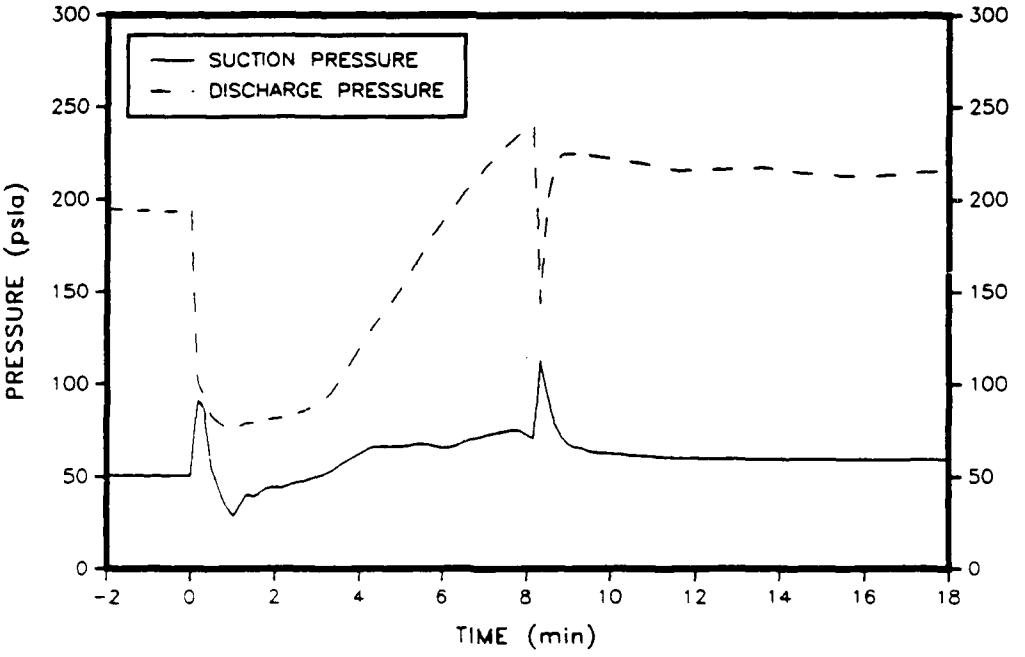

Figure 4.9. Compressor Suction and Discharge Pressures. (Base Case).

50 psia to 90 psia. With the decrease in pressure rise through the compressor, the refrigerant flow rate fell to almost zero and the heat pump power dropped from 2.8 kW to 1.8 kW(Figure 4.10).

The sudden decrease in pressure in the indoor coil caused the liquid refrigerant located in the indoor coil before defrost to vaporize in the coil and flush toward the accumulator. Figure 4.11 shows the refrigerant superheat/subcooling conditions leaving and entering the indoor coil and the coil capacity. Temperature 24(T-24) is a probe located in the vapor line after the indoor coil and temperature 25(T-25) is a probe located between the defrost expansion device and the coil(see Figure 3.6). The pressures at T-24 and T-25,(P-40 and P-41, respectively) are used to calculate the saturation temperatures(Tsat-24 and Tsat-25) and the difference between T and Tsat is the amount of superheat or subcooling(SHSC) of the refrigerant. A positive value for SHSC-24 means it is superheated and a negative value indicates subcooling. Also contained in Figure 4.11 is the capacity which is one indicator of the amount of refrigerant located in the indoor coil. When the coil contains no liquid refrigerant the capacity should be close to zero. As liquid refrigerant starts filling the

THE EFFECTS OF EXPANSION DEVICES ON THE TRANSIENT RESPONSE CHARACTERISTICS OF THE AIR-SOURCE HEAT PUMP DURING THE REVERSE CYCLE DEFROST

A Thesis

by

KURT T. PETERSON

Submitted to the Graduate College of
Texas A&M University
in partial fulfillment of the requirement for the degree of

MASTER OF SCIENCE

August 1988

Major Subject: Mechanical Engineering

(a) Complete Cycle

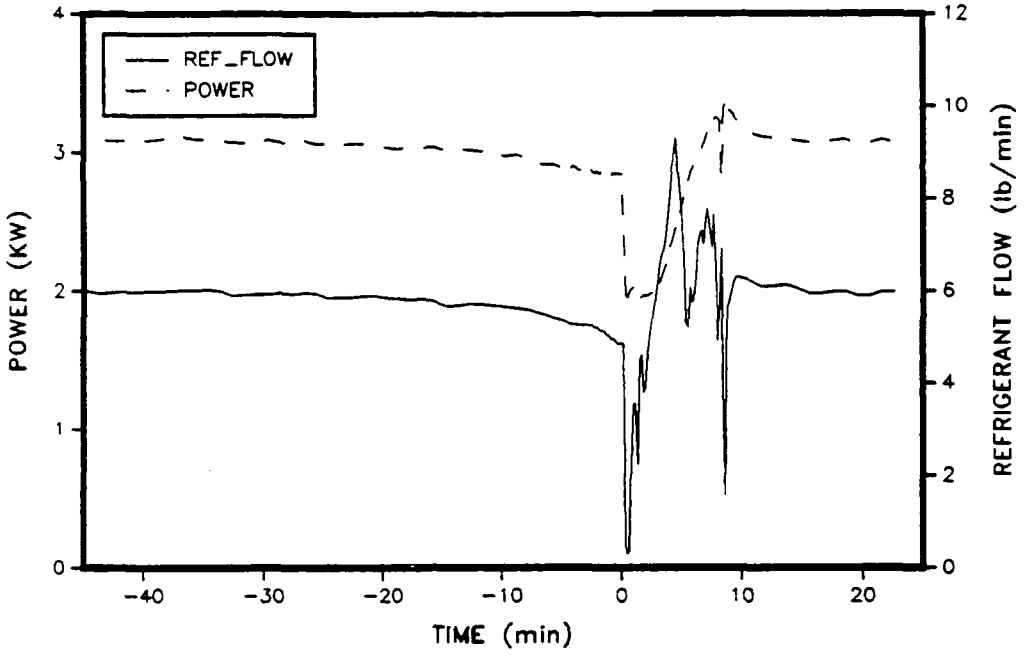

(b) Detail of Defrost

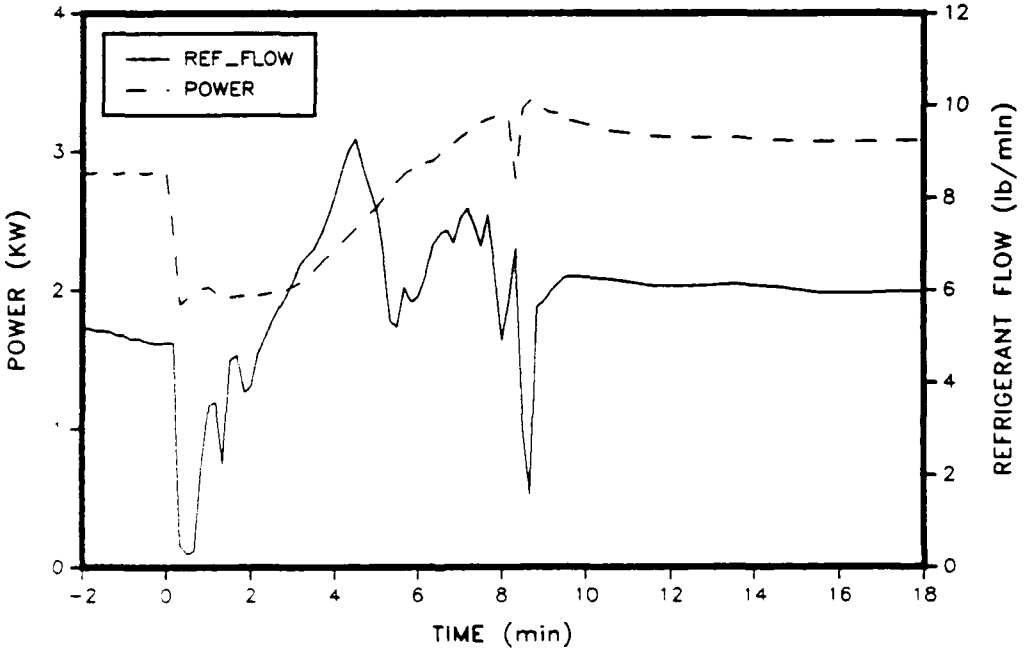

Figure 4.10. Refrigerant Flow Rate and Power Consumption. (Base Case).

(a) Complete Cycle

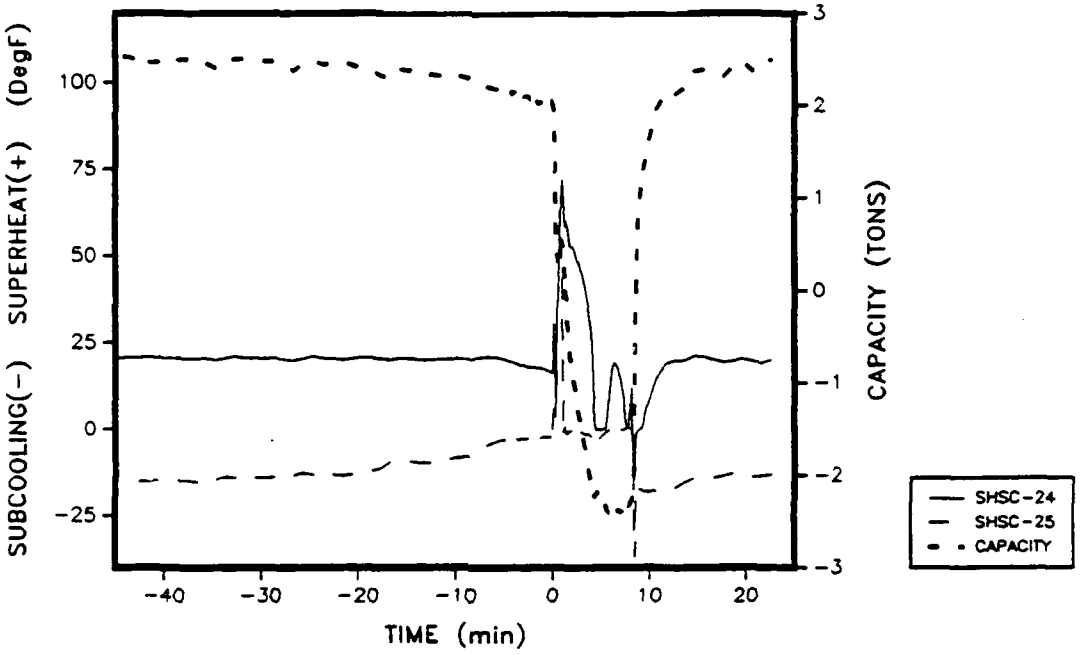

(b) Detail of Defrost

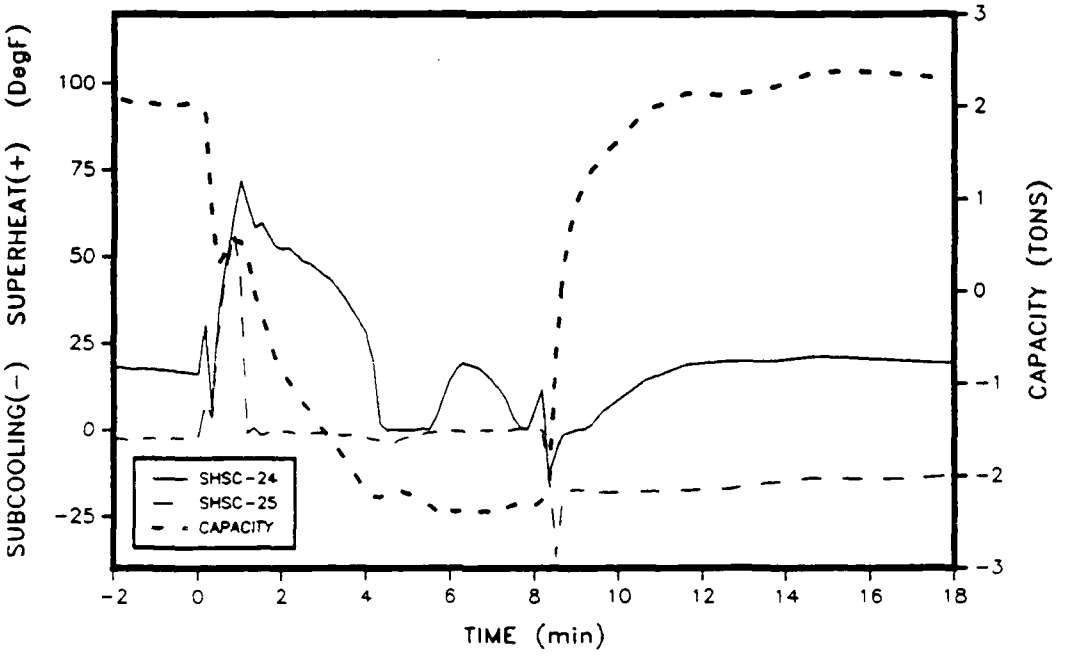

Figure 4.11. Superheat/Subcooling at T-24 and T-25 & Capacity (Base Case).

coil, the capacity should rise and reach a maximum when SHSC-24 is zero.

At defrost initiation, the capacity in Figure 4.11 fell from 2.0 tons to 0.3 tons within 20 seconds. This sudden drop in capacity was principally caused by the boiling of refrigerant from the indoor coil. The flow of liquid refrigerant out of the coil can also be inferred from SHSC-24. As defrost was initiated, SHSC-24 rose from 15°F to 30°F and then dropped to 4°F as the cool refrigerant vapor rushed out of the indoor coil. Since SHSC-24 did not drop to zero, as it would have if there had been liquid in the vapor line, all of the refrigerant in the outdoor coil apparently vaporized and no liquid went into the accumulator.

During this time, the refrigerant in the indoor coil, which was initially hot, boiled as the saturation pressure dropped. The accumulator was approximately 80% filled with refrigerant before defrost initiation and the level did not rise after initiation, indicating again that all of the refrigerant from the indoor coil vaporized before reaching the accumulator. With the indoor coil containing only low pressure vapor after defrost initiation, the compressor became temporarily "starved" of refrigerant and pulled the suction pressure down to 30 psia. As the suction pressure

fell, the refrigerant in the accumulator started to boil and the accumulator temperature(T-accum) decreased to 0°F as it lagged the saturation temperature(Tsat-20) which fell to -10°F(Figure 4.12b).

The refrigerant that remained trapped in the accumulator, was fed into the suction line of the compressor through the U-tube metering device at the bottom of the accumulator. The accumulator level dropped from 80% full at the beginning of defrost to 25% after 1 minute of defrost as the U-tube metering device fed the refrigerant into the compressor intake. Liquid refrigerant in the compressor intake was indicated by Figure 4.12b where T-20 was equal to Tsat-20. The heat from the compressor was used to boil the liquid refrigerant fed into the compressor from the accumulator. Since the indoor coil contained only low pressure vapor immediately after defrost initiation, the compressor was the only source of heat available to melt the frost from the outdoor coil during the first minute of the defrost cycle.

The liquid refrigerant was gone from the coil within 20 seconds from defrost initiation as indicated in Figure 4.11b with the superheated conditions at SHSC-24 and SHSC-25. With the liquid refrigerant gone from the coil, the capacity rose slightly to 0.5 tons because of some residual

(a) Complete Cycle

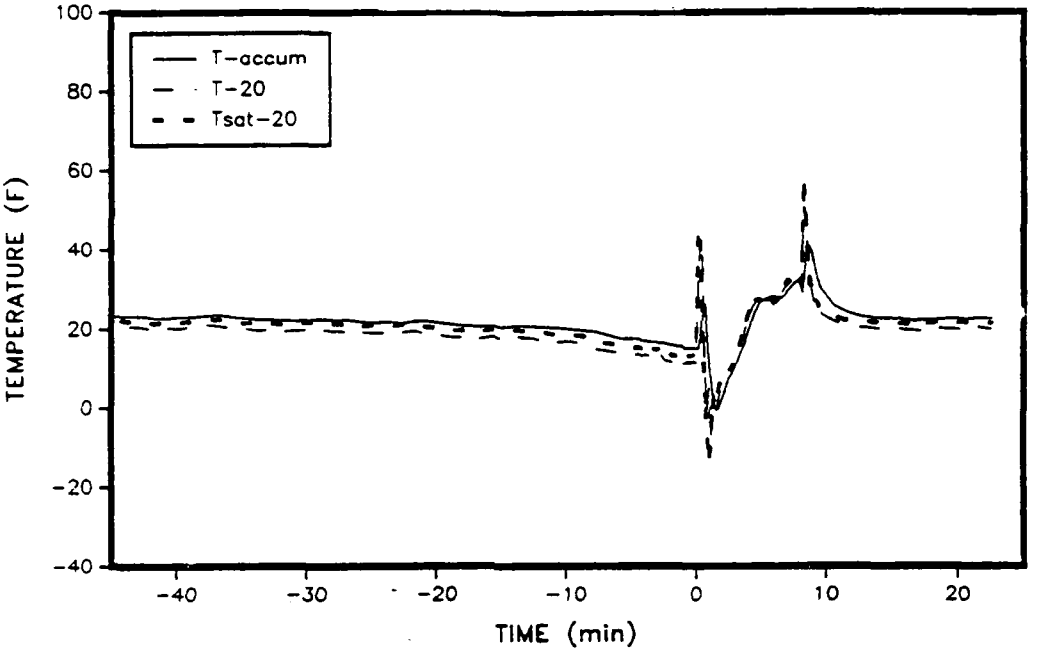

(b) Detail of Defrost

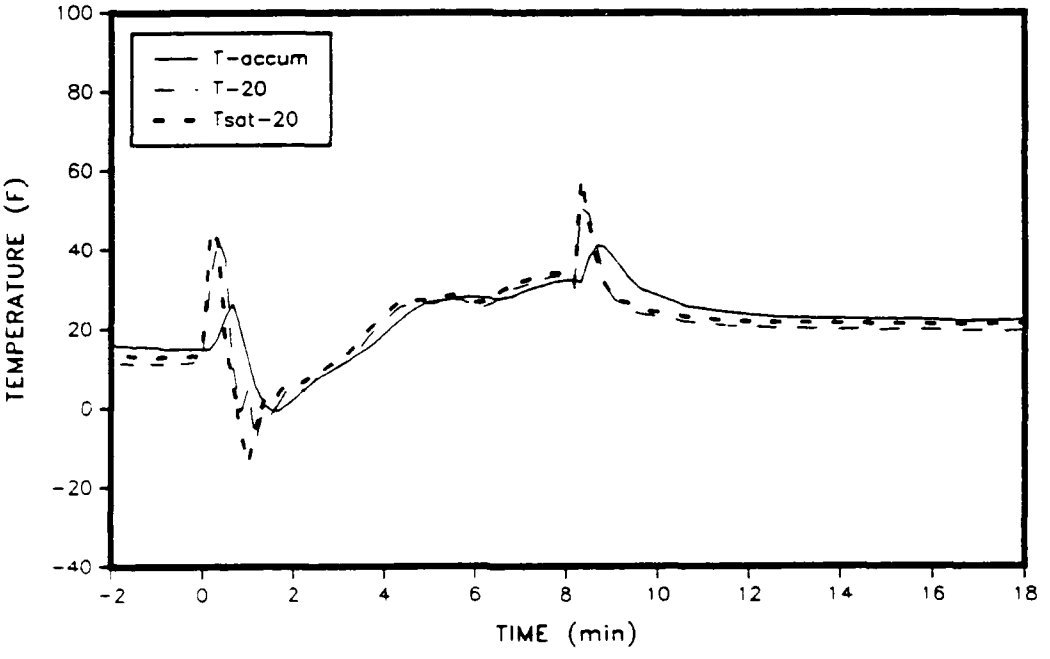

Figure 4.12. T-20, Tsat-20 and Bottom Temperature of Accumulator (Base Case).

heat still in the coil, duct and flow straighteners. The capacity started dropping again at 1.0 minutes as refrigerant was fed into the coil through the defrost expansion device(TXV #57). The flow of refrigerant into the indoor coil was indicated in Figure 4.11b by the drop in superheat of SHSC-25 to zero. Miller[13] showed the same trend in Figure 2.5.

MELTING FROST

1.0 to 4.2 minutes

After one minute into the defrost cycle, there was evidence of the frost melting from the outdoor coil. Up to this point, the indoor coil had not supplied a significant amount of heat to the system, since the coil had contained only vapor. At 1.0 minute, the indoor coil capacity began to increase(Figure 4.11b) from 0.5 tons at 1 minute to -2.3 tons at 4.2 minutes. This increase was coincident with the rapid rise in refrigerant flow(Figure 4.10b) from approximately 2 lb/min at 1 minute to 9 lb/min at 4.2 minutes. As the indoor coil reached a maximum capacity of 2.3 tons, SHSC-24 fell to zero as liquid refrigerant overflowed the indoor coil into the accumulator. At 4.5 minutes, the accumulator level was approximately 25% full

and started to rise as the suction line was filled with liquid refrigerant. The increasing saturation temperature from 1.0 minutes to 4.5 minutes was a result of the increasing flow of refrigerant vapor from the indoor coil to the compressor(Figure 4.10b) which increased the suction pressure from 30 psia to 70 psia(Figure 4.9b).

From 1.0 minute to 4.2 minutes into the cycle, frost was melted from the outdoor coil. Figures 4.13 and 4.14 show the defrosting coil at 2.0 minutes and 3.0 minutes. During this time, the temperature of the liquid refrigerant leaving the outdoor coil remained at 32^{o}F as the phase change occured from frost to water(Figure 4.7b). The subcooling of the liquid refrigerant leaving the coil increased to 30^{o}F during the same period as the compressor discharge pressure increased to 130 psia. These conditions greatly increased the capacity of the TXV and the refrigerant flow increased to 9.3 lbs/min(Figure 4.10b).

DRAINING MELTED FROST

4.2 to 8.1 minutes

At 4.2 minutes, most of the frost had melted from the outdoor coil and the melting phase ended as the average

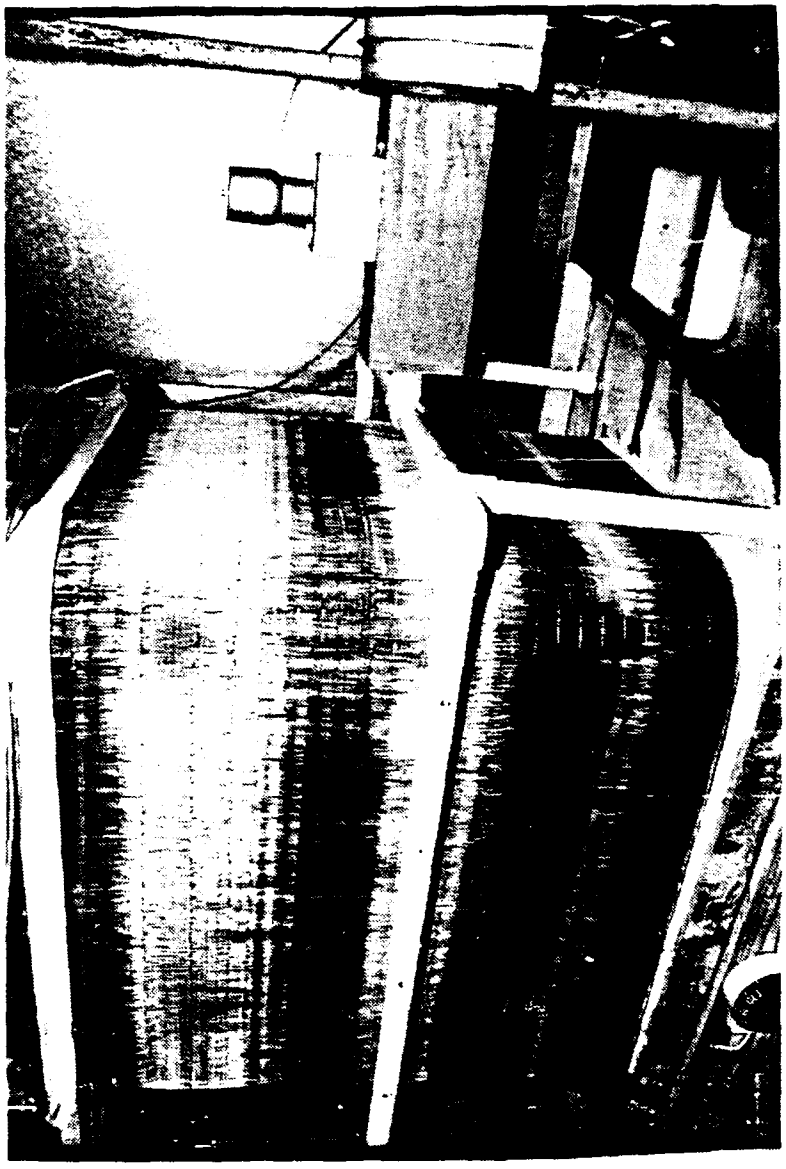

Figure 4.13. Outdoor Coil at 2 Minutes After Defrost.

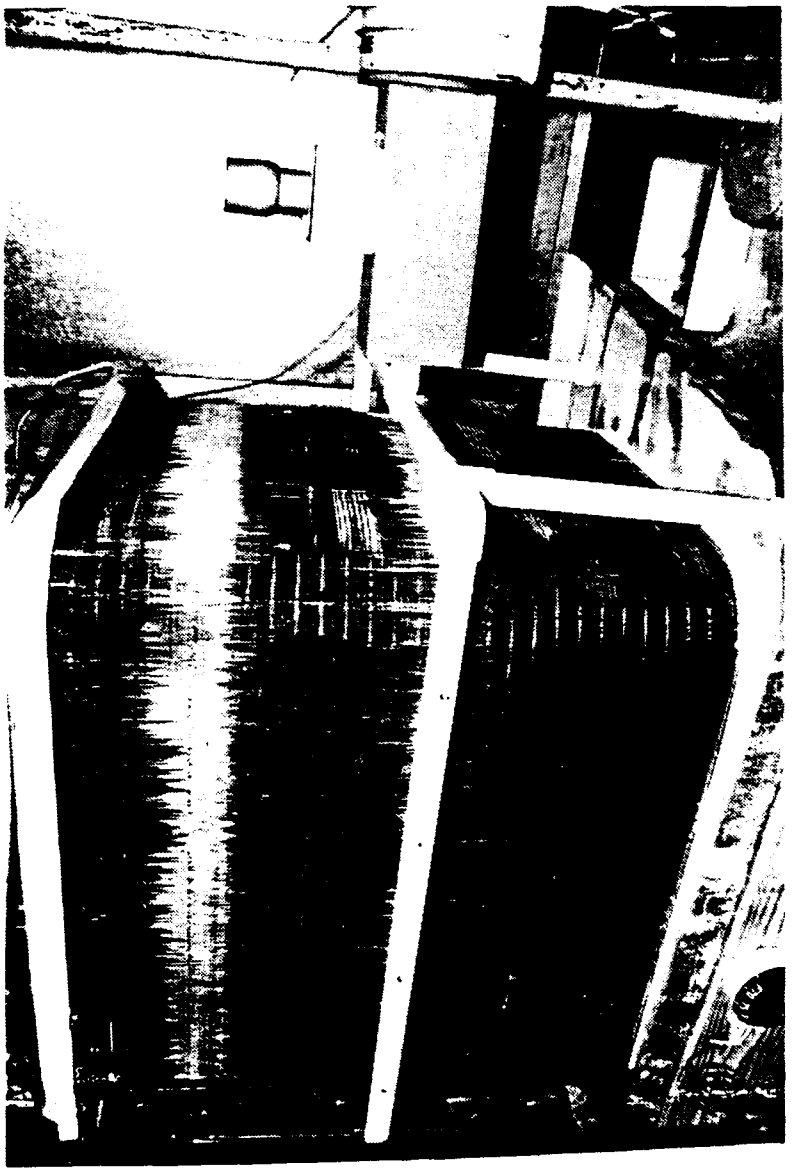

Figure 4.14. Outdoor Coil at 3 Minutes After Defrost.

leaving refrigerant temperature (T-17) rose above 32°F and continued to rise to 70°F in 30 seconds (Figure 4.7b). The end of the melting phase was determined when T-17 rose above 34°F. As T-17 rose to 70°F, the subcooling in the outdoor coil(SHSC-17) fell to approximately 4°F(Figure 4.15b). The subcooling upstream of the TXV (SHSC-26) did not fall as rapidly as T-17 and remained at approximately 10°F until 7 minutes.

While the internal movements of TXV #57 were not monitored during the defrost cycle, it is possible to infer its effects on the defrost cycle from the amount of superheat leaving the indoor coil(SHSC-24) and the refrigerant flow(Figure 4.11b). During the heating cycle, TXV #57 was bypassed, but its expansion bulb still sensed a superheated condition in the vapor line close to T-24. The TXV should have reacted to the superheated condition by opening its orifice to a maximum in an attempt to reduce the superheat. Thus, TXV #57 should have been wide open at defrost initiation and also during the melt phase. Refrigerant flow dropped to near zero at defrost initiation(0 minutes) as the reversing valve engaged. The flow rose steadily to over 9 lb/min at 4.5 minutes. The superheat at the outlet of the indoor coil(SHSC-24) remained over 30°F during this period, so TXV #57 should have

(a) Complete Cycle

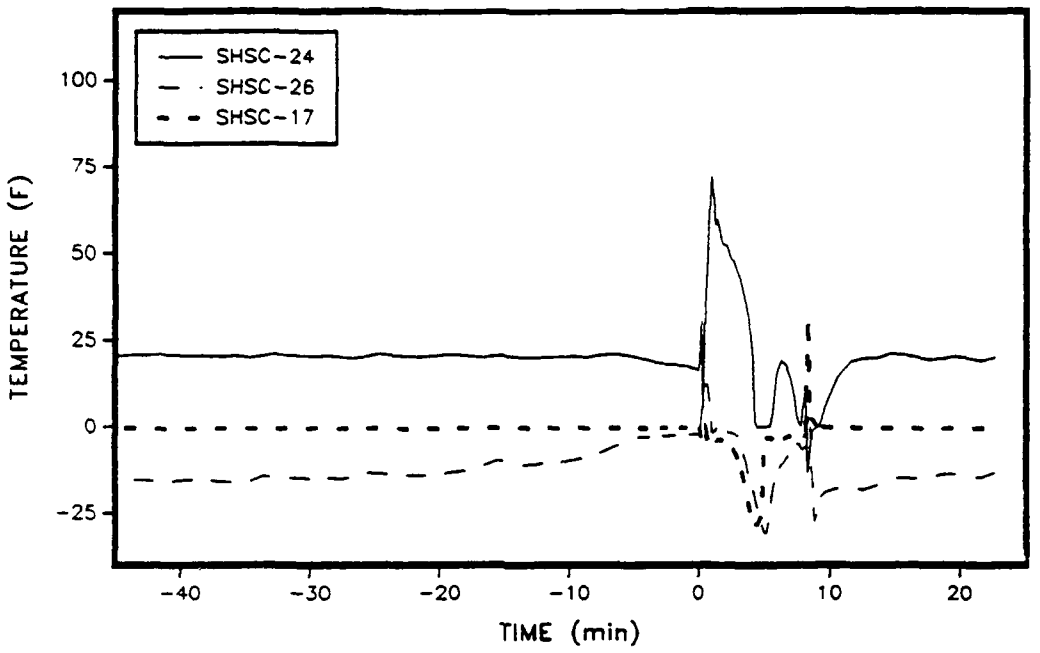

(b) Detail of Defrost

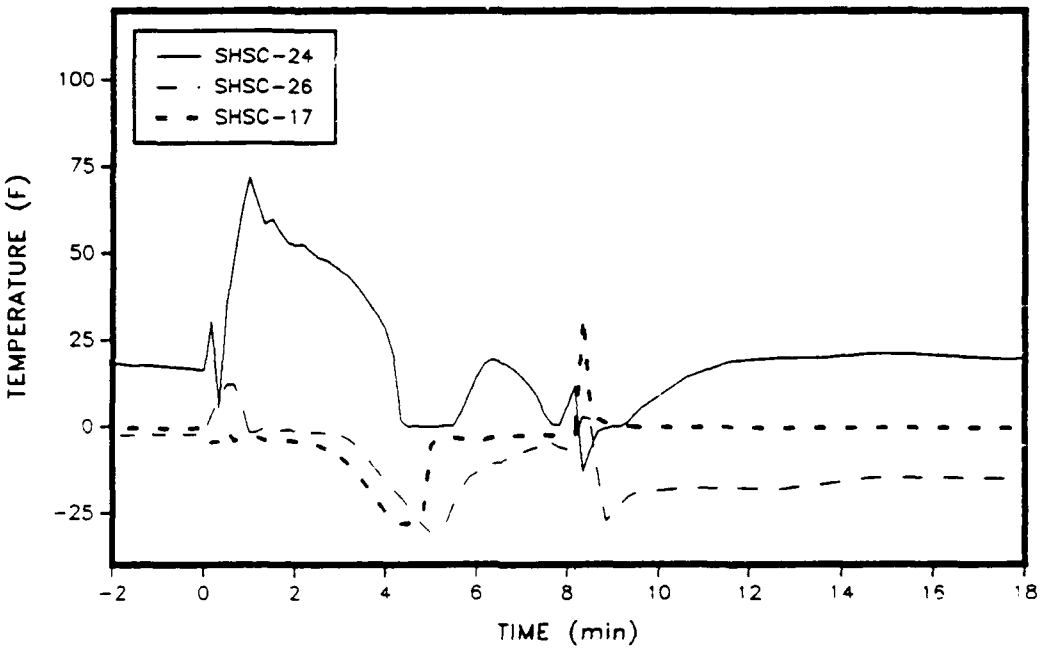

Figure 4.15. Superheat/Subcooling for T-17, T-25, and T-26 (Base Case).

remained wide open. At 4.4 minutes, the superheat dropped to zero as liquid refrigerant flooded the vapor line and TXV #57 closed down its opening and reduced the refrigerant flow from 9 lb/min at 4.5 minutes to 5.3 lb/min at 5.5 minutes.

When the refrigerant flow was reduced at 5.5 minutes, the indoor coil was able to increase the superheat as it rose to 20°F at 6.5 minutes. The TXV reacted to the increased superheat by opening larger and increasing the flow to 8 lb/min at 7.0 minutes. This reaction reduced the superheat to zero once more at 8.0 minutes. The TXV was unstable in its attempt to control the superheat(Figure 4.15b) and the instability (or hunting) continued until the cycle was terminated. At this point, TXV #57 was again bypassed in the heating mode.

During the drain phase of the defrost, the leaving refrigerant temperature(T-17) in the outdoor coil rose from 32°F at 4 minutes to 105°F at defrost termination(Figure 4.7b). The increasing coil temperature resulted in an increase in compressor discharge pressure from 110 psia to 240 psia for the same period(Figure 4.9b), which caused an increase in heat pump power from 2.2 kW to 3.2 kW(Figure 4.10b).

DEFROST TERMINATION AND RECOVERY

8.1 to 18 minutes

When the coil cleared of frost, the water produced by the melted frost was drained from the coil before terminating the defrost cycle. The outdoor coil had four parallel refrigerant circuits. The top circuit was designated as circuit 0. The middle circuits are 1 and 2. The bottom circuit is 3. In this test, termination was triggered when the temperature of the exiting bottom circuit(3) reached 65°F. This circuit and the termination scheme were chosen because they conformed to the manufacturers defrost termination scheme. The bottom circuit contained more liquid refrigerant during the defrost cycle and was also the coldest of the four circuits. Figure 4.16 shows a plot of the four circuit temperatures.

As the reversing valve was switched back to the heating mode, large pressure swings in both the liquid and vapor lines occured again in Figure 4.9. The pressure dropped 100 psi and then rose 80 psi in less than 20 seconds. The suction line received a similar shock of a 40 psi rise and drop in the same period. These pressure spikes are also reflected in Figure 4.9 as the power input to the compressor had a spike of -0.5 KW.

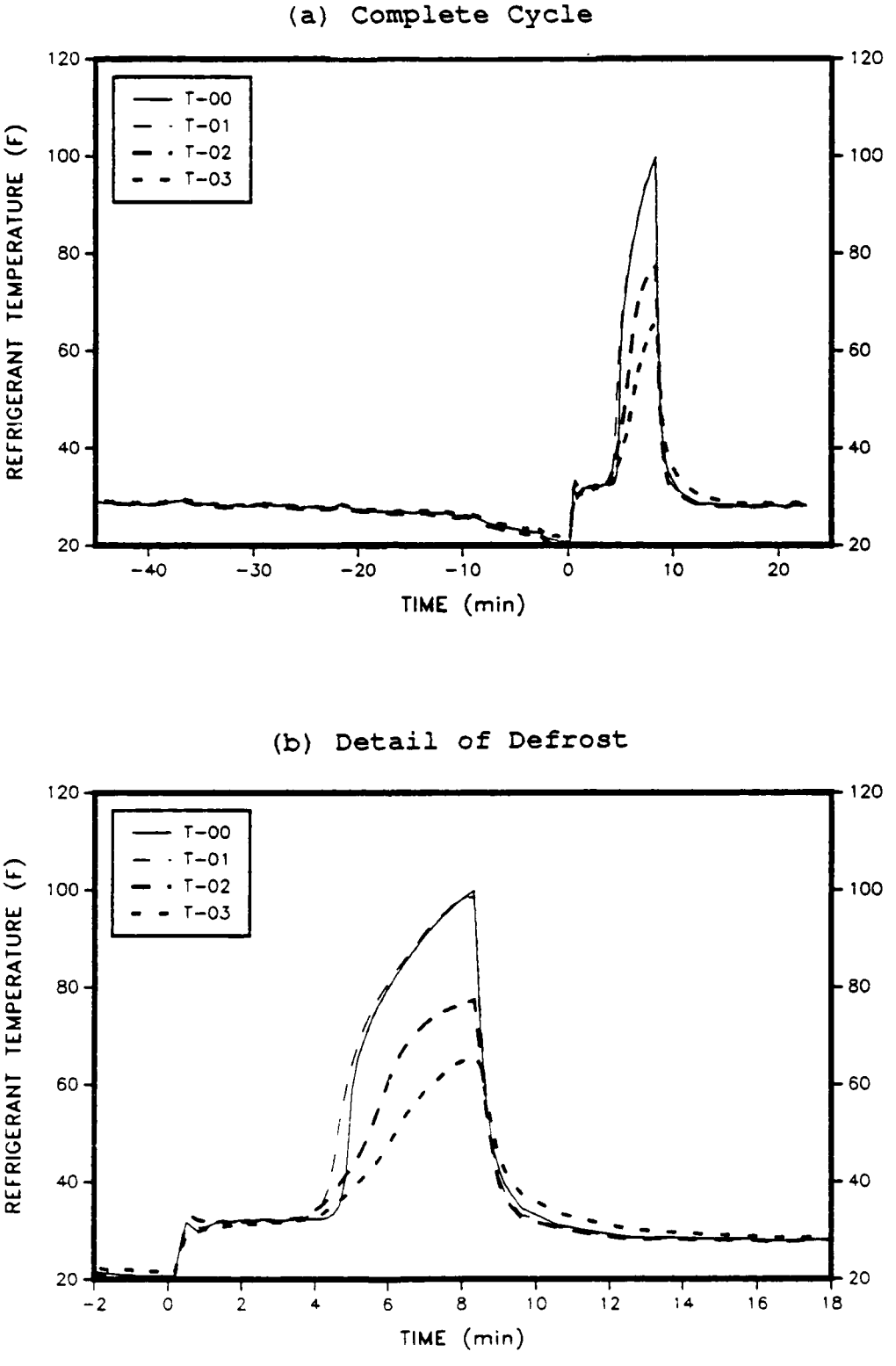

Figure 4.16. Outdoor Coil Circuit Temperatures at Defrost Termination (Base Case).

Unlike the beginning of the defrost cycle, where the indoor coil contained only low pressure vapor, the outdoor coil remained saturated after defrost termination, and the compressor was not starved for refrigerant. Figure 4.17 shows the refrigerant conditions in the vapor line(suction) at the outlet of the outdoor coil(T-18). After defrost termination, the vapor line remained saturated, providing sufficient refrigerant into the compressor. The refrigerant flow(Figure 4.15) also recovered within 30 seconds. This is in contrast to Figure 4.11 where there was a very high superheat(SHSC-24) and Figure 4.9 where there was a large drop in suction pressure. The condenser was also at 70^{o}F instead of 32^{o}F so the discharge pressure of the compressor remained above 200 psia. These factors resulted in a relatively fast recovery compared to the defrost initiation and the heat pump returned to 80% capacity in two minutes, although it took the unit nearly 10 minutes to reach 100% capacity.

SUMMARY OF BASE CASE

To evaluate the effects of different expansion devices on a heat pump during the reverse cycle defrost, a base case unit and test had to be established as a point of

(a) Complete Cycle

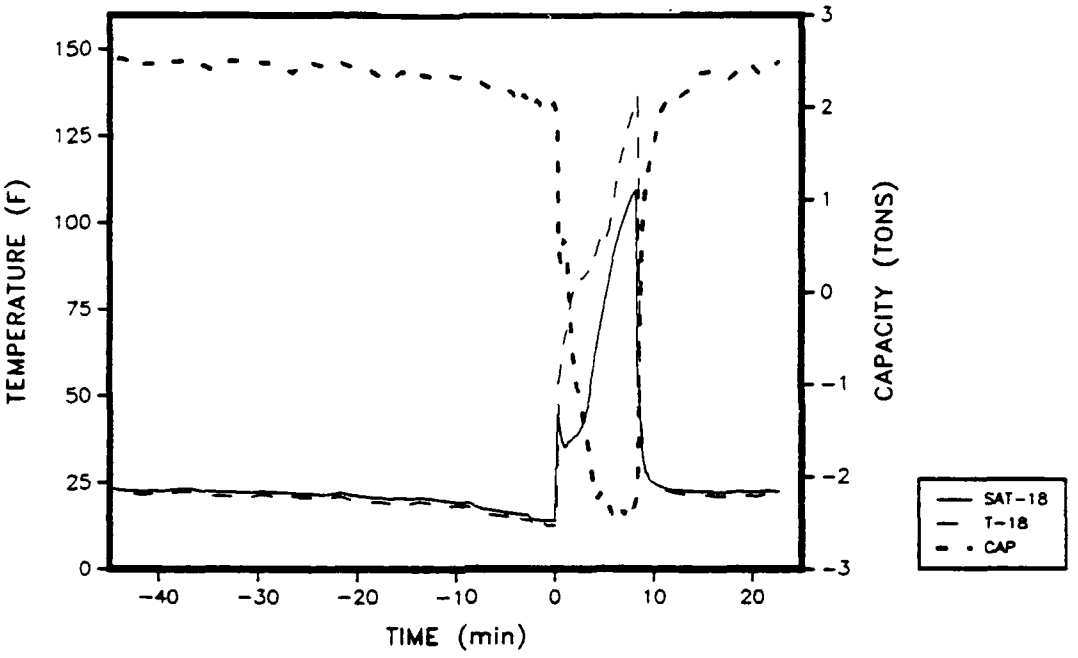

(b) Detail of Defrost

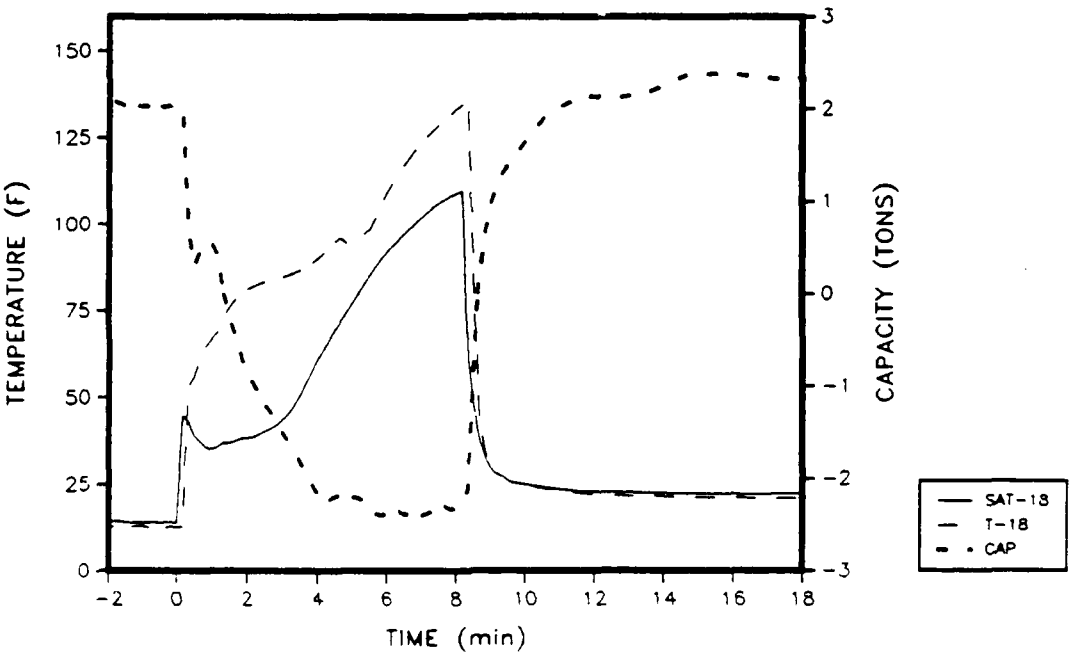

Figure 4.17. T-18, Tsat-18, and Capacity (Base Case).

comparison. The selected base expansion device was a thermal expansion valve labeled TXV #57 that was average in response. Several defrosting runs were made with TXV #57 and the base case performance was established. A detailed analysis of the base case test was also made, which was used in the analysis of the comparison tests.

CHAPTER V

COMPARISON OF TXVs WITH DIFFERENT RESPONSE TIMES

In addition to the base case thermal expansion valve (TXV), two other TXVs of the same model and capacity were installed in the heat pump to evaluate their effect on the defrost cycle performance. The only difference between the base expansion valve and the two others was in the response times to go from fully closed to fully open. These three TXVs were selected from a sample of nine TXVs provided by their manufacturer*. The three provided a sample of the slowest, fastest, and average response times. TXV #57, the base case TXV, was approximately the average of the group, while TXV #51 was the fastest and TXV #52 had the slowest response.

Figure 5.1 shows a plot of the response times of the three TXVs selected. The stroke range from fully closed to fully oper is 0.024 inches. In a full open position, the equivalent port area for the 2 1/2-ton TXV is 0.0059 $in.^2$, which is equivalent to a 0.086 inch diameter orifice. The time constant for each TXV is the time it takes for the

---

* Response tests were conducted by the TXV manufacturer at their test laboratories.

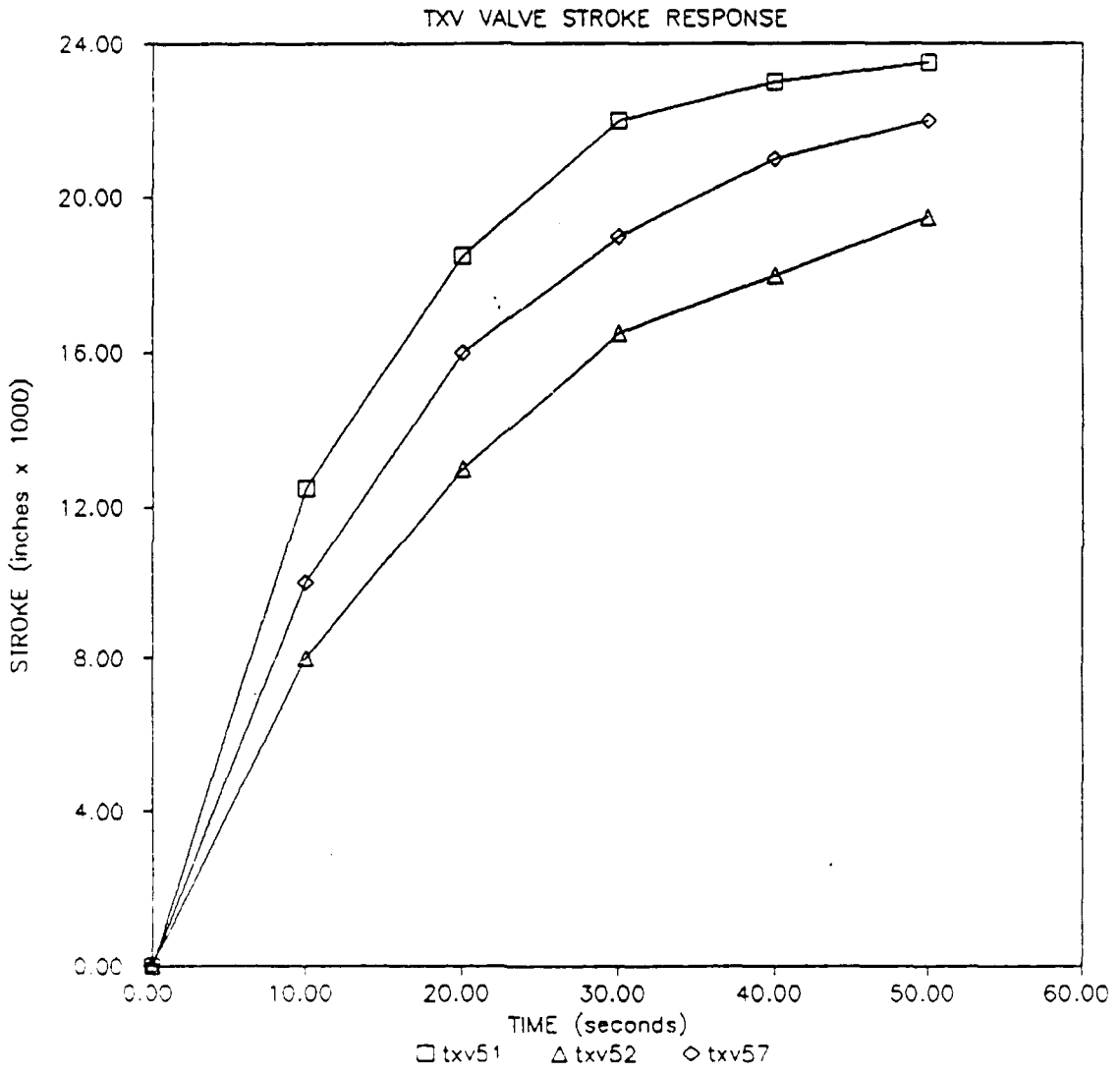

Figure 5.1. Response Times for Selected TXVs.

stroke to go from 0.0 to 63.2% of maximum stroke. All three of the TXVs have the same maximum stroke, so the time constant will be the time it takes the stroke to increase from 0.0 to 0.015 inches. Table 5.1 contains the TXV time constants.

Table 5.1. Time Constants for TXVs.

TXV #	TIME CONSTANT (seconds)
51	15
57	19
52	25

In comparing the impact of the TXVs on the heat pump system performance, four characteristics were considered: integrated COP, defrost time, melting time(the time required to melt the frost), and drain time(the period after the frost is melted and the water is draining from the coil). These values are presented in Table 5.2 for the three TXVs. The integrated COP is the ratio of the integrated heating output measured at the indoor coil over the integrated power consumption. The COP is measured over a complete frosting/defrost cycle which starts at the termination of the previous defrost and ends at the termination of the present defrost.

The characteristics for each TXV were averages taken from three consecutive runs. The average deviations during the tests were +/- 1% for the COPs and defrost times and +/- 2% for the melt and drain times.

Table 5.2. Comparison of Defrost Characteristics* for Three Thermostatic Expansion Devices.

DEFROST EXPANSION DEVICE	AVERAGE COP	DEFROST TIME (min)	MELT TIME (min)	DRAIN TIME (min)
TXV #57	2.26	8.06	4.22	3.83
TXV #51	2.22	8.33	4.39	3.94
TXV #52	2.16	8.28	4.00	4.28

* Characteristics are average values taken over three consecutive frosting/defrost cycles.

TXV #57(base case) had the best performance with a COP of 2.26 TXV #51(fast) was next with 2.22 and TXV #52(slow) had the lowest COP of 2.16. The difference between the COP for TXV #57 and TXV #51 was less than 1.8%, which was less than the combined experimental uncertainty, so statistically they are equal. The COP for TXV #52 was 3.7% less than TXV #57. Though the variation was small, it was greater than the experimental uncertainty, and it indicated a small variation in defrost performance.

In analyzing the defrost times for #57 and #52, the times were broken into two parts: the melt time and drain time. The melt time for TXV #52 was 5.2% (13 seconds) shorter than TXV #57, however the drain time was 11.7% (27 seconds) longer.

Figures 5.2 and 5.3 show the heating capacity and power consumption for TXV #57 and TXV #52, respectively. The power usage during the melt phase(approximately the first 4 minutes of defrost) stayed close to 2 kW because the constant temperature of 32^{o}F in the outdoor coil held the compressor discharge pressure below 100 psia for 1.5 minutes(Figures 5.4 and 5.5). This reduced the pressure rise through the compressor and also the power usage. During the same period, the heating capacity fell to zero, became negative and decreased to -2.3 tons at the end of the melt phase.

After the melt phase, the rising power and negative capacity during the drain phase produced a larger penalty to the overall COP during the drain time than during the melt time. Because the drain time for TXV #52 was 11.7% longer than the drain time for TXV #57, the integrated COP for TXV #52 was lower than TXV #57.

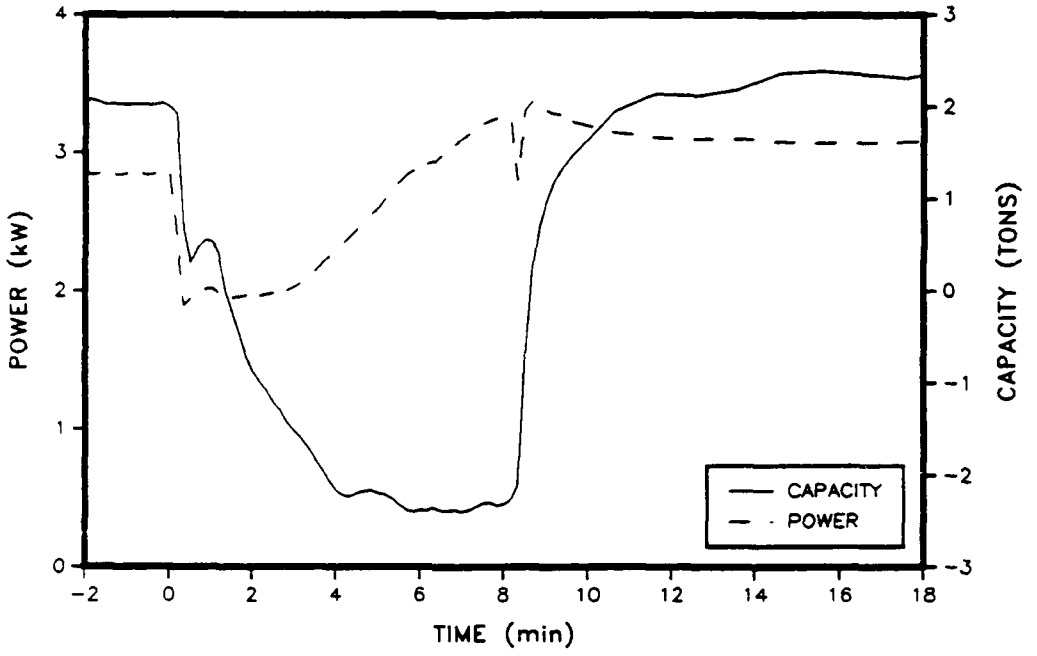

Figure 5.2. Power Usage and Heating Capacity for TXV #57 (Base Case).

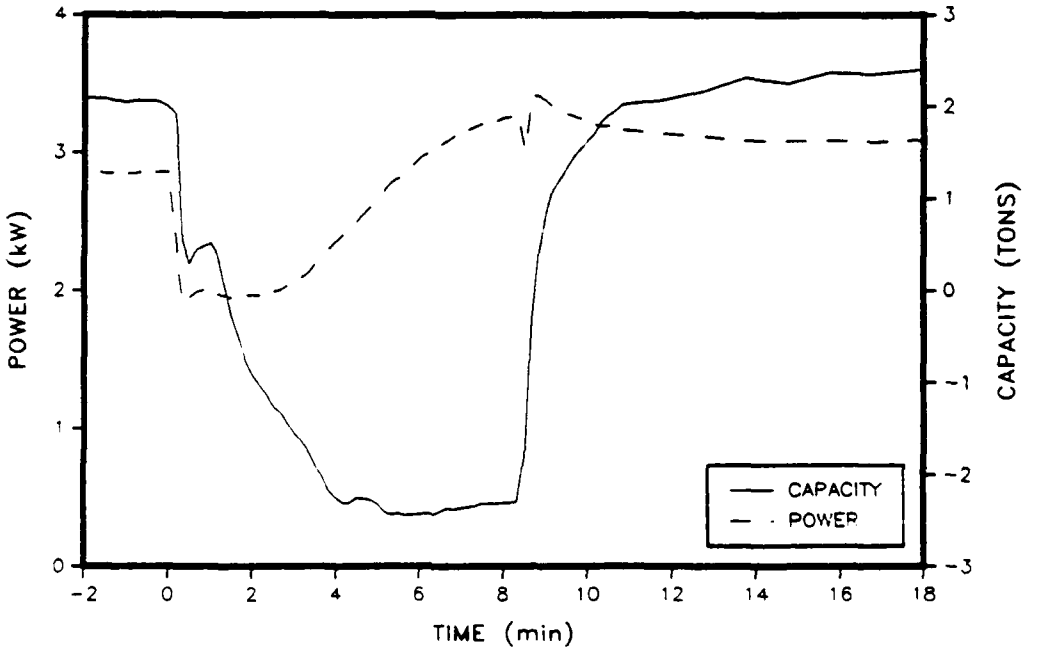

Figure 5.3. Power Usage and Heating Capacity for TXV #52.

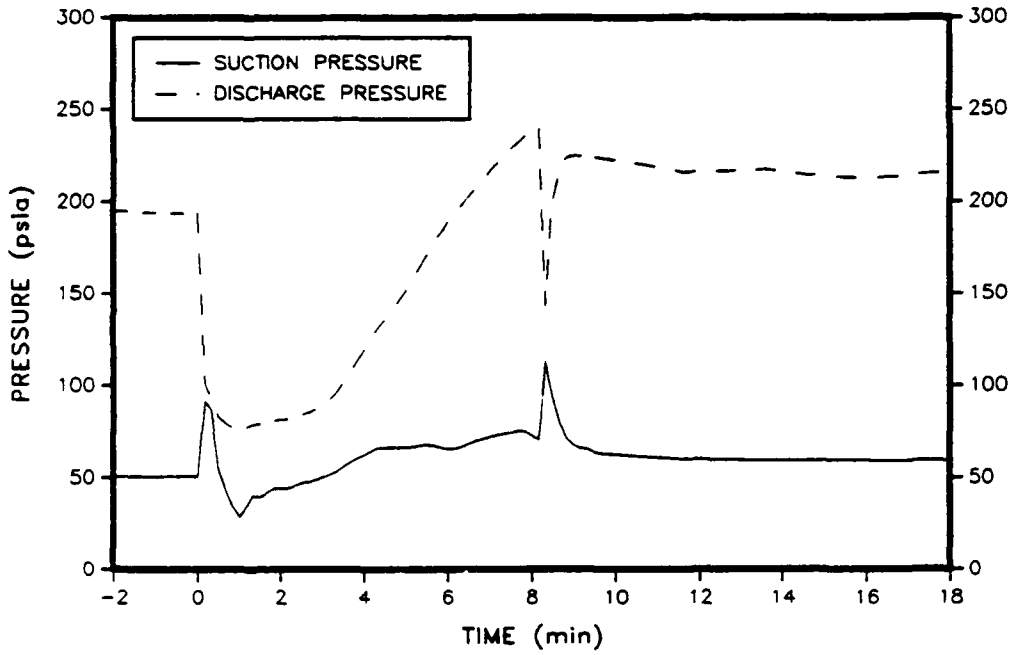

Figure 5.4. Compressor Suction and Discharge Pressures. for TXV #57 (Base Case).

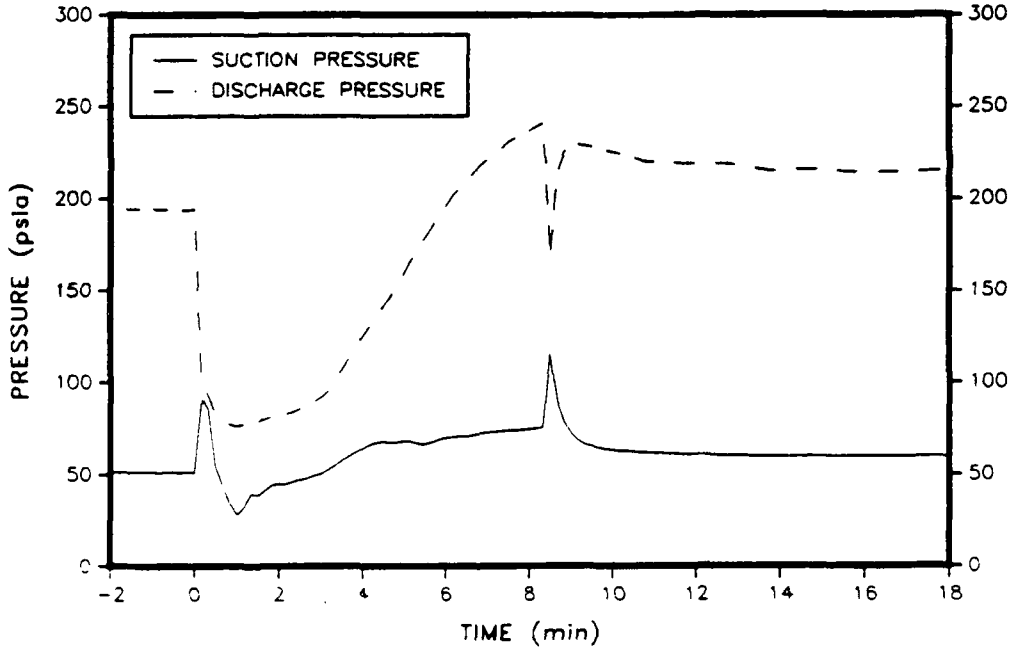

Figure 5.5. Compressor Suction and Discharge Pressures. for TXV #52.

The reason for the shorter melt time and longer drain time of TXV #52 can be explained with the use of the refrigerant flow characteristics in Figures 5.6 and 5.7. The maximum refrigerant flow during the defrost cycle for both TXVs is 9.1 lb/min. TXV #52 reduced the refrigerant flow at approximately the same time in the defrost cycle as TXV #57, but only to 5.8 lb/min instead of 5.1 lb/min for TXV #57. Figures 5.6 and 5.7 also show the superheat at the exit of the indoor coil(SHSC-24) for TXV #57 and TXV #52. After TXV #52 reduced the refrigerant flow, the superheat rose back to approximately 15°F at 5.5 minutes and then stabilized at 10°F at 8.0 minutes(Figure 5.7). The flow for TXV #52, during this time, rose up to 7 lb/min and experienced small oscillations between 6.2 and 7.2 lb/min. TXV #57 controlled differently as the superheat rose to 20°F at 6.5 minutes after reducing the flow. The superheat dropped to zero again as the flow increased to 7.8 lb/min. The flow did not stabilize before the end of the defrost cycle.

By stabilizing the flow, TXV #52 had a lower average refrigerant flow during the drain period then the unstable TXV #57. A smaller refrigerant mass flow rate for TXV #52 did not heat up the outdoor coil as fast as TXV #57 and delayed the termination of the defrost cycle, which is

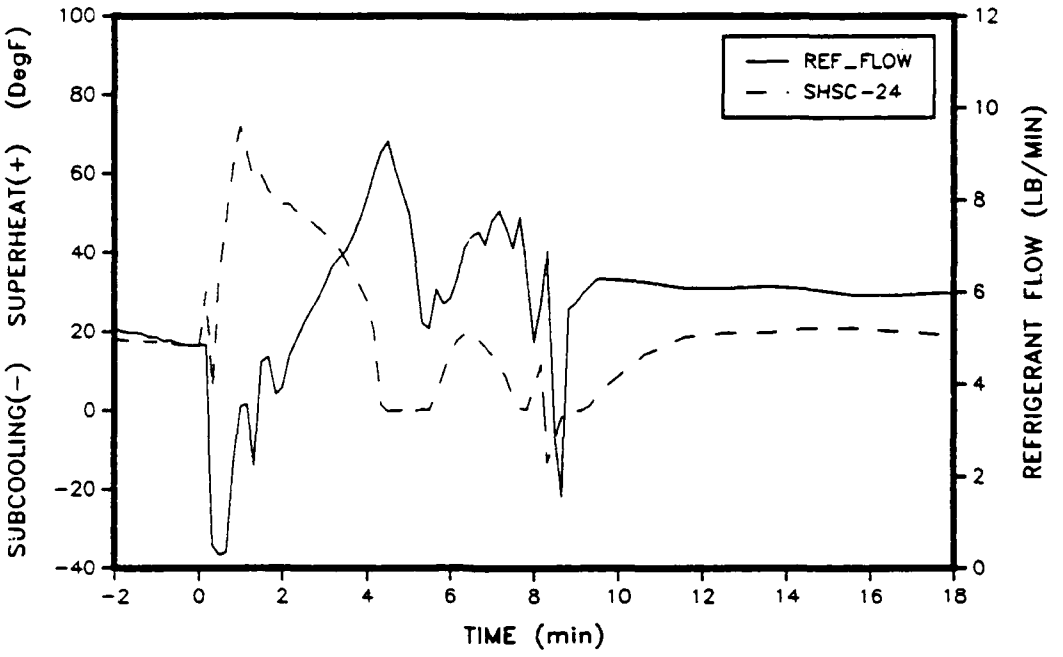

Figure 5.6. Superheat/Subcooling for T-24 & Refrigerant Flow for TXV #57 (Base Case).

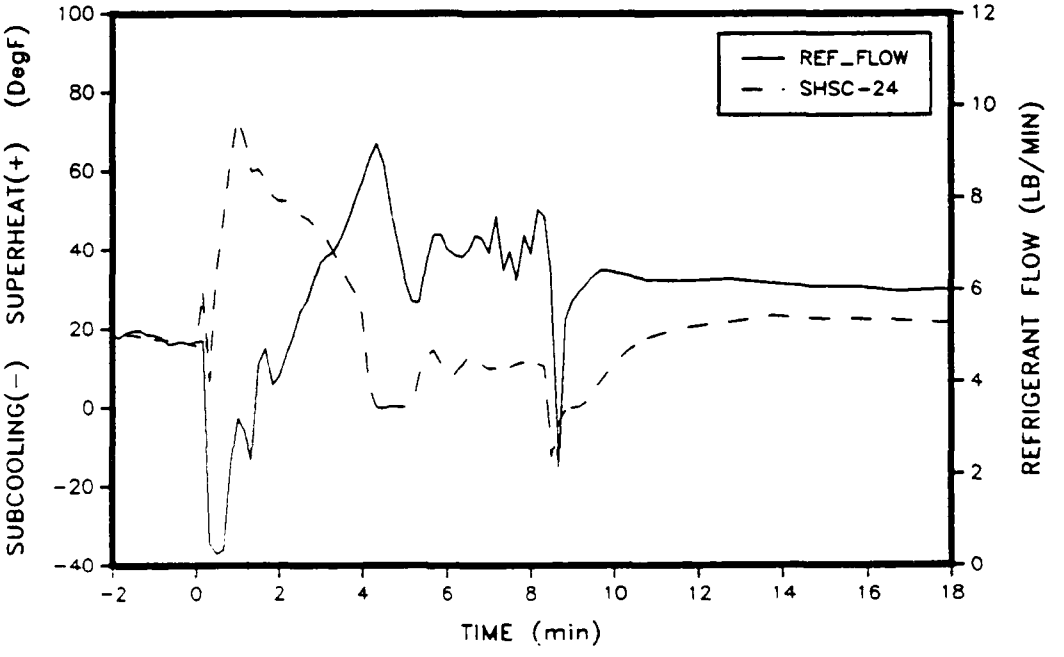

Figure 5.7. Superheat/Subcooling for T-24 & Refrigerant Flow for TXV #52.

triggered with outdoor coil temperature. The longer drain time penalized TXV #52 because it operated longer in the period where the cycle degradation is high, reducing the overall COP.

Figures 5.8 and 5.9 show the superheat and refrigerant flow characteristics for TXV #57 and TXV #51. The control characteristics of the TXVs are similar, but some variations are noticeable. SHSC-24 rose up to 75°F for TXV #51 which is approximately 5°F higher than TXV #57. After the initial drop in superheat, SHSC-24 rose to 18°F at 6.5 minutes, while SHSC-24 rose to 20°F. The response time of TXV #51, being faster then TXV #57 and TXV #52, was not evident in this investigation.

The speed of the TXVs did not establish a discernable trend for the COP as was expected. TXV #57 had the highest COP but was average in response time. The expected trend was either fast response time to slow or the reverse.

Further tests using TXV #57 revealed different control characteristics from those shown during the initial comparison testing. Figures 5.10 and 5.11 show the refrigerant flow and superheat at T-24 for two tests run with TXV #57 at different dates. For these tests the test

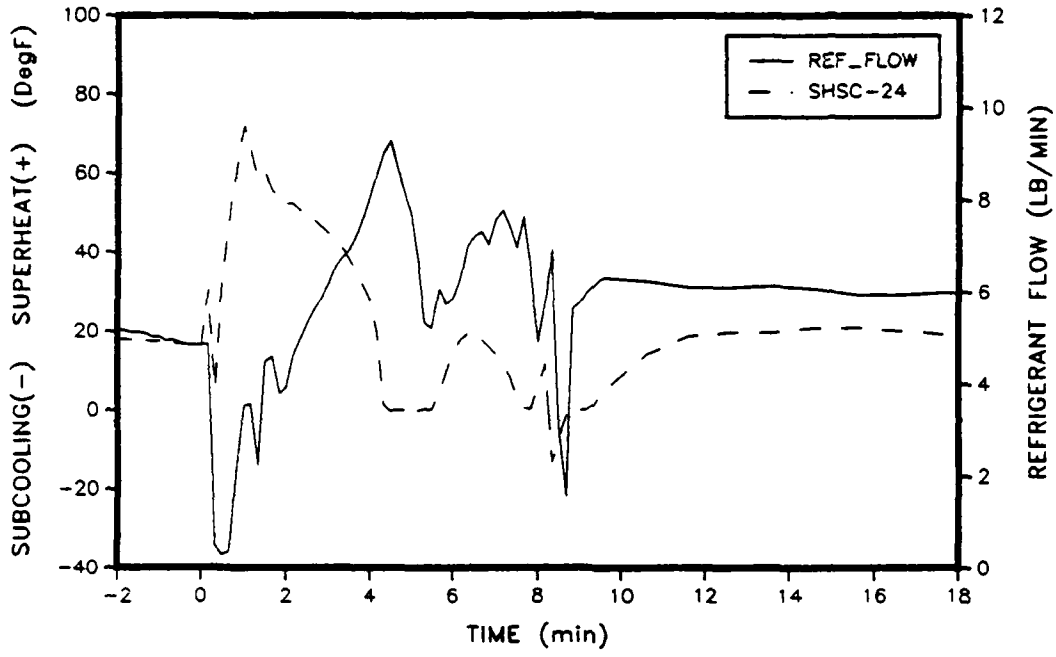

Figure 5.8. Superheat/Subcooling for T-24 & Refrigerant Flow for TXV #57 (Comparison with TXV #51).

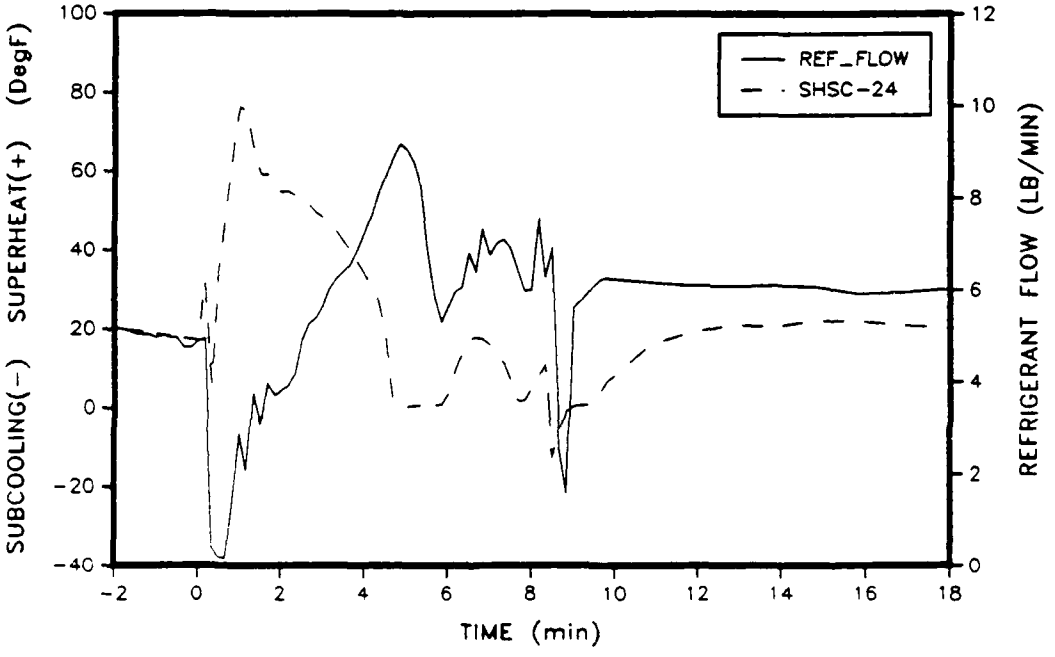

Figure 5.9. Superheat/Subcooling for T-24 & Refrigerant Flow for TXV #51.

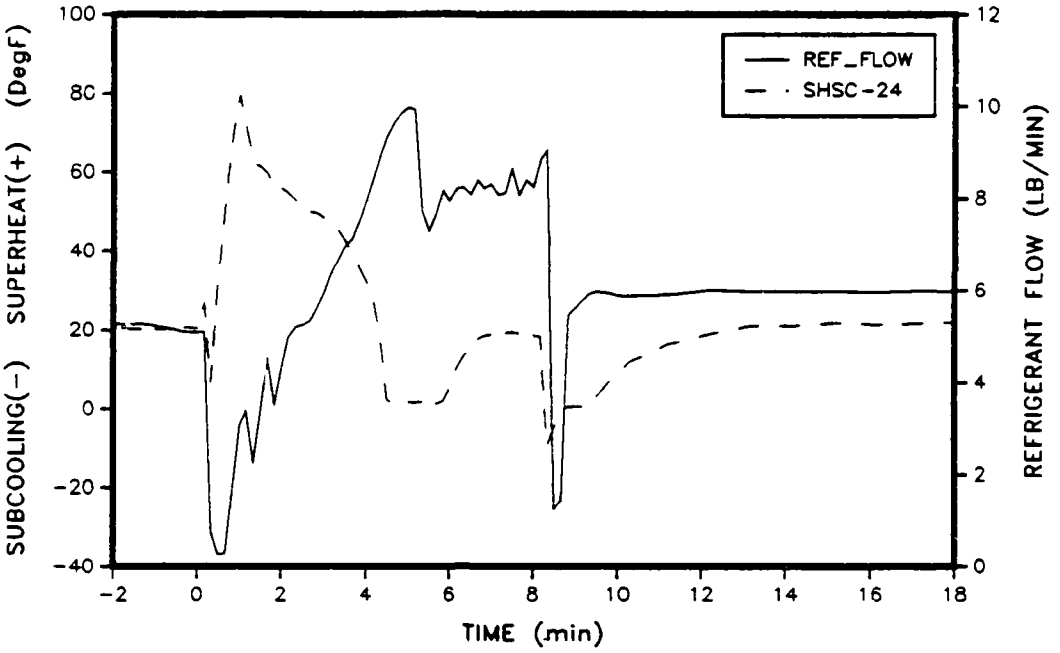

Figure 5.10. Superheat/Subcooling for T-24 & Refrigerant Flow for TXV #57 - Test #1.

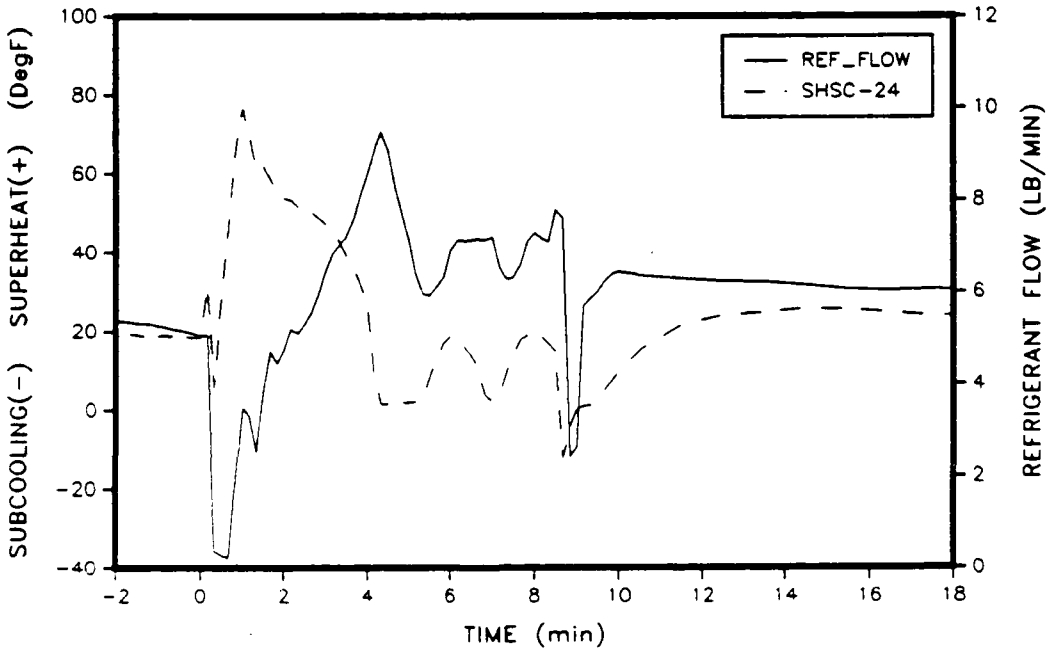

Figure 5.11. Superheat/Subcooling for T-24 & Refrigerant Flow for TXV #57 - Test #2.

unit was disassembled and reassembled which means the TXV bulb was removed and then remounted to the suction line.

The differences between Figures 5.10 and 5.11 and the base case(Figure 5.8) are dramatic. Figure 5.10 shows the largest variation from the base case as the refrigerant flow rose as high as 10 lb/min and only dropped to 7.5 lb/min before rising steadily to 8.5 lb/min at defrost termination. The superheat(SHSC-24) leaving the coil initially fell to zero like the base case but then rose to 20°F and remained there until termination. The refrigerant flow in Figure 5.11 is similar to the base case, but the similarities in this test using TXV #57 are not as close as the comparison between TXV #51 and TXV #57 in Figures 5.7 and 5.9.

The control variations in TXV #57 indicate the importance of the expansion bulb contact on the suction line. While the expansion bulb was mounted in the same position for every test, small variations in expansion bulb contact caused the control characteristics of TXV #57 to change drastically. The conclusion to this is that the TXVs internal response time was of secondary importance to the expansion bulb contact on the suction line and the test results were more a factor of bulb contact than the internal response of the TXV.

SUMMARY OF TXV COMPARISON

Three TXVs of different response times were tested, resulting in the highest COP for the base case TXV #57. The COP for TXV #51(fast response) was slightly less than TXV #57 and had similar control charactersitics. TXV #52 (slow response) had the most stable control of refrigerant and superheat, but also had the lowest COP. Analysis showed that the stable control of TXV #52 allowed less refrigerant to flow to the outdoor coil which delayed the termination of the defrost, causing the reduction in COP.

Further testing with the base case revealed variations in refrigerant control characteristics using TXV #57. The variations were caused by expansion bulb remounting after the test setup was disassembled and reassembled between tests. The variations in the control characteristics for the three TXVs were not as great as that of TXV #57 with slight differences in bulb placement.

CHAPTER VI

COMPARISON OF DIFFERENT DIAMETER ORIFICES

The orifice analysis starts with a comparison of the control characteristics of the base case TXV #57 and an orifice whose flow diameter is comparable to the maximum flow diameter for TXV #57. The orifice is labeled ORF 090. The ORF is an abbreviation for orifice and the number 090, refers to the diameter of the orifice in thousandths of an inch. Following the comparison of ORF 090 and TXV #57, the analysis continues with a comparison of the operation of six different sizes of orifices: ORF 059, ORF 070, ORF 076, ORF 090, ORF 101, and ORF OPEN. ORF OPEN is the orifice holder with the orifice removed, giving an approximate opening diameter of 0.300 inches, essentially no restriction.

CONTROL DIFFERENCES BETWEEN A TXV AND AN ORIFICE

As mentioned in Chapter V, the base case expansion device(TXV #57) had an equivalent port area, when fully open, equal to a 0.087 inch diameter orifice. Since the diameter of ORF 090 is approximately equal to 0.087 inches, it was selected for comparison with TXV #57 during the

reverse cycle defrost. Table 6.1 shows the effects of the two expansion devices on the defrost cycle.

Table 6.1. Comparison of Heat Pump System Characteristics Using TXV #57 and Orifice 090.

DEFROST EXPANSION DEVICE	INTEGR. CYCLIC COP	DEFROST TIME (minutes)	MELT TIME (minutes)	DRAIN TIME (minutes)
TXV #57	2.26	8.06	4.22	3.83
ORF #90	2.28	7.83	4.83	3.00

The overall performance of TXV #57 and ORF 090 were essentially equal as the COP varied by less than 1% and the defrost times by less than 3%. This similarity did not hold true for the melt and drain times. TXV #57 was able to melt the frost on the coil 12.6% (36 seconds) faster than ORF 090, but TXV #57 took 27.7% (49 seconds) longer to heat the coil and terminate the defrost during the drain time. The variations in melt time and drain time indicated differences in control characteristics even though the overall performances were similar.

The system refrigerant flow characteristics and the subcooling(SHSC-26) at the inlet of TXV #57 and ORF 090 were

shown in Figures 6.1 and 6.2, respectively. For the first 2 minutes into defrost, the refrigerant flow for both expansion devices followed similar trends. After defrost initiation, the refrigerant flow dropped close to zero and then rose into a period of unstable flow. This unstable flow was caused by the saturated condition at the inlet to the expansion device(T-26) as shown in Figures 6.1 and 6.2. T-26 was superheated during the first minute of defrost and at 1 minute became saturated as liquid started flowing through the expansion device into the indoor coil. At 2 minutes, characteristics between the two expansion devices started changing as the subcooling for TXV #57(T-26) started increasing and reached -16^{o}F at 4 minutes(Figure 6.1). During the same period in Figure 6.1, the refrigerant flow stabilized and rose from 4 lb/min to 8 lb/min. In Figure 6.2, T-26 did not become subcooled for ORF 090 until after 3 minutes. This delayed the rise in refrigerant flow for ORF 090 as it reached 6.5 lb/min at 4 minutes. Since the flow for ORF 090 was lower than that for TXV #57 during the melt phase , less hot refrigerant was pumped into the outdoor coil and the melt time was longer for ORF 090 than TXV #57.

Shortly after 4 minutes, the refrigerant flow for TXV #57 rose to 9.3 lb/min and then fell to 5.3 lb/min at 5.5 minutes. The flow for ORF 090 surpassed TXV #57 during this

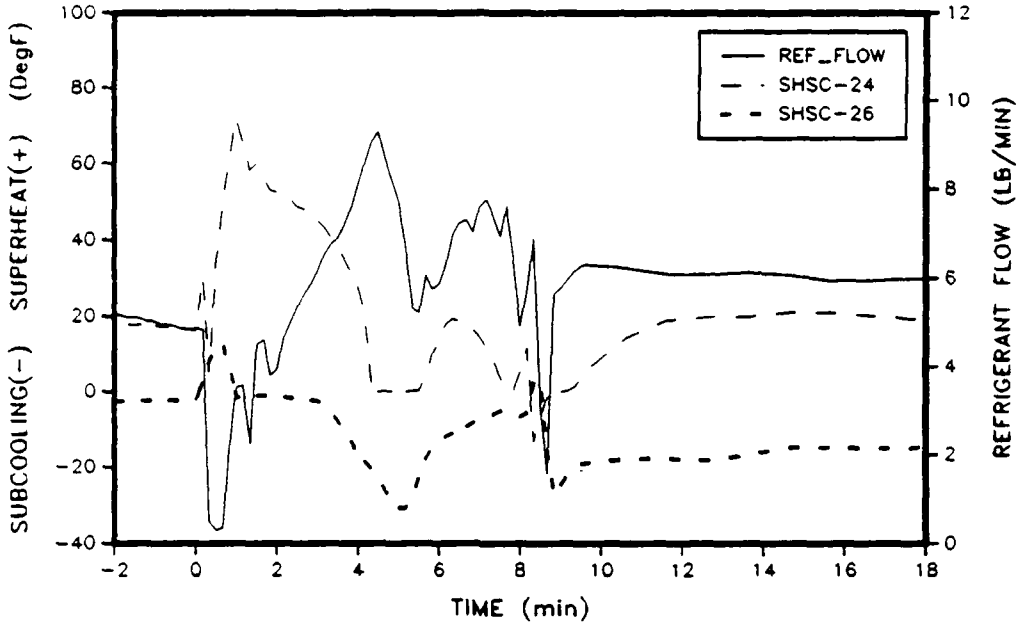

Figure 6.1. Superheat/Subcooling for T-24,T-26 & Refrigerant Flow for TXV #57 (Base Case).

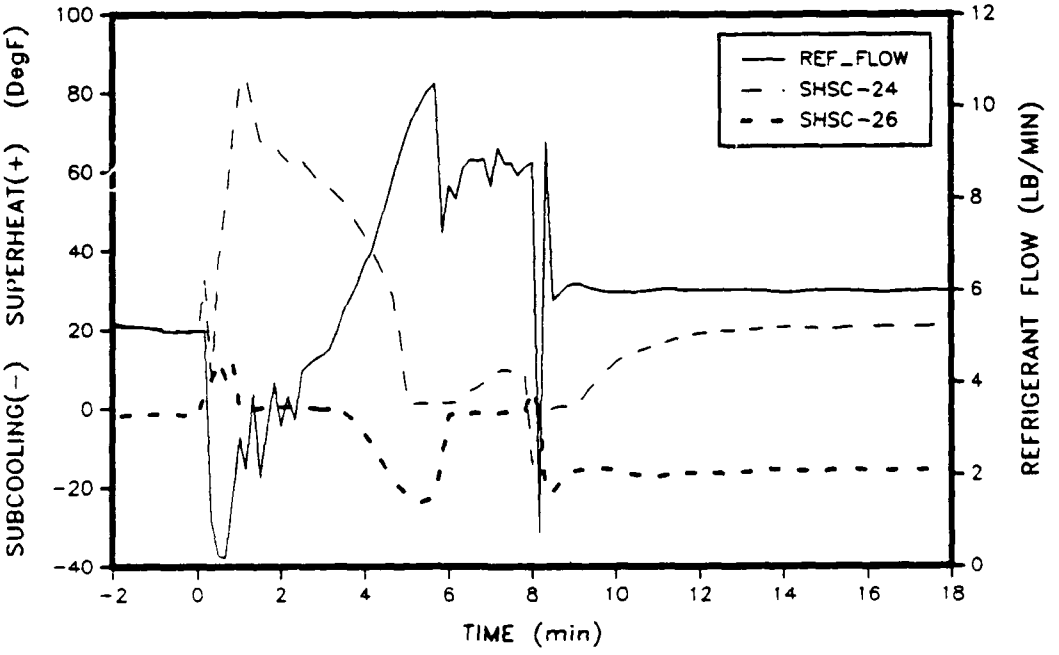

Figure 6.2. Superheat/Subcooling for T-24,T-26 & Refrigerant Flow for ORF 090.

phase and rose to 10.6 lb/min at 5.5 minutes. During the remainder of the defrost, the refrigerant flow for ORF 090 averaged approximately 8.5 lb/min, while the flow for TXV #57 averaged 6.5 lb/min. ORF 090 allowed 30% more hot vapor into the coil during the drain phase than did TXV #57. This shortened the drain time by 50 seconds from that of TXV #57.

In Chapter IV, the control of refrigerant flow by TXV #57 was discussed in detail. The drop in refrigerant flow from 9.3 lb/min to 5.3 lb/min(Figure 6.1) at 4.5 minutes was probably caused by the closing down of the TXV port after the superheat at T-24 fell to zero at 4.4 minutes (Figure 6.1). ORF 090 had a similar reduction in its flow as it fell from 10.5 lb/min to 7 lb/min at 5.5 minutes in Figure 6.2. Since the orifice was stationary, the flow control must have been caused by the refrigerant conditions at the inlet to the orifice. Figure 6.2 contains the subcooling (T-26) of the refrigerant entering the orifice. The start of the refrigerant drop at 5.7 minutes coincided with the drop in subcooling from -25°F at 5.5 minutes to -5°F at 6 minutes. Figures 6.3 and 6.4 show the inlet pressures and subcooling for TXV #57 and ORF 090, respectively. At 5.5 minutes the pressure for ORF has risen to 120 psia and the pressure for TXV #57 is 150 psia.

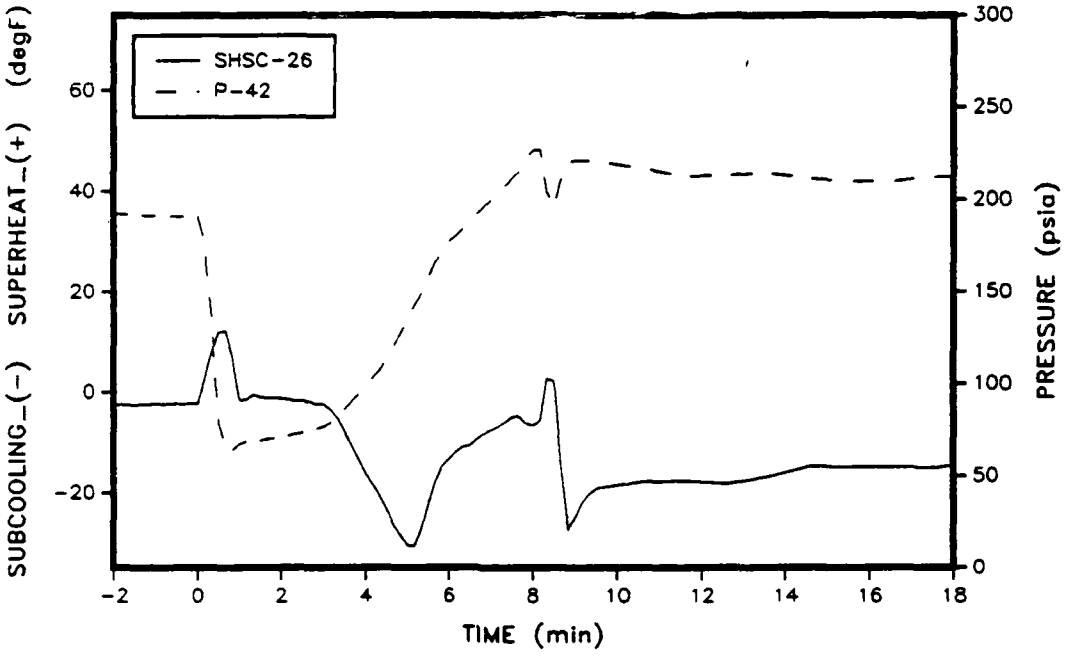

Figure 6.3. TXV #57 Inlet Pressure and Subcooling (Base Case).

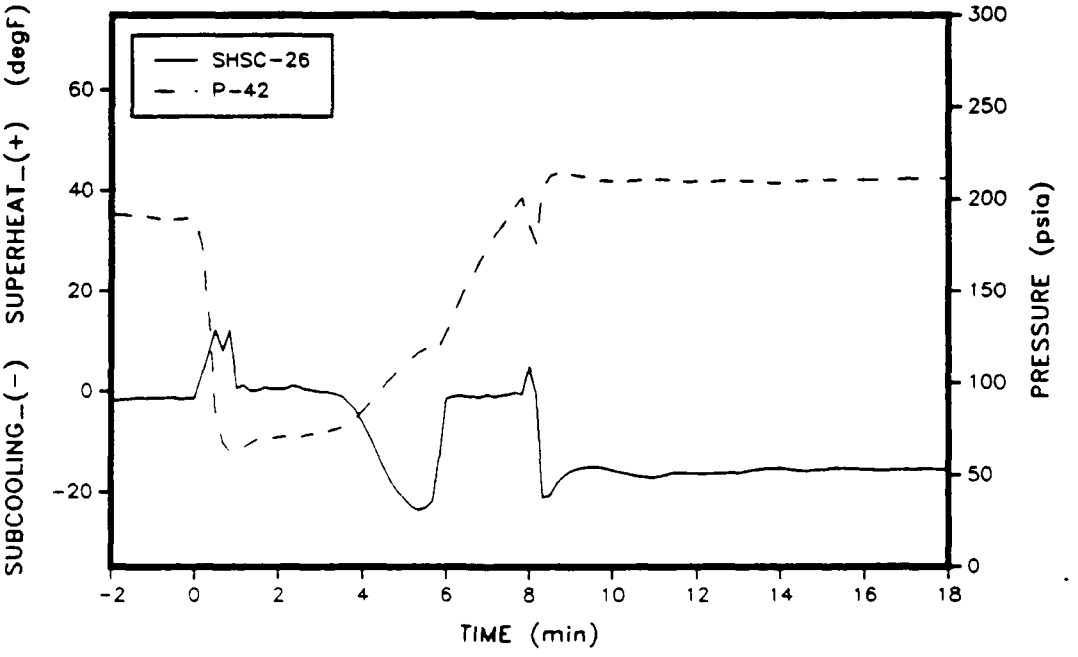

Figure 6.4. ORF 090 Inlet Pressure and Subcooling.

Assuming the flow characteristics for an orifice are similar to a capillary tube as stated by Krakow and Lin[22], the reduced flow rate through the orifice can be obtained from the Basic Rating Curves for capillary tubes in the ASHRAE 1988 Equipment Handbook[23]. From Figure 38 in Chapter 19 of the Equipment Handbook, the mass flow rate for 25°F subcooling and 120 psia inlet pressure resulted in a normalized mass flow rate of 90 lb/hr. The reduced normalized flow rate with -5°F subcooling and the same inlet pressure was found to be 59 lb/hr, a 34% reduction. Applying the same percentage reduction to 10.5 lb/min in Figure 6.2 at 5.5 minutes yielded a reduction to 6.9 lb/min. The flow actually dropped to 7.0 lb/min, a 33% reduction. Thus it would appear that the change in flow conditions at the inlet to the orifice were responsible for the reduction in refrigerant flow.

COMPARISON OF DIFFERENT DIAMETER ORIFICES

This section focuses on the defrost cycle effects of using different diameter orifices for the defrost expansion device. The orifice diameters ranged from 0.059 inches to approximately 0.300 inches (no restriction). As was done in previous sections, the overall performance of the orifices

are discussed first, followed by a detailed analysis of the refrigerant dynamics.

Table 6.2 contains the COP and defrost times for the different orifices. The COP increased with the size of orifice from a low of 2.03 for ORF 059 to a high of 2.30 for ORF OPEN. Directly responsible for the variation in COP was the trend of decreasing defrost times with increasing orifice size, which agrees with Young's study[12]. The defrost times are plotted in Figure 6.5 along with the melt and drain times. The relationship between orifice size and defrost time is nearly linear except for ORF 059. ORF 059 is consistent with the melt times of the other orifices, but

Table 6.2. Comparison of Heat Pump System Characteristics Using Various Diameter Orifices.

DEFROST EXPANSION DEVICE	INTEG. CYCLIC COP	DEFROST TIME (minutes)	MELT TIME (minutes)	DRAIN TIME (minutes)
ORF #59	2.03	14.53	6.72	7.61
ORF #70	2.21	9.71	6.00	3.71
ORF #76	2.22	9.33	5.44	3.90
ORF #90	2.28	7.83	4.83	3.00
ORF #101	2.30	7.33	4.44	2.94
ORF OPEN	2.30	6.61	3.72	2.89

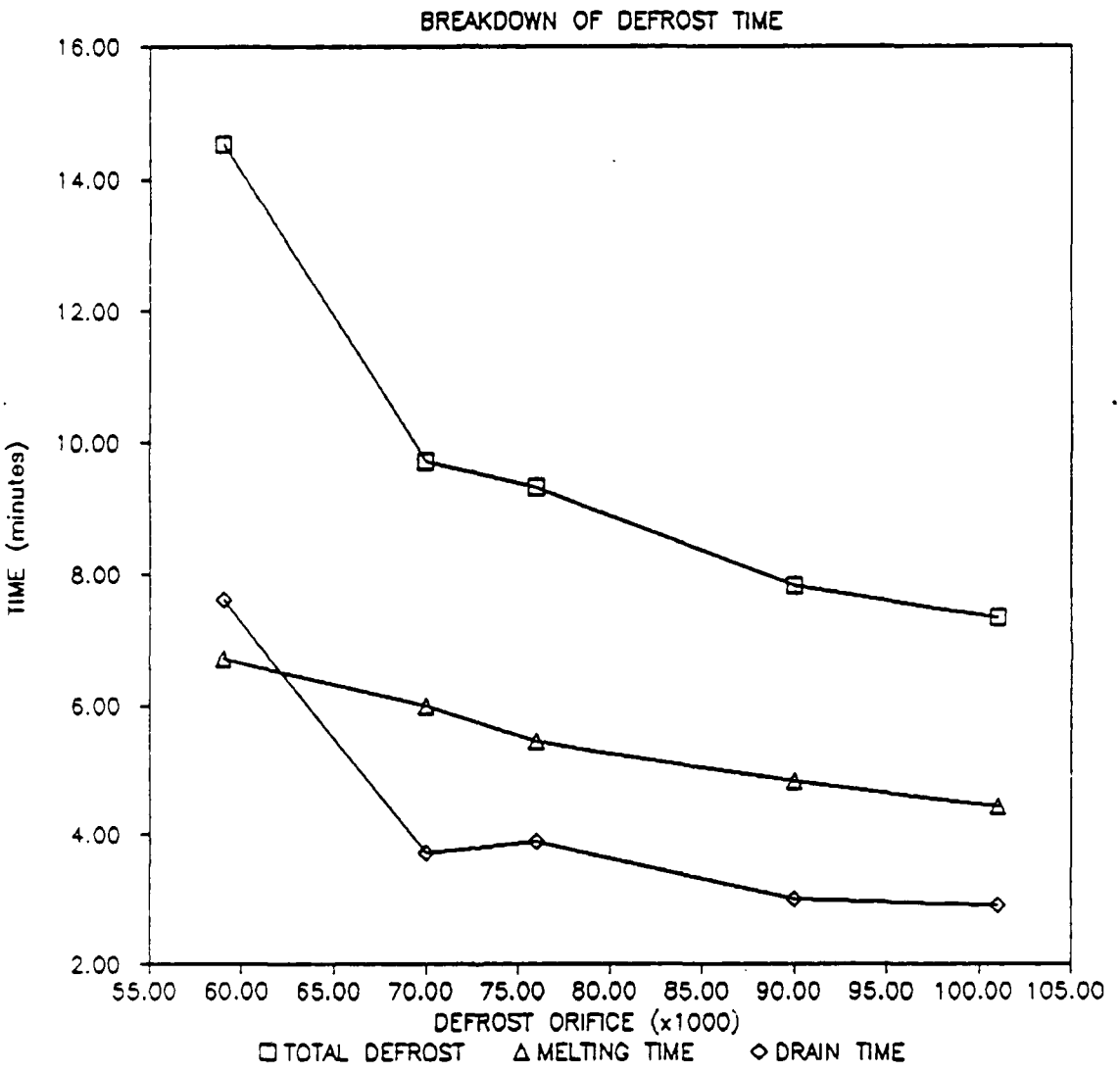

Figure 6.5. Graph of Defrost Times in Relation to Orifice Size.

during the drain time, ORF 059 takes over twice as long as the other orifices to terminate the defrost.

Some of the operating conditions of the orifices are listed in Table 6.3. The minimum suction pressure and the maximum superheat are related to each other and are directly related to the restriction of refrigerant flow by the defrost orifice. At the initiation of defrost, the orifice metered refrigerant into the indoor coil and eventually into the compressor intake. A small orifice provided less refrigerant to the compressor which caused the suction pressure to drop as indicated in Table 6.3. Note, that with the small orifice, ORF 059, the suction pressure went below atmospheric pressure.

Table 6.3. Operating Conditions for Different Diameter Defrost Orifices During the Reverse Cycle Defrost.

DEFROST EXPANSION DEVICE	MINIMUM SUCTION PRESSURE (psia)	MAXIMUM DISCHARGE PRESSURE (psia)	MAXIMUM SUPERHEAT @ T-24 (F)	MAXIMUM REFRIG. FLOW (LB/MIN)
ORF #59	13	283	112	6.8
ORF #70	16	244	100	8.8
ORF #76	18	245	96	9.5
ORF #90	23	230	84	10.5
ORF #101	27	220	75	11.2
ORF NONE	35	220	59	11.4

Because the indoor coil contained only low pressure vapor shortly after defrost initiation (Chapter IV), the reduced suction pressure lowered the saturation temperature which raised the superheat at T-24. The maximum superheat was the highest for ORF 059 with 112°F and decreased with increasing orifice size to 59°F with ORF OPEN.

In general, the larger the orifice size used during the reverse cycle defrost, the larger the refrigerant flow into the outdoor coil. The large orifice allowed more refrigerant to flow into the outdoor coil which melted the frost quicker and heated the coil up faster than with a smaller orifice. This shortened the defrost time and increased COP for the complete cycle.

The refrigerant flow for ORF OPEN and ORF 059 are shown in Figures 6.6 and 6.7. After defrost initiation, the refrigerant flow dropped to zero and then immediately rose to 5 lb/min at 1 minute. From 1 minute to 2 minutes the flow was unstable similar to ORF 090 but at a higher flow rate. The refrigerant flow increased rapidly from 2 minutes until 4 minutes where it reached a maximum flow rate of 11.4 lb/min. Figure 6.6 also shows the subcooling at the entrance to the orifice(SHSC-26). As the subcooling at 4.2 minutes dropped from -10°F to -2°F, the refrigerant flow dropped from 11.4 to 6 lb/min. Figure 6.2 displays the same

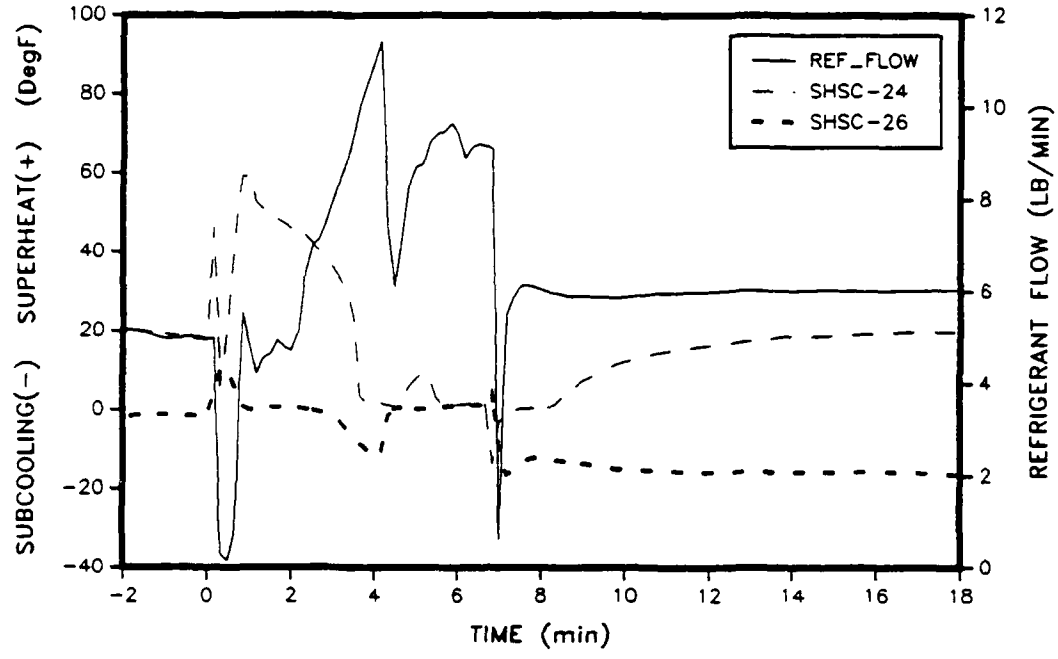

Figure 6.6. Superheat/Subcooling for T-24,T-26 & Refrigerant Flow for ORF OPEN.

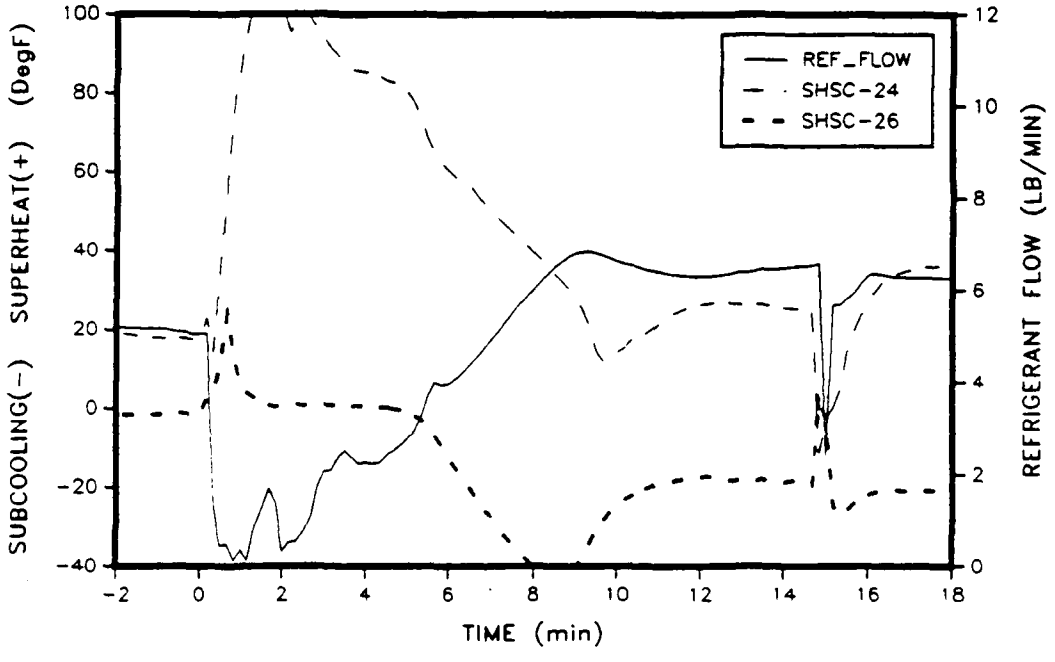

Figure 6.7. Superheat/Subcooling for T-24,T-26 & Refrigerant Flow for ORF 059.

characteristics for ORF 090, but the flow was only 10.5 lb/min and the subcooling was at -24°F before it fell to 2°F.

The control characteristics of ORF OPEN and ORF 090 were similar to the other orifices tested except for ORF 059. Figure 6.7 shows the refrigerant flow for the system using ORF 059 as the defrost orifice. The flow dropped to zero at 1 minute and stayed under 3 lb/min until 5 minutes. ORF 059 reached a peak flow of 6.8 lb/min at 9 minutes and stayed at 6.5 lb/min until defrost was terminated. There was no drop in refrigerant flow and the subcooling remains at -20°F for the remainder of the defrost cycle.

Figures 6.8 and 6.9 show the potential problem of compressor slugging caused by the high refrigerant flow from ORF 090 and ORF 101, respectively. In Figure 6.8, the refrigerant condition at the compressor discharge(T-19) is shown for ORF 090. At 6 minutes, T-19 dropped toward Tsat-19 but rose immediately to maintain a superheated condition at the compressor discharge. If T-19 had dropped down to Tsat-19, the outlet of the compressor would have been saturated and the compressor would have pumped some liquid, which could have caused damage to the compressor valves. Figure 6.9 shows saturated vapor in the compressor discharge for ORF 101. At 6 minutes, T-19 dropped down to Tsat-19

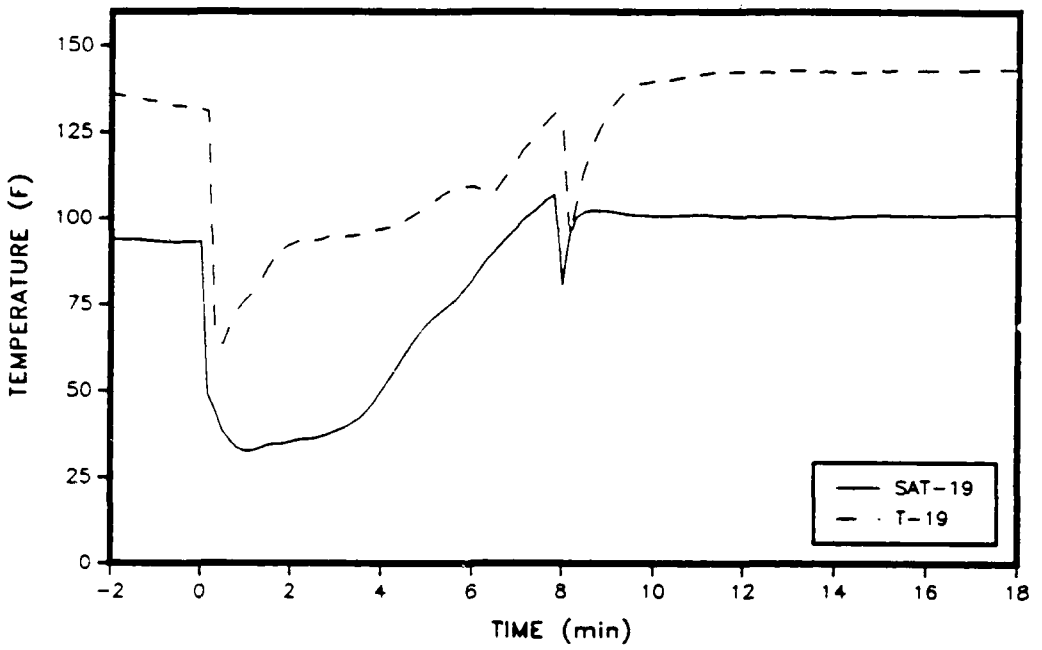

Figure 6.8. Refrigerant Conditions at Compressor Discharge for ORF 090.

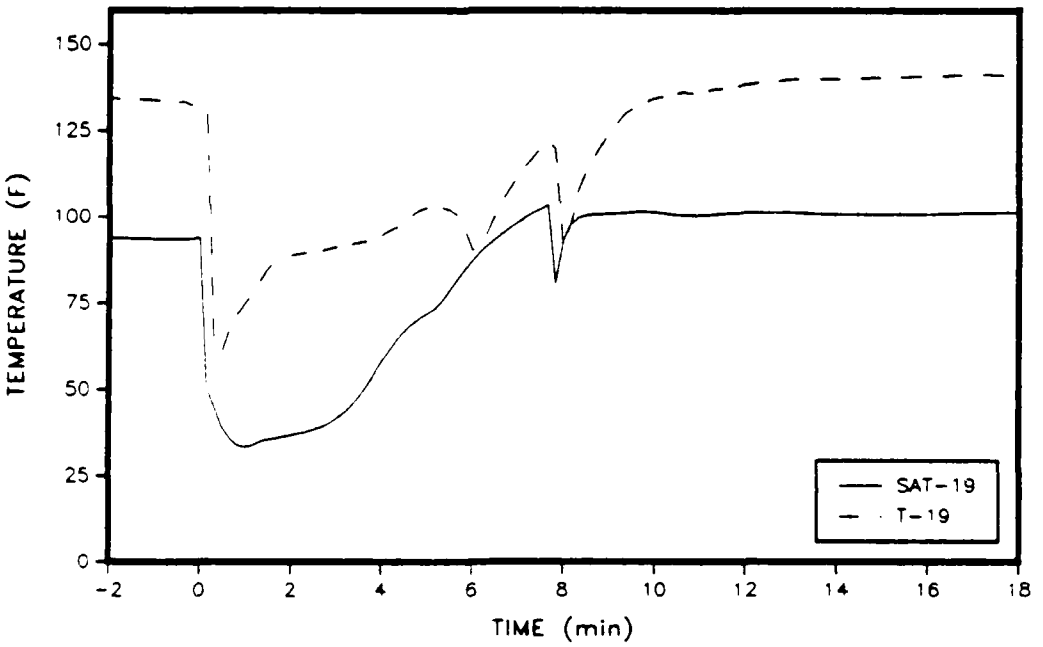

Figure 6.9. Refrigerant Conditions at Compressor Discharge for ORF 101.

where the flow was saturated for a short period. The saturated condition indicated some liquid had passed through the compressor and there was a possibility of compressor damage. For the orifices smaller than ORF 090, the compressor discharge remained superheated. ORF 101 and ORF OPEN both had conditions that indicated compressor slugging.

SUMMARY OF ORIFICE COMPARISON

The refrigerant flow characteristics of an orifice and a TXV were compared. Though the TXV melted the frost off the coil faster than an equivalent diameter orifice, the TXV reduced the flow of refrigerant during the drain period of the defrost and took longer to complete the defrost cycle.

Five different size orifices were also compared for their effect on the reverse cycle defrost. In general, the larger the orifice, the more refrigerant is supplied to the outdoor coil during the defrost and the quicker the defrost. The larger orifices reduced the maximum discharge pressure, the minimum suction pressure, and the maximum superheat leaving the indoor coil during the defrost cycle. Slugging of the compressor was indicated in the largest orifice, while the smallest orifice more than doubled the defrost time from the other orifices.

CHAPTER VII

CONCLUSIONS AND RECOMMENDATIONS

There are general limitations in current published studies involving the transient performance of heat pumps. These limitations include the uniqueness of each experiment and the lack of documentation for comparison with results from other work. The need for additional research with adequate documentation is required to provide a better understanding of the heat pump transient performance.

A 3-ton air-to-air heat pump was instrumented and installed in two psychrometric rooms to analyze the transient performance of the heat pump during a frosting/defrost cycle. The investigation focused on the effects of various defrost expansion devices on the overall performance of the heat pump and the refrigerant dynamics during the cycle. Variations in the defrost expansion device included: TXVs with different response times and orifices with different diameters.

The results of the experimentation showed that the slow response TXV provided better control of the refrigerant flow during the defrost cycle, but had a slightly longer

defrost cycle and lower COP than the faster response TXVs. A reduced refrigerant flow rate caused the decrease in COP for the slow response TXV. The orifices showed a trend of faster defrost times as the orifice diameter was increased. This was a result of a higher refrigerant flow rate. Comparison between the TXVs and an equivalent size orifice revealed that the frost melted from the coil faster with a TXV, but the defrost cycle was longer because the TXV reduced the refrigerant flow rate during the last half of the defrost cycle.

CONCLUSIONS

During the testing, it was discovered that the response times of the TXVs were greatly dependent on the bulb position on the vapor line. Further investigation showed the TXV response time was effected more by the bulb position than the bulb charge. This means that while the TXV tests were able to characterize the effect of the TXVs on the system, the tests did not necessarily give an accurate account of the effects caused by the different response times of the individual TXVs.

Several other conclusions were reached from the study. First, the TXVs are well suited for defrost expansion since

the high superheat in the indoor coil keeps them in a wide open position during the first half of defrost when the frost is being melted from the coil. Secondly, the larger the orifice the better during the melt phase of the defrost, but during the drain phase the larger size orifice can cause two phase flow in the compressor. Third, the drain phase of the defrost has the largest penalty on COP, so the shorter the drain phase the higher the COP. Lastly, the stall of the outdoor unit fan motor prematurely caused the initiation of defrost by dropping the airflow through the outdoor coil which reduced system capacity.

RECOMMENDATIONS

From the study, some recommendations for heat pump equipment and operation, as well as future research, are suggested.

Modifications to the test unit that would improve defrost performance are: (1) installation of a more powerful outdoor fan that could maintain the airflow longer and increase the time between defrosts and (2) installation of an electronic valve that would open wide during the defrost, but close to a smaller setting when operating in the cooling mode.

In heat pump operation, two options are identified for improvement in the defrost cycle: (1) the drain time could be initiated with the rise in refrigerant temperature leaving the outdoor coil. When the leaving refrigerant temperature rises above 34°F, a timer could be initiated to allow adaquate time for the water to drain from the coil. This would limit the drain time and lower the COP. (2) when the leaving refrigerant temperature rose above 34°F, the compressor could be shut off during the drain phase, since the heat is no longer required to melt the ice.

While performing the testing, several ideas for improving the test setup were developed: (1) To improve repeatability, an orifice could be used for the base case expansion device, since its performance is not dependent on mounting. (2) An automatic control on the outdoor chamber damper would improve testing ability, since more observations could be done during the test instead of monitoring the airflow through the outdoor coil. (3) Mounting flow meters between the compressor and the outdoor coil and between the indoor coil and the accumulator would provide a better analysis of the refrigerant inventory.

REFERENCES

1. American Society of Heating, Refrigeration and Air-Conditioning Engineers, ASHRAE Handbook: 1985 Fundamentals, p. 1.4, Atlanta, Georgia, 1985.

2. "Standard for Unitary Heat Pump Equipment," Standard No 240-76, The Air-Conditioning and Refrigeration Institute, Arlington, Va.

3. Didion, David A.; and Kelly George E., "New Testing and Rating Procedures for Seasonal Performance of Heat Pumps," ASHRAE Journal, Vol. 21, No. 9: pp. 40-44, September, 1979.

4. Baxter, V.D.; Abbatiello, L.A.; and Minturn,R.E., "Comparison of Field Performance to Steady State Performance for Two Dealer-Installed Air-to-Air Heat Pumps," ASHRAE Transactions, Vol. 88, Part 2:941-953, 1982.

5. Wildin, M.W.; Fong, A.; Wilson, C.; and Nakos, J., "Analysis of The Effects of Cycling on Energy Use of Installed Air-to-Air Heat Pumps in Albuquerque, New Mexico." Third Annual Heat Pump Technology Conference, Sponsored by Oklahoma State University, April 1978.

6. Goldschmidt, V.W.; and Hart, G. H., "Heat Pump System Performance: Experimental and Theoretical Results," ASHRAE Transactions, Vol. 88, Part 1: pp. 479-488, 1982.

7. Bittle, B.B.; and Goldschmidt, V.W., "Effect of Cycling and Frost Formation on Heat Pump Performance," ASHRAE Transactions, Vol. 89, Part 2: pp. 743-754, 1983.

8. Baxter, V.D.; and Moyers, J.G., "Air-Source Heat Pump: Field Measurement of Cycling, Frosting and Defrosting Losses," ORNL/CON - 150, 1981-83.

9. Tanaka,N.; Yamanaka,G.; and Ikeuchi M., "Experimental Study on the Dynamic Characteristics of a Heat Pump," ASHRAE Transactions, Vol. 88, Part. 2: pp. 345-353, 1982.

10. Miller,W.A., "Laboratory Examination and Seasonal Analysis of Frosting and Defrosting for an Air to Air Heat Pump," ASHRAE Transactions, Vol. 93, Part. 1: pp. 289-301, 1987.

11. Mulroy, W.J., "The Effect of Short Cycling and Fan Delay on the Efficiency of a Modified Residential Heat Pump," ASHRAE Transactions, Vol. 92, Part 2: pp. 813-826, 1986.

12. Young, David J., "Development of a Northern climate Residential Air-Source Heat Pump," ASHRAE Transactions, Vol. 86, Part 1: pp. 671-686, 1980.

13. Miller, W.A., "Frosting Experiments for a Heat Pump Having a One-Row Spine-Fin Outdoor Coil," ASHRAE Transactions, Vol. 90, Part 1: pp. 1009-1025, 1984.

14. Trask, Allen, "The Heat Pump Defrost Problem," Fifth Annual Heat Pump Technology Conference, Sponsored by Oklahoma State University, April, 1980.

15. West,James E., "Defrosting Air to Air Heat Pumps Present and Future," Fourth Annual Heat Pump Technology Conference, Sponsored by Oklahoma State University, April, 1979.

16. Department of Energy(DOE) - Test Procedures for Central Air Conditioners, Including Heat Pumps(1979).

17. "Laboratory Methods of Testing Fans for Rating," ANSI/ASHRAE Standard 51-1985(ANSI/AMCA 210-85).

18. "Methods of Testing for Seasonal Efficiency of Unitary Air-Conditioners and Heat Pumps," ANSI/ASHRAE Standard 116-1983.

19. American Society of Heating, Refrigeration and Air-Conditioning Engineers, ASHRAE Handbook: 1985 Fundamentals, pp. 6.12-13, Atlanta, Georgia, 1985.

20. Kartsounes,G.T.; and Erth R.A., "Computer Calculation of the Thermodynamic Properties of Refrigerants 12, 22, and 502," ASHRAE Transactions, Pgs. 88-103, 1971.

21. American Society of Heating, Refrigeration and Air-Conditioning Engineers, ASHRAE Handbook: 1988 Equipment, pp. 3.2-3.3, Atlanta, Georgia, 1988.

22. Krakow,K.I.; and Lin S., "Refrigerant Flow Through Orifices," ASHRAE Transactions, Vol. 94, Part. 1: pp. 250-261, 1988.

23. American Society of Heating, Refrigeration and Air-Conditioning Engineers, ASHRAE Handbook: 1988 Equipment, p. 19.26, Atlanta, Georgia, 1988.

APPENDIX A

Equipment Used in the Testing Apparatus.

EQUIPMENT	SIZE/ RANGE	MAKE/MODEL	ACC.[1]
HEAT PUMP[2]	3 TON	PAYNE/544AJ036	
COMPRESSOR	3 TON	TECUMSEH/AV5535E	
ACCUMULATOR	163 OZ	TECUMSEH/51066-1	
OUTDOOR FAN	1/10 HP		
DATALOGGER	65 CHAN	ACUREX/AUTODATA	
WATT/WATT-HOUR TRANSDUCER	20 KW	OHIO SEMITRONICS/W-53	0.5%
PRESSURE TRANSDUCER	0-300psig	FOXBORO/1225-12G-K42	0.5%
DIFF.PRESSURE TRANSDUCER	0-2 INWG	CELESCO/LCCD 110 (CD) LCVR (TRANS)	0.1%
FLOW METER	0-26 LBPM	MICRO-MOTION/D-12	0.3%
DEW POINT SENS.	0-100°F	GENERAL EASTERN/DEW-10	0.5°F
THERMOCOUPLES	30 AWG	OMEGA/TYPE T	0.5°F

[1] Percentages are percent of span or range. Temperatures are deviations (+/-).

[2] Original unit supplied for testing. The modifications to the original unit included using a different indoor coil, installing a different accumulator, and replumbing of the refrigerant lines.

VITA

Kurt T. Peterson [redacted], the first son of [redacted] He graduated from Gilbert High School in Gilbert, Minnesota in 1974. He enrolled in LeTourneau College in Longview, Texas, in 1979, and received his B.S. Degree in Mechanical Engineering in 1983.

He is currently employed as a Captain in the United States Air Force as a Civil Engineering Officer.

He is married to the former Wendy Helene Wuotila of Gilbert, Minnesota, and is the father of a son, Seth Thomas, and two daughters, Kimberly Helene and Amy Jolene.

Mr. Peterson's permanent residence is in McKinley, Minnesota with a mailing address of P.O. Box 225 , McKinley, Minnesota 55761.